School of Mining Engineering

UNIVERSITY OF THE WITWATERSRAND, JOHANNESBURG

GEOSTATISTICAL MODELLING OF FLOOR AND ROOF HAZARD DATA IN THE HIGHVELD COALFIELD – A NEW DENMARK COLLIERY CASE STUDY

Quintin Hall

A research report submitted to the Faculty of Engineering and the Built Environment, University of the Witwatersrand, Johannesburg, in partial fulfilment of the requirements for the degree of Master of Science.

Johannesburg, 2024

DECLARATION

I declare that this research report is my own unaided work. It is being submitted for the degree of Master of Science at the University of the Witwatersrand, Johannesburg. It has not been submitted before for any degree or examination to any other university.

I have familiarised myself with the University of the Witwatersrand Student Academic Misconduct Policy (SAMP). I hereby declare that the work I am submitting for assessment is my original work. I affirm that I have not plagiarised, misrepresented, or colluded with any other person or source. I have properly acknowledged, cited, and referenced all the sources that I have used in my work. I also declare that I have used artificial intelligence (AI) tools only as a means of guidance. The ideas and arguments presented in my work are my original thoughts and interpretations. I acknowledge that any academic misconduct, such as plagiarism or collusion will result in serious consequences. These consequences may include a reduced grade, a fail mark, or disciplinary action according to the SAMP. The School of Mining Engineering has my consent to investigate any potential academic misconduct in my work. This investigation may include the use of similarity and AI detection software to check the originality of my work. I undertake to abide by the decision of any such investigation.

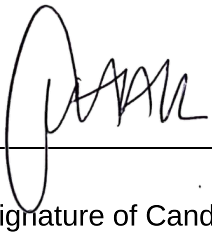

____

(Signature of Candidate)

18 day of March, 2024

(month) (year)

"The greatest power on Earth is the magnificent power we all of us possess... the power of the human brain!"

Professor X

ABSTRACT

New Denmark Colliery (NDC) is an underground coal mine located between Standerton and Bethal in the Mpumalanga province of South Africa. Due to the nature of the coal seam and the mining method in the research study area, mining operations are in constant contact with floor and roof lithologies which introduce operational challenges. To mitigate these challenges floor and roof hazard plans are used for operational planning purposes. Existing floor and roof hazard plans are deficient of both sound theoretical and procedural formality in their construction. This lack of formality in the hazard modelling was most concerning.

The research establishes a methodology for the generation of meaningful floor and roof hazard plans from empirical and theoretical applications to both interpreted and measured variables relevant to the floor and roof hazards encountered. This methodology; developed for easy operational implementation, is supported by a formal system of procedures that allow for continuous updating, validation and monitoring. The quantitative and qualitative hazard data available in the study area required bridging. For this, the author introduces the concept of applying scorecards to the hybrid data and develops the scoring logic to convert the hybrid hazard information to numeric values, usable in quantitative analyses.

The estimation software in place at NDC is limited to inverse distance weighting (IDW). The research therefore sought to determine whether the application of this classical technique would suffice for the creation of hazard plans. IDW, ordinary kriging and conditional sequential Gaussian simulation were applied to measured structural variables. The estimation results were visually compared. This would then confirm the suitability of applying IDW to the research data.

The research takes a turn when the hazard scorecard numbers become the focus of the research as opposed to the structural variables. Floor and Roof hazard scores are individually classified, respectively representing either “competent”, “moderately competent” or “incompetent” floor conditions and “normal”,” cautionary” or “high risk” roof conditions. An innovative method of defining hazard indicators sets is introduced. IDW estimation is applied to each hazard indicator set. Results are interpreted, and inflection points on the slopes of the cumulative distribution plots of the estimates are used to identify cut-off values to clearly distinguish the hazard conditions mentioned. Resulting in updated Floor Hazard and Roof Hazard Plans for NDC aligned to a formal analytical process and estimation methodology. With this in place, the research goals were accomplished through the construction and validation of reliable and easily implementable floor and roof hazard plans. Procedures for applying hazard scorecards to newly drilled boreholes and for updating the hazard models appear in the Appendices.

ACKNOWLEDGMENTS

Words cannot express my gratitude to my supervisor Prof Dohm for her challenging questions, unwavering support, constructive feedback. Through this process my knowledge, insight, and frame of reference significantly increased.

I also could not have undertaken this journey without the financial support of my sponsor, New Denmark Colliery.

I am also grateful to my colleagues in industry and in the office for their insights and thoughts. Thanks also to my line supervisor who allow me to undertake such a monumental task.

Finally, I would like to thank my family and friends for their unending encouragement and support. Your words of kindness and emotional support meant the world to me.

TABLE OF CONTENTS

LIST OF FIGURES

LIST OF TABLES

1 INTRODUCTION

New Denmark Colliery is located between Standerton and Bethal in the Mpumalanga province of South Africa. This mine is currently mining the No 4 Seam at an average depth of 189 m. The method of coal extracting includes bord and pillar mining, as well as coal pillar stooping. As an underground coal mine, NDC has a seam thickness which requires the mining height to be more or equal to the thickness of the coal seam. Due to this reality the underground operations are in constant contact with the roof and floor lithologies. Both the roof and floor lithologies possess properties which, when encountered, create operational mining challenges for the affected underground sections.

This research investigates methods to be applied to qualitative and quantitative floor and roof hazard data to generate more reliable two-dimensional (2D) hazard forecasting models, than the unsatisfactory legacy methodology currently in place at NDC. With improved hazard forecasting, geotechnical specialists and operational geologists will be able to improve Life of Mine (LOM) planning and support designs.

1.1 Research Background and Context

NDC Strata Control Officers (SCOs) and Rock Engineers review borehole data close to active or planned mining panels and request the Survey Department to amend the roof hazard plan. The roof hazard plan is then manually updated by the Survey Department. The updating of the roof hazard plan is triggered with the movement of underground mining sections into new areas. Because the plan has not been updated recently, new boreholes will not have been reviewed for the plan. In addition to not including new borehole information, the plan was constructed by students and SCOs without documenting their process.

This practice of manually updating the roof hazard plan lacks in a formal procedure or guide of how to perform the task of roof hazard identification. This shortcoming introduces risks such as human bias and room for incorrect interpretation which, in turn could result in the unintentional exclusion of relevant information in the process of producing an updated roof hazard plan. Currently the entire mining lease is divided into so called ‘good’ and ‘bad’ roof regions; an example is shown in **Figure 1** below.

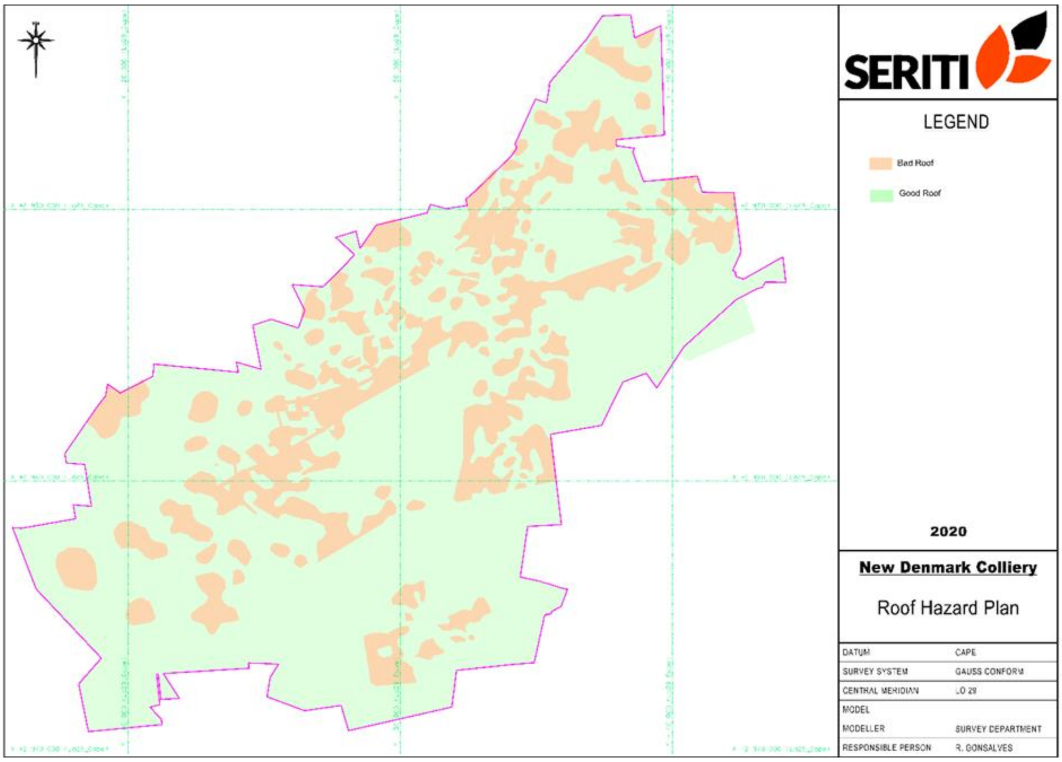

***Figure 1**: The 2020 NDC roof hazard plan.(New Denmark Colliery Mine Survey Department, 2019).*

The floor hazard planning on the other hand underwent two major initiatives in the recent past. Initially, the floor hazard plan was developed by geology interns at NDC. Concerns with the interns’ approach were raised by the resident geologists. It was suspected that the interns, due to inexperience, might have disregarded or ignored information such as the presence of geological structures or the effect of various lithologies on the competence of the floor. The 2016 floor hazard plan is presented in **Figure 2**. Furthermore, this plan was also not conducive to the addition of new information when it became available; thus, a new floor hazard plan was requisitioned in 2017.

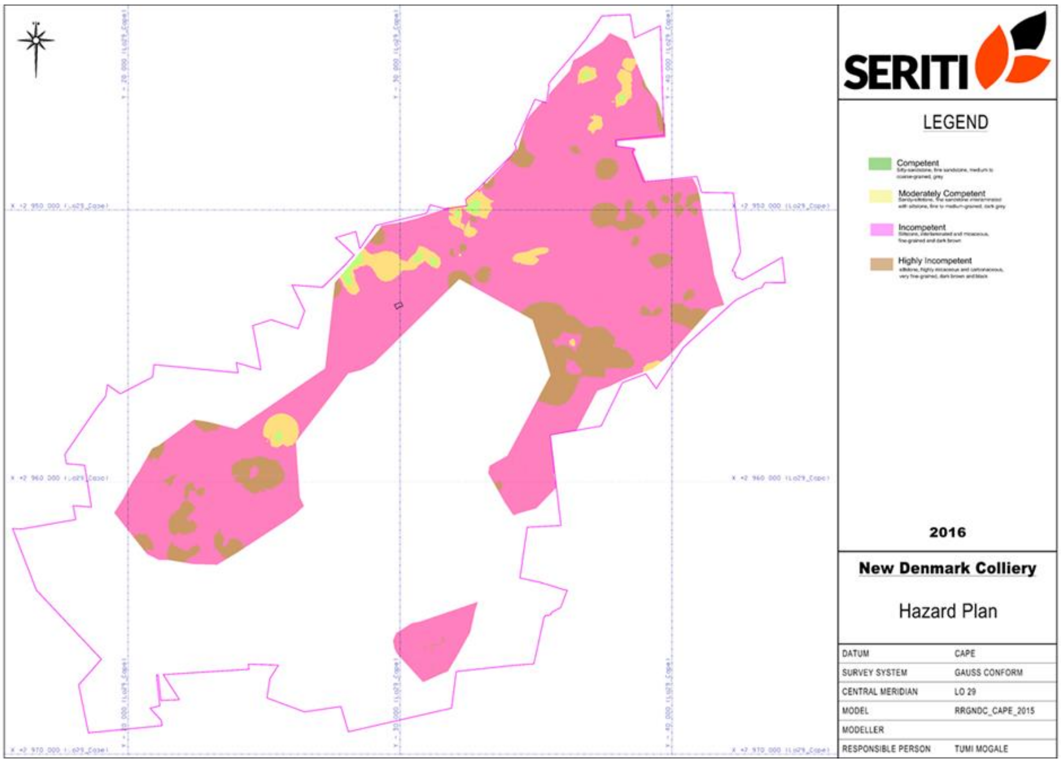

***Figure 2**: Original (2016) floor hazard plan constructed by interns at NDC (New Denmark Colliery Geology Department, 2016).*

After considering the information available on the two plans the consensus was reached that new borehole information were to be added to the 2016 plan. Visual alterations were made by resource geologists resulting in the floor hazard plan currently in use at the mine and shown in **Figure 3**. Unfortunately, the methodology applied to create the plan was not formalised or documented, again limiting future updates to conform to previous practice.

At the onset of this research, it was clear that both roof and floor hazard plans were in serious need of an update. Neither of the floor hazard plans then in existence, included relevant drilled boreholes information post 2016 and 2018, nor were these plans representative of the entire mine lease area. Moreover, a concern was expressed that the visual alterations made in 2018, may have involved different classification criteria and interpretation, which raised questions of uncertainty in the plans in use.

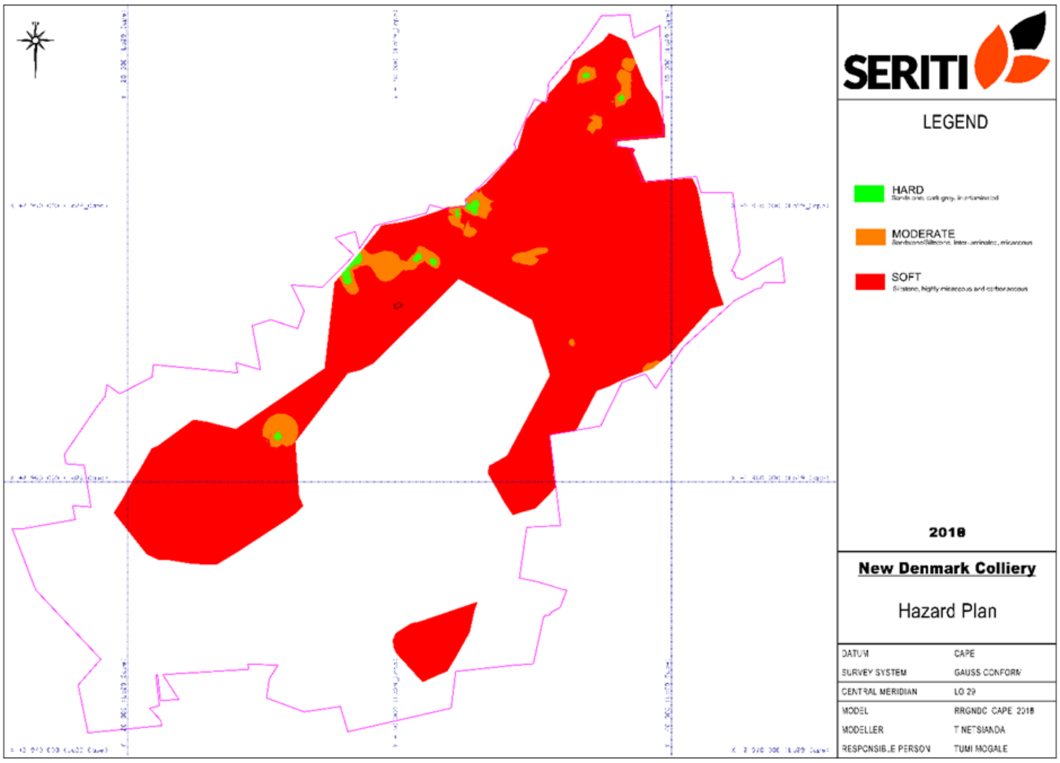

Figure 3*: Current floor hazard plan (2018) used at NDC(Anglo Coal Geological Services (ACGS) Resource Geology Department, 2018).*

1.2 Problem Statement

The above background highlights that both the current roof and floor hazard plans were deficient of solid theoretical and procedural formality in their construction. The lack of formality in the current hazard modelling is most concerning; as it is impossible to incorporate and update the models with new drilling information as it becomes available, and validation is also challenging. To appropriately manage roof and floor hazard at NDC an improved methodology for forecasting such hazards is required. The research question to address is thus: Can this research identify a practical methodology to accurately highlight and forecast the extent of floor and roof hazards for the No 4 seam at NDC?

1.3 Justification for Research

Current methodologies for the prediction of floor and roof hazards do not supply NDC with meaningful information and are unsatisfactory and outdated. If roof and floor hazard prediction can be done more efficiently, and with higher certainty, it is envisaged that this would lead to reduced operational costs, improved mining performances, and increased planning optimisation. The requirement of an option for continuous updating and validation, of these predictive models, form an integral part of this research study.

A successful research outcome would assist in predicting regions where increased contamination is expected to occur (floor hazard) and regions where additional support may be required (roof hazard). It is envisaged that more reliable contamination forecasting will lead to improved quality predictions for grade control (floor hazard), and a more informed understanding of roof hazards will lead to improved planning optimisation and a reduction in support costs with improved support design. These improvements in understanding would then lead to increased trust in operational commitments and mining performance indicators.

1.4 Research Objectives

The objective of this research was to investigate whether a meaningful floor and roof hazard plan models for NDC could be generated and if systems for continuous monitoring, updating, and validating of the plans could be developed for easy operational implementation. Having such a Coal Resource Management tool would improve planning optimisation and reduce costs, which would lead to increased trust in operational commitments and performance indicators.

1.5 Research Approach

The research is empirical in nature and the research study approach was split into three phases. The research approach is described in the following paragraphs. The first phase included the creation of floor and roof hazard scorecards based on the identification of hazardous roof and floor properties from hybrid data types; qualitative (interpreted) and quantitative (measured) attributes associated with a borehole. To convert the hybrid data types, algorithms were developed to distinguish hazard categories and generate individual floor hazard and roof hazard indexes for each borehole. This was done to facilitate mathematical operations and analyses in the next phases of the research. The second phase was to establish whether inverse distance weighting (IDW) can be used as a substitute for geostatistical estimation techniques such as kriging and conditional simulation, in the spatial modelling of hazardous floor and roof occurrences; NDC only has access to IDW estimation software. In phase three the knowledge from phases one and two were combined to produce a method that would meet the research study objectives. This method would be easily reproducible and documented for future roof and floor hazard assessment.

1.6 Sources of Data

The research study is reliant on a database with structural and hazard-specific information that was extracted and constructed from the vast NDC geological information repository. All boreholes that inform on floor and roof hazard identification are considered. The research source data thus includes boreholes beyond the mine boundary; the hazards are geospatial in nature and are not limited by surface mine boundaries. The research data for was obtained from the NDC vertical borehole database and includes structural properties such as roof and floor lithology, presence, and extent of geological structures. The data for the research study is captured in the Cape Lo29 Coordinate system within a Northing range of -2 940 000 m to -2 970 000 m, and Easting range of 15 000 m to 45 000 m (30 km x 30 km). Relevant structural variables such as coal seam thickness, coal seam depth and coal seam floor elevation were also extracted.

1.7 Research Methodology

A broad outline of the research methodology applied in the research is highlighted in this section. The two objectives; developing scorecards for the floor and roof hazard and then establishing whether IDW could be used as a proxy methodology for OK. Successful achievement of these objectives would finally result in a practical methodology for floor and roof hazard risk management maps at NDC. The methodology followed is largely a function of the mixture of qualitative and quantitative floor and roof hazard data and qualitative measured geological structural variables. Both data types will be used to generate a combined quantitative dataset to be used in numerical analyses.

Development of a scorecard procedure for converting qualitative and quantitative floor and roof hazard data to numeric scorecard risk indexes for the two individual hazards were the initial focus in the research. Followed by the application of analytical techniques to achieve the second objective of this research study.

1.7.1 Qualitative research

The qualitative properties inform on the severity of the hazardousness of the roof and floor strata within the underground coal mine. These properties are used to guide and provide recommendations to underground section managers assisting them to plan for operational delays due to hazardous ground. Qualitative rock properties such as lithology, sedimentary structure and devolatilised/burnt coal are recognised as properties of interest with regards to the hazardousness. The qualitative data with some quantitative data are considered via the scorecard system developed by the author in alignment with the first phase in the research approach. The development and creation of the scorecard indexes for floor and roof hazard data is detailed in Chapter 4

1.7.2 Quantitative research

Quantitative data that inform on hazardousness, are bed thicknesses and sill proximity, as well as structural variables, such as seam thickness, seam floor elevation and seam floor depth. Quantitative and qualitative data that inform on hazardousness are included in the generation of both roof and floor scorecard indexes. These numerical values, reflect the severity of the individual hazards, and are used in the scorecards for further quantitative analysis.

1.7.3 Analytical research

Extraction of relevant research data from the NDC geological data repository was followed by a validation process that included both logical and analytical assessments. Relevant statistical assessments were carried out on both discrete (hazard indexes) and continuous data (measured structural) variables. Quantitative and qualitative data of all the variables considered were subjected to the same analytical processes outlined below and discussed in Chapter 3.

The analytical process applied to the scorecard results (discrete data) and the continuous measured structural data is listed below.

- Exploratory Data Analysis (EDA)
- Visual presentation an interpretation of results
- Inverse Distance Weighting Squared (IDW2) estimation
- Ordinary Kriging (OK) estimation
- Comparison of spatial outcomes and interpretation
- Conditional Sequential Gaussian Simulation (CSGS) and Conditional Sequential Indicator Simulation (CSIS) as relevant
- Comparison of result with previous outcomes and interpretation.

1.8 Research Validation

This research study mainly concerns the comparison between the IDW2 models and Geostatistical models of the hazard data. The need for the IDW technique is a direct consequence of the nonexistence of geostatistical software at NDC, a limitation highlighted earlier. Drawing IDW2 estimation plans in parallel with the geostatistical estimation plans allows for visual comparisons. If the visual IDW2 estimation plots reasonably compare with the OK estimation plots a conclusion can be drawn that IDW2 can be used as a proxy for the estimation of spatial variables being estimated.

1.9 Structure of the Research Report

This research study consists of six chapters. Chapter 1 is the introduction and covers the background of the research topic, the problem statement, the justification for the research, and the research objectives. The research methodologies followed by this study and the sources of the information are introduced. The research validation criteria, as well as the contribution to knowledge in the form of scoring hazards and comparing the IDW2 estimates with Geostatistical methods, are considered.

Chapter 2 outlines the literature review which establishes an academic frame of reference for the methods used in the research. The literature review firstly concentrates on establishing an understanding of the geological setting and the lithological challenges which create hazardous environments underground. Followed by literature reviews focussing on the concept of using scorecards for establishing confidence, and finally geostatistical methodologies relevant to the research namely kriging and simulation.

Chapter 3 presents the process and methodology undertaken in this research. The process of constructing usable numerical values from the borehole data with the use of scorecards is detailed. Also, the data analysis and various estimation techniques used to generate estimation maps for comparison and correlation purposes.

Chapter 4 describes the process that was undertaken to collect floor and roof hazard data and construct the database for the research. The scorecard process developed is detailed and a summary of the research data is presented.

Chapter 5 contains the analysis and findings of the research. The kriging and simulation of structural variables with their spatial correspondence to the hazard data is presented and discussed. This is followed by the indicator interpolation and geostatistical evaluation of the hazard data. Finally, the construction of floor and roof hazard plans are presented.

Chapter 6 details the concluding remarks and recommendations of this research study. The key learning from the results and discussion after the applied methodology are summarised. The achievement of the objective is stated and future work is noted. The recommendation is a high-level summary of future work to be carried out as a consequence of this research study.

2 LITERATURE REVIEW

It was envisaged that a deeper understanding three technical fields would lead to the development of a relevant floor and roof risk assessment methodology that would be reliable, straight forward, updatable and within the software knowledge and skills available at NDC. With this vision in mind, the extensive literature review, carried out in preparation of the research study is summarised in this chapter. Commencing with a background to coal mining and specific coal geology. Followed by a literature review of scorecard approaches relevant to turning a combination of qualitative and qualitative information into quantitative data that can be subjected to numerical analyses. Concluding with a review of some geostatistical estimation and simulation applications, and uncertainty assessments of geospatially correlated data.

2.1 Coal Mining Background and Geology

Coal is an important resource for the South African economy and has been since its discovery in Witbank in the 1800s (Jeffrey *et al.*, 2015). Currently, there is an international sentiment that coal, as a thermal product, has no future. However, experts suggest that coal will remain part of human lives regardless of the pressure from developed nations for the move to green energy (Mineral Council South Africa, 2020).

Due to coal's long period of exploitation in South Africa (RSA), logic dictates that most of the higher quality and easily accessible coal reserves have been extracted. '*Easily extractible resources are depleted*' is however a subjective statement but easily explains why many mining operations are investigating the extraction of previously undesirable coal resources (De Korte, 2015).

The cost of coal extraction in RSA has seen a general increase which can be partly attributed to the increased exploitation of these previously undesirable coal reserves (Snyman & Botha, 1993). This general increase has created a cost-cutting culture as other developing nations can sell their coal at a cheaper rate which in turn undermines the RSA coal mining sector.

Increased cost and mining difficulties have raised concerns regarding the viability of coal extraction. Many projects factor in the most cost-effective way of extraction to allow for a profitable venture. Combining proven multidisciplinary techniques to achieve such goals is thus the order of the day.

Coal deposits are present over a large area of South Africa, the distribution of the coal deposits and their respective coalfield divisions are highlighted in **Figure 4** (Jeffrey, 2005). This map highlights the subdivision of the coal hosting deposits into coal regions, introduced for sake of geographical and structural simplification (Hancox & Götz, 2014). Most of the coal in South Africa is hosted within the Karoo Supergroup which was deposited in the shallower waters of the Karoo Basin (Cairncross & Cadle, 1991).

After the deposition of the Karoo sediments, the supercontinent broke up and resulted in hypabyssal intrusions (Snyman, 1991). These intrusions (dolerite dykes and sills) altered, crosscut and displaced the coal seams as a result (Snyman & Botha, 1993). Burning of coal due to the inherent heat of the intrusions, as well as the adverse ground condition (sympathetic structures like faults) are challenges that significantly increase the difficulty of coal's economic extraction (Poonam *et al.*, 2017).

The study area for the research falls within the Highveld Coalfield which is south of the Witbank Coalfield. The Highveld Coalfield is similar in stratigraphy, however, the two coalfields are separated by the Smithfield Ridge which is a region between the coalfields where no coal exists (Falcon, 1986). In the southern part of the Highveld Coalfield the lower two-seam present in the Witbank Coalfield, that is, No 1 and No 2 Seams, are absent (Jeffrey, 2005).

More specifically the research area is located within the southern portion of the Highveld Coalfield where only the No 4 Seam is economically extracted. The No. 4 Seam was deposited after the No 3 Seam and is commonly interlaminated by sediments ranging from laminated shales to poorly sorted gritstones (Hagelskamp *et al.*, 1988).

The No 4 Seam and No 3 Seam are separated by an interburden (floor rock) that ranges from a few centimetres to several metres thick. This parting consists of micaceous, fine-grained sandstone with cross-bedding and horizontal laminations (Jeffrey, 2005). The floor rocks of the No. 4 Seam is thus the upper portion of an upward finning sequence, which mainly comprise of shales and siltstones

(Hagelskamp *et al.*, 1988). The No. 4 Seam is overlain (roof rock) by coarse gritty material which suggests the depositional environment present after coal deposition exhibited channel erosion associated with rapid -high energy fluvial sedimentation, suggesting channel switching.

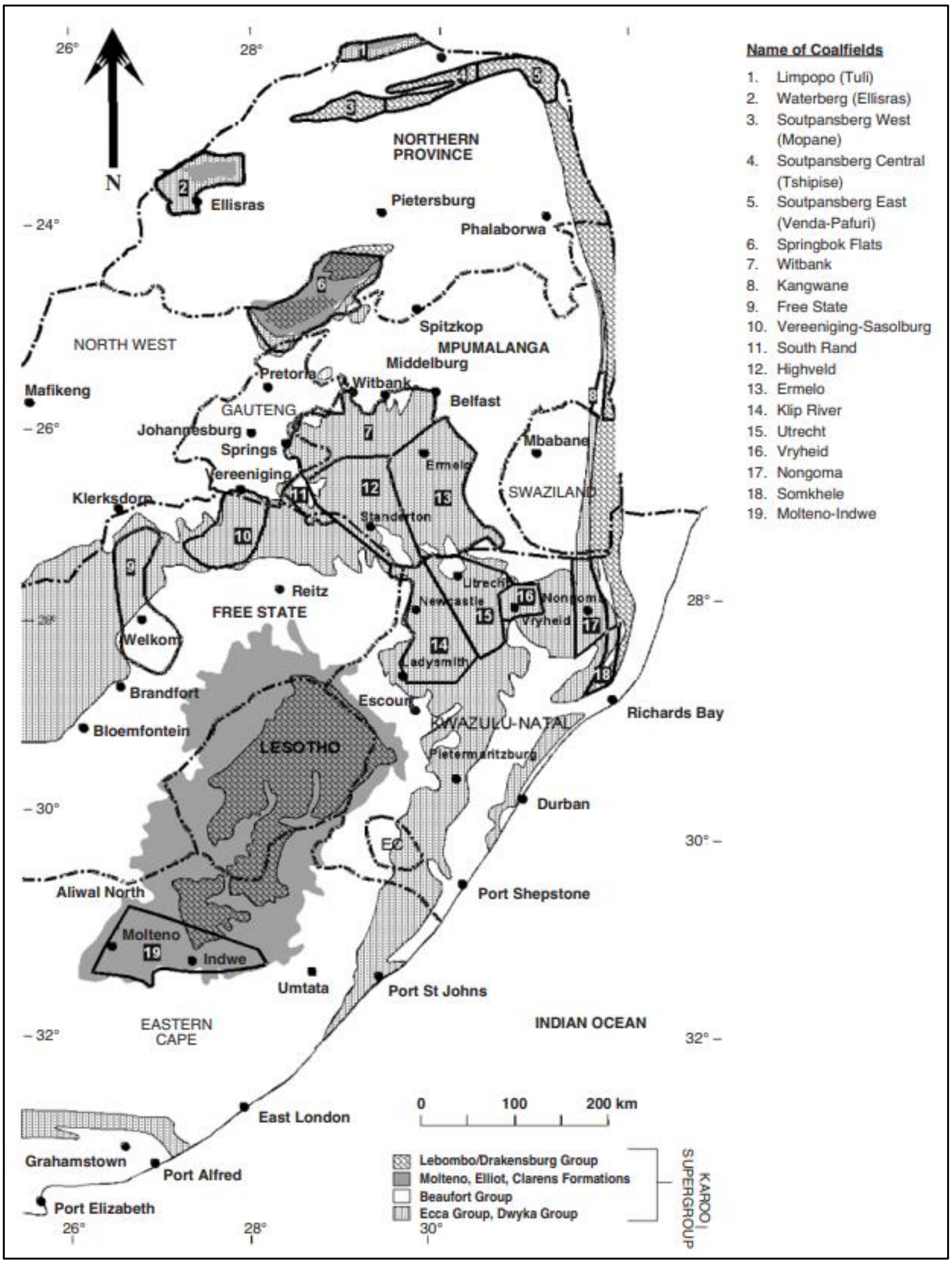

***Figure 4**: Distribution of coal deposits in South Africa and their respective coalfield divisions(Jeffrey, 2005).*

The Sasol Bosjiespruit – Twisdraai resources are located to the North-North-East (NNE) of the study. According to Hagelskamp (1987) a graben structure is present which downthrows the local coal seams, including those in the research study area, from the greater Highveld Coalfield. An approximately 80 m transgressive sill also forms part of the downthrown stratigraphy which resulted in additional structural complexity. Additionally, igneous intrusions resulted in areas where the coal was burnt beyond economic extraction and are linked to increased groundwater penetration due to the influence on the surrounding host rocks (Jeffrey, 2005).

2.2 Scorecard Methodologies and Applications

At this stage NDC does not have a reliable or documented method of identifying hazardous floor and roof ground. The current process involves the physical evaluation of borehole logs for the boreholes drilled in an underground panel. Multiple quantitative and qualitative attributes are evaluated, and a decision on hazardousness is made. The decision process is not documented or auditable which most likely introduced bias and unknown assumptions into play. For this reason, a documented and structured method is required to formally combine the various lithological and structural attributes into numeral data. The method identified as most suitable for this process is a scorecard approach. Knowledge, insight and understanding on the generation and application of scorecards gleaned from the literature review is summarised in this subsection.

In this research two types of hazard data, quantitative and qualitative, are to be combined for numerical analysis. Despite a difference in data type the scorecard methodology can be applied to the quantitative and qualitative hazard attributes and will allow for an overall scorecard value which can be used in a numerical analysis.

A balanced scorecard is a business tool that was created by Kaplan and Norton (1992) for organisations to measure performance with the use of a more balanced collection of performance measures (Dearlove & Crainer, 2011). The balanced scorecard has been deemed a game-changer as it allowed multi-measurable factors to be combined to give an overall ‘measure’ of success.

One of the first Mineral Resource sectors to employ a scorecard methodology was the De Beers Group. Diamond deposits are known for being geologically complex which results in significant difficulty in estimating and controlling grades (Grills *et al.*, 2017). Therefore, Diamond Resource evaluation and classification are challenging. De Beers noted this difficulty and invested significantly into developing a method for identifying and scoring elements of uncertainty during Mineral Resource Classification. Their result was a 'best practice Mineral Resource Classification System (MRCS) within DeBeers'. The MRCS involved the development of a scorecard consisting of key questions and possible ranges of answers for the different elements. The outline of the scorecard was important and included all relevant measures and their possible outcomes were required to be logical, provide a meaningful result on the associated confidence for the different elements (Grills *et al.*, 2017).

Parker and Dohm (2014) noted that the use of scorecards for Mineral Resource classification enhances transparency and understanding in Public Reports. This level of transparency is directly related to the general outline and type of scorecard used. These scorecards consider factors assumed relevant, in any unique Mineral Resource evaluation and classification process. Weights are assigned to different factors depending on their importance in the resource estimation. These factor weights are then combined to produce an assigned confidence rating resulting in a discrete score which would inform on Inferred, Indicated and Measured Resource classifications.

Rock engineering also use scorecards for rock competence classification purposes. Rock Mass Rating (RMR) systems are widely used and are of prime importance in the development of techniques for the control of rock masses (Aksoy, 2008). Some of the methods for the development of a site-specific rock mass scoring system will be tested in this research as the importance of one identified hazard cannot be placed ahead of another. The general conditions for the development of such a scoring system in a mine setting are described by Laubscher (1990).

Requirements for a scorecard are that it should be straightforward and possess a strong affinity toward the geological properties. The scoring should allow for all possible variations and colour should be used to illustrate differences in classes on plans and sections. The accuracy of the classification depends on the sampling in the area as well as scorecard validation on sampling coverage. The final classification should be accompanied by good guidelines for a mine (Laubscher, 1990).

2.3 Geostatistical Estimation

Geostatistics deals with the calculation of values in a probability topography, generated from known samples gathered from an orebody that is geographically distributed. This probability topography or 'topo-probabilistic', idea was originally introduced by Krige (1951) and supported by the work of Sichel (1947), however, it was not formally termed at the time. This 'idea' was later referred to as the Random Function (RF) (Matérn, 1987) and later coined by Matheron (1962) as 'Geostatistics'.

Early on, the uniqueness of ore bodies resulted in research regarding the applicability of random functions. Reconstructing the probability distribution of ore bodies are never possible without certain assumptions that usually do not hold in practice. However, later research suggested that the assumed intrinsic random function of an orebody would fulfil the requirements to generate estimates. Thus, variograms (intrinsic RFs) were used rather than covariances (Stationary RFs) (Matheron & Kleingeld, 1987).

Classical statistics assume that all sample data reflect a normal distribution of a population and that all samples are spatially independent of one another. In geostatistics, the underlying geological information is used to interlink sample data. The interlinked data's probability distribution can be skewed, and the data could possess spatial correlation. Taking this into consideration geostatistical methods can be used in two ways, estimation and simulation (Zhange, 2011).

Kriging estimation refers to the calculation and generation of a 'best' estimate (map) and focuses on the minimisation of estimation errors. This method takes into consideration the variogram of the sample data as well as the modelled spatial correlation of the sample data. Due to its reliance on the determination of the most accurate spatial correlation different estimators with the same data can produce different estimates. The kriging techniques consist of three variants, namely simple kriging (SK), ordinary kriging (OK) and universal kriging (Ma, 2019).

OK, and IDW, are both linear estimates in that they are a weighted sum of Regionalised Variable (RV) values. The RV is the weight assigned to a conditioning value when estimating an unknown point. For IDW this weight is calculated by inversing the distance between the known points and the point being estimated. However, an OK estimate is the function of a RV, or variogram model (γ(h)), that captures the spatial variability of the variable as a function of distance and direction (h). This function was laid out by George Matheron in his work *The Theory of Regionalised Variables* in the 1960s.

Clark and Harper (2000) noted that the estimate should be accompanied by confidence. The OK method optimises the weights of the known points which are used to estimate an unknown point to minimise the estimation error. This error is referred to the Kriging Variance (KV). Compared to IDW estimation, the OK estimation process distances between the known points and the point to be estimated and the distances between all the known points used in the estimation are considered.

Simulation assumes that variances will exist in possible variograms and so focuses on the reproduction of heterogeneities of geospatial properties of variables. Multiple varying estimates are generated allowing the level of uncertainty to be assessed and heterogeneity to be highlighted. Commonly used simulation techniques are conditional and unconditional sequential Gaussian simulation and domain frequency or spectral simulation (Ma, 2019).

Lam (1983) summarised spatial interpolation as the interpolation of point data and areal data. Further subdivisions under these two categories (estimation and simulation) classify geostatistical techniques as presented below in **Figure 5**. The point interpolation methodologies listed in **Figure 5** were grouped into ‘exact’ and ‘approximate’ by Wren (1973). The ‘exact’ methodology refers to the preservation of the original sample data within the generated surface, whereas the ‘approximate’ approach does not preserve these points. Exact methodologies will most accurately fulfil the purposes of this research.

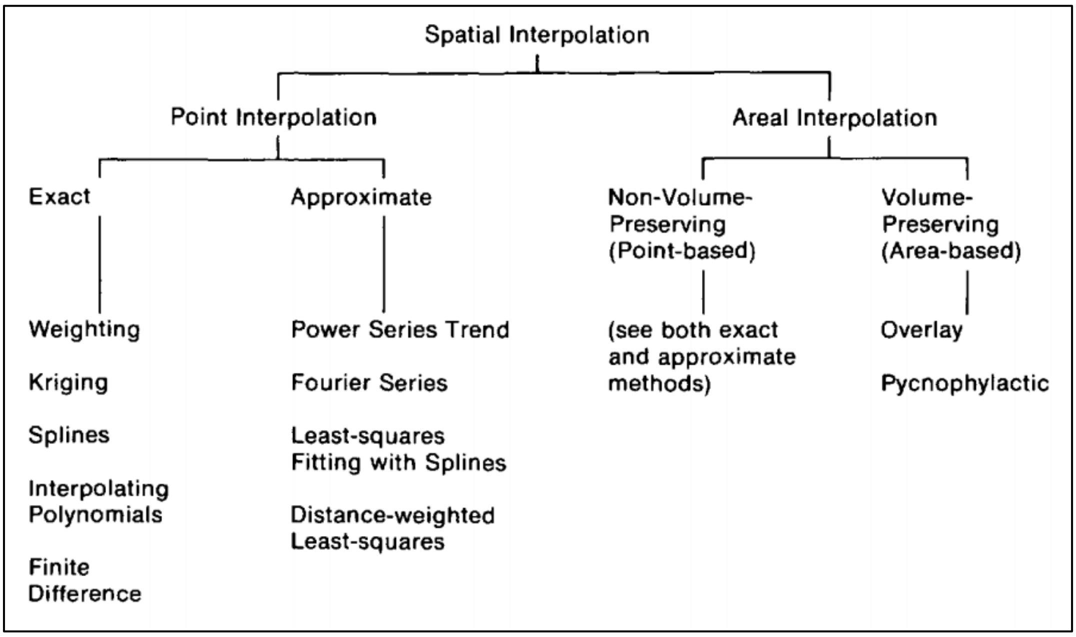

***Figure 5**: The division of geostatistical techniques for certain spatial interpolation methods (Lam, 1983).*

Zhange (2011) notes that the ultimate goal of geostatistical methods is forecasting through spatial distribution which usually takes the form of a group of maps or plans. The process for mapping with the use of Geostatistics can be restated as spatial interpolation. With the assistance of geostatistical techniques, spatial interpolation deals with the generation of a surface that will best predict values at a certain location (Atkinson & Lloyd, 2009).

In coal deposits, due to its simplicity and speed, inverse distance weighting (IDW) is the most common spatial interpolation method used (Maxwell, 2020). IDW is a geostatistical technique where a sample weight is the inverse of the distance between the known sample points and the location to be estimated (Abzalov, 2016).

The IDW estimation methodology is based on the geometry between samples and is independent of the spatial correlation between the samples. Many geological modelling software packages also include IDW as an estimation option. Despite being the most popular method of estimation in coal mining, IDW is not necessarily the most accurate. As more informative results are desired, and the fact that qualitative rock properties are being modelled, application of a sound method will aid in establishing whether the proposed roof and floor hazard models are robust.

2.4 Geostatistical Simulation

Geostatistical conditional simulation methods for both continuous and discrete variables are applied in this research. The R package ”gstat” is used to conduct the conditional sequential simulations. In conditional sequential simulations the input data is used to sequentially simulate continuous or discrete, values at unknown nodes of a grid from the known data following a random path on the grid. Simulated node values become part of part of the “known”’ data base (conditioning the simulation) as the simulation progresses until all nodes on the grid has been simulated. Every complete simulation is considered a realisation and, if multiple simulations are run, there will be multiple realisations for each node and for the deposit.

Simulation allows for the evaluation of joint uncertainty (accuracy) at multiple locations and provides a more realistic picture of natural complexity and heterogeneity relative to kriging (Chiles & Delfiner, 1999). The simulation can also provide an idea of “best,” “most likely” and “worst” cases for a given problem-bounding case.

To assess the robustness of the models generated multiple interpolation and geostatistical methods have been considered in the research. As the method for generating these models on the mine will most likely be IDW, geostatistical methods evaluated would be used to evaluate the validity of the IDW estimation by comparing it to the Geostatical models which have accompanying certainty.

3 RESEARCH APPROACH

To achieve the objectives of this research a structured research design was followed. As stated in the introduction the objectives of this research were to investigate and determine whether meaningful floor and roof hazard plan can be generated and if a system can be developed and implemented for cyclic updating of the plans without laborious geostatistical methods.

NDC uses inverse distance weighting squared (IDW2) estimation thus there is no quantitative measure of variability or certainty in the plans. This situation creates a challenge as confidence in hazard prediction needs to be justified, as it will inform on decisions and actions of recommendation which could affect the operation of the mine as well as the safety of the employees. With the geostatistical methods it is possible to obtain confidence in the estimates and confidence through the probability derived from simulation models.

Comparing the results of the geostatistical model to that of the IDW2 plot will be integral to confirm successful achievement. The comparison will allow for the measure of confidence in the IDW2 model. If comparisons can be drawn between the geostatistical models and IDW2 estimation meaningfulness can then be attributed to the IDW2 model.

The research study includes the collection and validation of relevant data, estimation, and simulation of variables and finally the comparison of geostatistical and interpolation models. The research methodology followed against this background is outlined in the subsections below.

3.1 Data Source and Software

Due to the fact that both quantitative and qualitative data are required for this research the full lithological log and collar files for each borehole were required. To preserve confidentiality of information, only the borehole information necessary for the research were extracted from the NDC geological data repository and compiled in a database relevant to this research study.

The data selected for the research database included borehole ID, coordinates, and topographical elevation. From the physical logs the structural variables: seam quality and bed thicknesses were extracted. Considering the type of information used to assess the hazardousness of floor and roof lithologies, it was deemed most appropriate to score the observed hazard information at each borehole location with the use of a scorecard. The scoring method developed distinguishes between the severity levels of the individual hazards according to some rules applied. The resulting categorical numerical values or hazard indexes which are used to generate hazard models.

Two scorecards were created during this research, one for the floor and one for the roof. These scorecards are based on hazardous properties associated with floor and roof conditions at NDC. Scoring of vertical boreholes required the identification of hazardous floor and roof properties from the quantitative and qualitative data extracted from the NDC vertical borehole database. These hazardous properties were converted from their hybrid state with the use of algorithms developed by the author to score the floor and the roof. The numerical scores, or hazard indexes, formed the basis for the research study as they would facilitate mathematical operations and analyses.

The quantitative and qualitative data which informed on the scorecards were not included in the data export, however, the results of the scorecard variables were extracted. In other words, if a floor of a specific borehole had a thick and massive sandstone its scorecard qualifier result would be ’Competent’. This scorecard qualifier results were included in the research dataset and not the detailed log description.

For a borehole’s hazard data to be included in the database all information pertaining to the hazard qualifiers needed to be present in the research database. For example, in old boreholes where the roof and floor lithology were not captured in detail, the boreholes were disqualified for use in this research.

The scorecards outcomes for each hazard were analysed and reviewed, resulting in a reduction in hazard categories or Hazard Index Numbers (HIN) from nine to three, Hazard Index Classification (HIC), reflecting classes of hazard severity.

To evaluate the data multiple software packages were considered however, the statistical and data visualisation software R (R Core Team, 2022) was chosen. As R is a multi-developer and community collaboration environment not all preloaded functions could be used to evaluate the data for this research. Thus, additional software packages were considered, the main software packages used are:

- gstat (Gräler *et al.*, 2016)
- mstats (Trueman, 2019)
- sp (Bivand *et al.*, 2013)
- tidyverse (Wickham *et al.*, 2019)
- gridExtra (Auguie, 2017)
- ggplot2 (Wickham, 2016)
- ggspatial (Dunnington, 2023)
- ggpmisc (Aphalo, 2023)
- ggpubr (Kassambara, 2023)
- ggvoronoi (Garrett *et al.*, 2022)
- paletteer (Hvitfeldt, 2021)

3.2 Estimation and Simulation Methodology

From the data extracted from the NDC repository there is a clear distinction between the structural variables (seam thickness, floor elevation and seam depth) and the floor and roof hazard data. This distinction between data types is attributed to the fact that the hazard data of some of the boreholes were excluded as mentioned above.

As the structural dataset is more abundant than the hazard dataset, the first step was to compare the structural variables with the hazard data. This comparison included correlation plots and visual spatial comparisons between hazard data and structural data estimates and simulations in attempt to inform on spatial domaining of NDC floor and roof hazards.

The structural variable comparison stage included the following:

- Exploratory Data Analysis (EDA) of the roof and floor HIN.
- Voronoi Diagrams of the roof and floor hazard data.
- EDA of the structural variables.
- Correlation comparison of the structural data with the HIN and HIC.
- Structural data variography (experimental variograms, varmaps, and variogram models).
- IDW2 and OK estimation of structural variables at a 25 m x 25 m block size
- NSCORE transformation of the structural variables.
- NSCORE variography (NSCORE varmaps, experimental variograms and variogram models) on the structural data.
- Conditional Sequential Gaussian Simulation (CSGS) on the structural data at a 25 m x 25 m block size.
- Back transformation of the structural NSCORE data.
- E-type estimate plans of structural data for comparisons to hazard estimate models.

These steps allowed for the identification of possible hazard domaining based on the results of the structural data estimates and simulation. Form this a comparison between the IDW2 models and Geostatistical models was established.

After the structural variable comparisons with the hazard classes, it was noted that it could be advantageous to also evaluate the hazard data sets on their own. For this evaluation the floor and roof hazard classes were converted into 0-1 indicators. The 0-1 indicators were then evaluated using indicator estimation and simulation techniques.

The indicator evaluation stage included the following:

- Conversion of the HIC dataset into two 1-0 data sets. Here the HICs of the floor and roof are compared to one another, i.e., the good floor/roof is compared to the moderate to poor floor/roof and the good and moderate floor/roof are compared to the poor floor/roof. This resulted in 4 new data sets to be analysed, two for each hazard.

- EDA of the HIC indicator data.
- HIC indicator variography (varmaps, experimental variograms and variogram models)
- Estimation (IDW2 and OK) of the HIC indicator.
- Standardisation of HIC indicator variogram
- CSIS of the HIC indicator.
- Probability calculations and probability plots for comparisons to estimate models.
- Combination of simulated probability plots of the 2 respective indicator data sets for each of the floor and roof HIC. This will be the generation of the simulated floor and roof hazard plan.
- IDW2 estimate of the HIC data. If indicator probabilities are chosen in line with the comparative estimate plans the IDW2 hazard plans should be comparable to the simulated hazard plan.

At the onset of this research, it was envisaged that a methodology could be developed to identify areas where the hazard index is high, together with a measure of certainty associated with the index. For this to be achieved, simulation was the route to be explored (the method of choice), or more specifically CSIS.

The research approach outlined here has been designed to evaluate the available data in a manner which will result in the most meaningful results. The combination of qualitative data collection and incorporation with quantitative data is innovative for NDC and will result in meaningful numerical data. The numerical data will then be geostatistically evaluated and the standard interpolation method proposed, to be used at NDC, is expected to give meaning to updated roof and floor hazard maps.

4 HAZARD SCORECARD DEVELOPMENT

The data for the research comprise of quantitative measurements and qualitative observations. To achieve the objective of the research, it was firstly important to convert the qualitative data into meaningful quantitative values. All subsequent analyses hinge on the success thereof. The resulting numeric values are used in the geospatial analyses presented in Chapter 5.

In **Table 1** the number of boreholes within the study area, as well as the number of boreholes extracted with relevant information necessary for the research are shown. Discrepancies in the numbers are mainly due to the fact that many boreholes drilled in the past were only drilled for structural data such as coal thickness, coal depth, coal qualities, etc. Therefore, many of these older borehole records do not contain detailed lithological loggings (logs).

Table 1*: Number of boreholes used in the research.*

	Number of boreholes
Total number of boreholes	3 290
Number of boreholes used for floor hazard	1 919
Number of boreholes used for roof hazard	1 414

4.1 Floor Hazard Data

The qualitative data comprises of lithological qualifiers from the geological database for qualifying boreholes drilled within the study area. These qualifiers are used by mine geologists to predict whether underground sections are expected to experience poor floor conditions.

For the No 4 Seam, the floor qualifiers are lithology sedimentary structure (bedding), and signs of coal devolatilization/burning. In some instances, quantitative data has been used to explain poor floor conditions, and thus, certain quantitative data was also extracted for the No 4 Seam which included the dolerite sill proximity, coal seam thickness, coal seam floor elevation and borehole collar elevation.

During this research the author developed a floor hazard scorecard method and logic to assess each individual borehole not only for the complete competency of the floor but also individual competencies of the different floor hazard qualifiers (rock type, strata bedding and geological structures). The scorecard is designed in a table or matrix format consisting of rows (hazard qualifiers) and columns (floor competency levels). The four floor hazard qualifiers considered are Composition, Bedding, Structural Proximity and Coal Seam Devolatilisation. The three qualitative floor competencies considered are Competent, Moderately Competent and Incompetent.

The logic of scoring the floor competency for a borehole is as follows, each of the floor hazard qualifiers (rows) are considered in turn and a competency identifier ("X") is placed in the appropriate informed floor competency column for each qualifier. Once all the floor hazard qualifiers have been considered the number of 'X' occurrences in each competency column are totalled and the scoring can take place.

The scorecard is designed to assign the worst-case competency scenario to a borehole. In other words, if one qualifier is regarded as incompetent the borehole has to be incompetent in terms of the coal seam floor. Allocating a floor hazard score or floor hazard index number (FHIN) for any borehole in the database is based on the following logic:

- ✓ If all floor hazard qualifies are ***competent*** the borehole is allocated FHIN value of one
- ✓ If one of the floor hazard qualifiers are in the ***moderately competent*** column the FHIN will increase to two. The FHIN will increase by one for every additional qualifier that is classified as moderately competent. Thus. if all four qualifiers are classified as moderately competent the FHIN would be five.
- ✓ If one floor hazard qualifier is ***incompetent*** the borehole floor is deemed to be incompetent floor and is allocated a FHIN value of six, irrespective of where the other qualifiers rank (competent or moderately competent). The count for incompetent will increase by one for every qualifier that is classified as incompetent. If all qualifiers are classified as incompetent the borehole will have a FHIN value of nine.

The algorithm for applying this logic to produce a FHIN for any qualifying borehole in the database is:

```
if (count(Number of "X's" in the Incompetent column)>0) {
        count(Number of "X's" in the Incompetent column) + 5
        } else if (count(Number of "X's" in the Moderately competent column)>0) {
                count(Number of "X's" in the Moderately competent column) + 1
                } else {
                1
                }
```

This method of scoring the competency of the floor always considers the worst-case scenario for the competency of the floor. This is important as encountering for example a carbonaceous floor will be hazardous for a section even if all other qualifiers are competent. This method of assessing the hazard qualifiers will result in nine potential categories for a FHIN to fall within.

The principle of the scorecard is to generate a meaningful number, or index, to represent the qualitative floor competency category of a borehole. **Figure 6** below illustrates a dummy borehole being scored with the floor hazard scorecard.

In **Figure 6** “X” indicates an identified floor hazard qualifier in the competency columns of the scorecard. Based on the above algorithm, two qualifiers are in the Incompetent column and the first “IF” statement of the algorithm is true and the FHIN is thus two plus five resulting in the FHIN of seven, in the box on righthand side of the scorecard.

New Denmark Colliery

Floor Hazard Scorecard

			Competent (3)	Moderately Competent (2)	Incompetent (1)
Composition *Composition refers the facies of the rock - Mudstone, shale, sandstone, siltstone, etc.			Gritstone to Coarse grained Sandstone C-factor: **5.8 - 5.7**	Sandstone, Medium grained siltstone, Sandstone/Siltstone C-factor: **5.6 - 5.4**	Carbonaceous mudstone, shale, fine grained siltstone C-factor: **5.4 - 5.2**
					X
Bedding *Bedding refers to the depositional layering or lack of layering - laminated, beds, massive, etc			Massive	Interbedded	Laminated, Interbedded & interlaminated
					X
Geological Structures	**Structure Proximity** *Intrusions and other stress related structures can influence the structural rigidity of the floor.	**Sill**	>5m	5m - 1m	<1m
				X	
	Devolatilisation *Devolatilisation/burning occur when heat from igneous intrusions alter the host rock. This heat can alter the matrix in the floor rock and thus can degrade the floor conditions.		No Evidence	Devolatilised coal on floor rock	Burnt coal on floor rock
			X		

InC2
7

***Figure 6**: Floor Hazard Scorecard an example.*

The FHIN bar chart in **Figure 7** highlights that the majority of the FHINs fall within FHIN 2 (~33%) representing boreholes with all but one floor hazard qualifier in the competent floor column and within FHIN 6 (~46%) reflecting the boreholes with one floor hazard qualifier within the incompetent column, The FHIN locations appear in **Figure 8** and spatially the dominance of FHIN 2 and 6 is also clear.

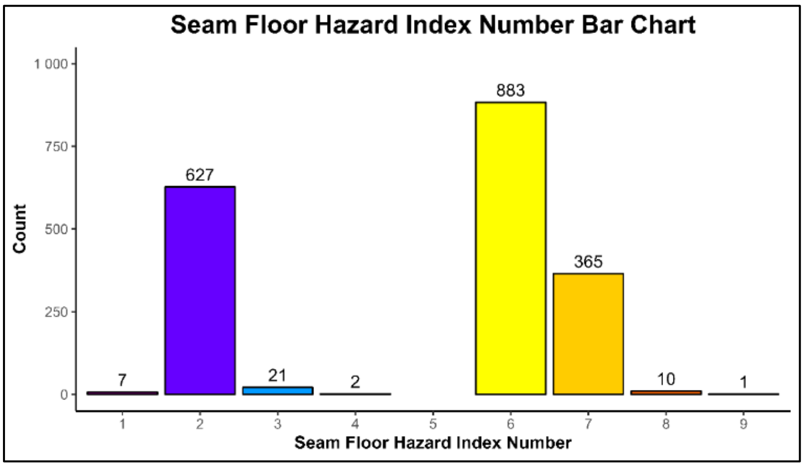

***Figure 7**: Floor Hazard Index Number Bar Chart*

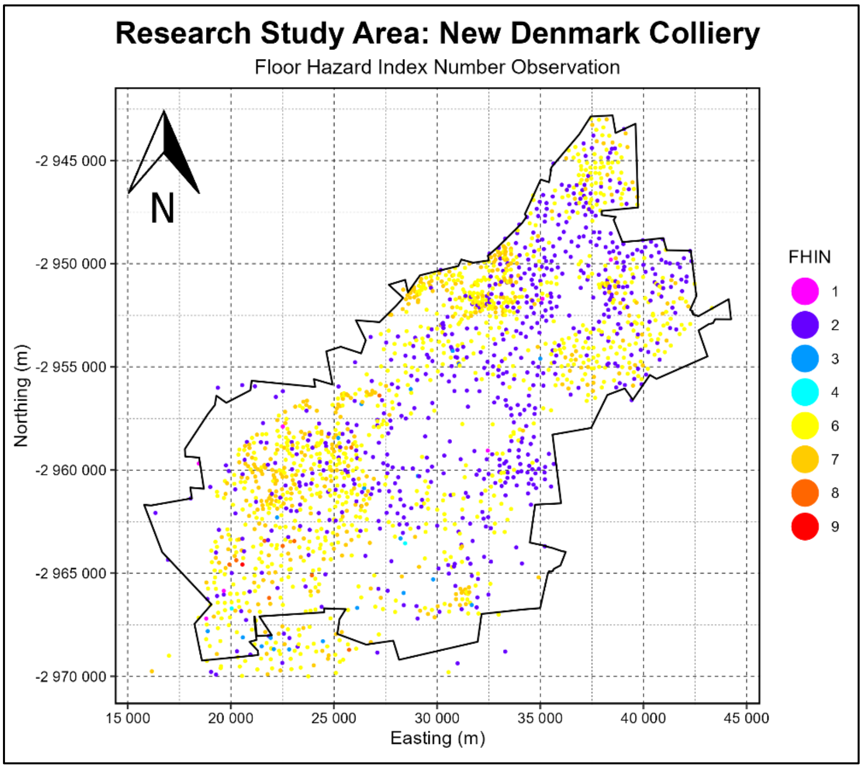

***Figure 8**: FHIN location plot within the study area.*

4.2 Roof Hazard Data

The author also developed a roof hazard scorecard to score roof hazard qualifiers of boreholes. The roof hazard qualifiers differ from the floor hazard qualifiers and the Strata Control Offices and Rock Engineers use different properties to establish if the roof is good (standard support), or bad (requires additional support). The only qualitative properties required for the roof hazard are the lithology of the immediate roof and the bed separation contact type (mainly referring to the sedimentary bedding contact type).

The calculation of the roof hazard index number (RHIN) for a borehole is based on a similar matrix to that of the FHIN, with the roof hazard qualifiers (rows) aligned to the Rock Engineering vocabulary at NDC. The roof hazard qualifiers are bed separation (distance), roof lithology, sill proximity (distance) and geological structures (proximity).

The roof hazard risk (columns) informs on 'Normal' ground, 'Cautionary' ground and 'High Risk' ground. This terminology indicates to the underground section crew which safety precautions have to be taken. The roof hazard plan will be important as it will assist in the identification of specific safety measures to be implemented once a mining section enters into 'Cautionary' or 'High Risk' zones. Allocating a roof hazard score or roof hazard index number (FHIN) for any borehole in the database is based on the following logic:

- ✓ If all roof hazard qualifies are ***normal*** the borehole is allocated RHIN of one
- ✓ If one of the roof hazard qualifiers are in the ***cautionary*** column the RHIN will increase to two. The RHIN will increase by one for every additional qualifier that is classified as cautionary. Thus. if all four qualifiers are classified as cautionary the RHIN would be five.
- ✓ If one floor hazard qualifier is ***high risk*** the borehole roof is deemed to be high risk and is allocated a RHIN of six, irrespective of where the other qualifiers rank (normal or cautionary). The ***high risk*** count will increase by one for every qualifier that is classified as high risk. If all qualifiers are classified as high risk the borehole will have a RHIN of nine.

For any qualifying borehole in the database, the algorithm for applying this logic for producing the RHIN score is given by the following code:

```
if (count(Number of "X's" in the High Risk column)>0) {
        count(Number of "X's" in the High Risk column) + 5
        } else if (count(Number of "X's" in the Cautionary column)>0) {
                count(Number of "X's" in the Cautionary column) + 1
                } else {
                1
                }
```

The RHIN bar chart in **Figure 9** highlights that RHIN 1 (normal ground conditions) were mostly encountered. The remaining significant RHIN values are RHIN 2 (roof conditions with one cautionary qualifier) and RHIN 6 (roof conditions with one high risk qualifier). **Figure 10** below illustrates the application of this the above algorithm to generate a RHIN score for a dummy borehole.

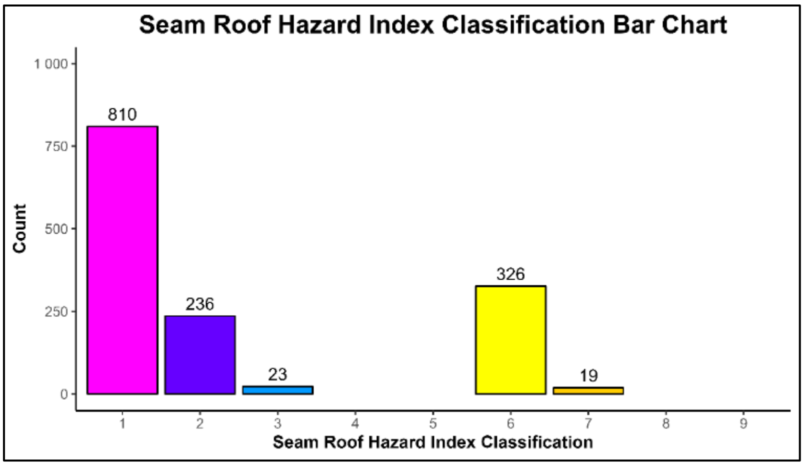

***Figure 9**: Roof Hazard Index Number Bar Chart*

The spatial dominance of RHIN 1 is visually also confirmed in **Figure 11** below.

In **Figure 10**, “X” indicates an identified roof hazard qualifier in the floor condition (risk) columns of the scorecard. Based on the above algorithm, two qualifiers are in the High Risk column and the first “IF” statement of the algorithm is true and the RHIN is thus two plus five resulting in the RHIN of seven, appearing in the box on righthand side of the scorecard.

New Denmark Colliery

Roof Hazard Scorecard

		Normal Ground	Cautionary	High Risk
Bed Seperation *Refers to the thickness of rock layer that has to be anchord with roofbolts or long anchors		Gradational Contacts **<0.6m & >2.0m**	Gradational Contacts, Laminated Contacts **1.0m - 0.6m**	Laminated contacts **2.0m - 1.0m**
			X	
Roof Lithology *The depositional sedementary rock (immediate roof) with its attributed structures - shale, mudstone, sandstone, siltstone, etc.		Massive Gritstone - Sandstone, Hyperbyssal	Bedded Sandstone - Siltstone	Laminated Shale, Siltstone, Mudstone
				X
Structure Proximity *Intrusions and other stress related structures can influence the strucural integrety of the floor.	**Sill** *Proximity to roof	>5m	5m - 1m	<1m
			X	
	Structures in roof *Structures in close proximity to the roof as per borehole information - joints, faulting, slips, etc.	>10m	10m - 5m	<5m
				X

HR2
7

***Figure 10**: Roof Hazard Scorecard an example.*

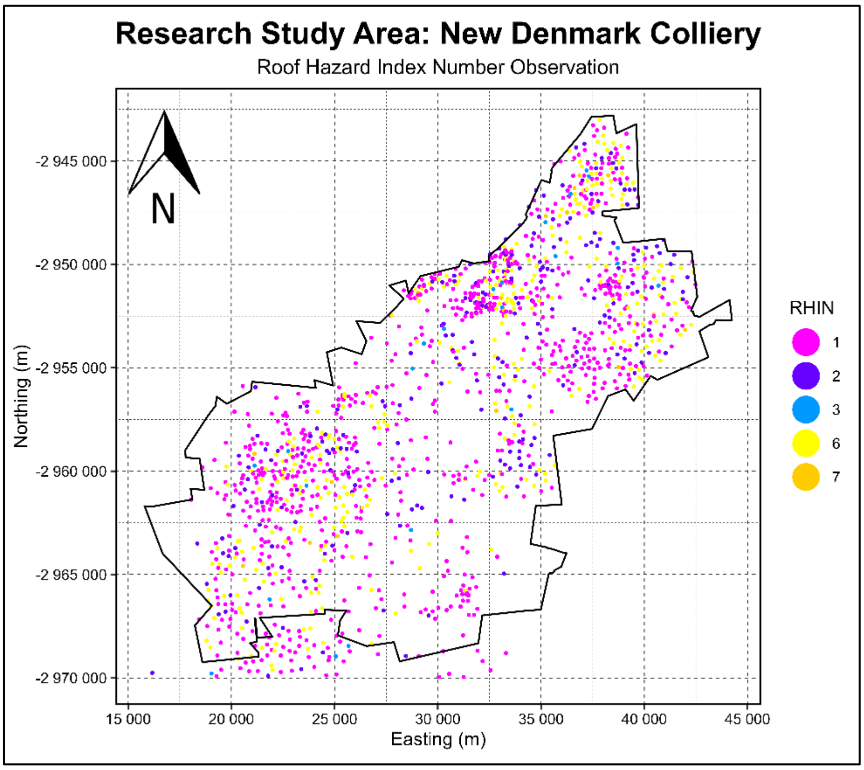

***Figure 11**: Roof HIN location plot within the study area.*

In Chapter 4 the development of distinctly different floor and roof hazard scorecards, consisting of both quantitative and qualitative data and applied to all boreholes was outlined. The process of generating individual hazard indexes numbers using the two scorecards was explained and illustrated. The discrete numeric FHIN and RHIN scores for the floor and roof hazards will be used in the quantitative methodologies to evaluate their geospatial relationships in the next chapters.

5 ANALYSIS AND FINDINGS

As highlighted in Chapter 4 the amount of observed structural data is more than double that of the hazard data (**Table 1**). In addition, the spread of the FHIN and RHIN across the nine identified scorecard categories reflected by the bar charts in **Figure 7** and **Figure 9**, highlighted that some FHIN and RHIN values were more likely than others. In Chapter 5 the statistical and spatial analyses and findings of the research investigations are detailed.

It was assumed necessary to investigate if correlations between the structural data and the hazard data exist. This was considered a significant aspect of the research because, if a spatial association of the structural variables could be linked to the floor or roof hazard locations it would be an advantage for hazard map generation using estimation and simulation processes.

Two spatial estimation methods (OK and IDW2) were explored and applied to the continuous structural data and the discrete hazard index data. The resulting spatial outcomes were appraised and visually compared in an endeavour of discovering regionalised variables that could be used in the hazard map generation. Extensive statistical and geostatistical analyses including conditional simulation applications were pursued as it was initially argued that spatial association between structural variables would be a stronger guide to be used in the floor and roof hazard assessment. These analyses did, however, not lead to that envisaged outcome.

Nonetheless, knowledge about software applications was gained and this is an advantage to NDC estimation applications. It was then important to proceed with an investigation on the spatial correlation of the hazard data itself. Culminating in the definition of hazard indicator classes (HIC) based on individual grouping of FIN and HIN and indexes. Finally OK and IDW2 indicator estimation and simulation were carried out on the HIC, the results were interpreted, compared and evaluated.

5.1 Hazard Index Classification

The spatial spread of the individual FHIN and RHIN values gave rise to the notion that grouping of the roof and the floor HIN categories in classes would be more realistic and sensible option to consider in the quest for finding a spatial solution for hazard identification. Creation of the Hazard Index Classifications (HIC) for the respective floor and the roof HIN competency classifications appears **Table *2*** .

Table 2: *FHIC and RHIC Classification based on FHIN to RHIN competencies.*

Floor Hazard Index Classification (FHIC)		Roof Hazard Index Classification (RHIC)	
FHIN 1 FHIN 2 FHIN 3	Floor Hazard Index Class1 ***Competent floor***	RHIN 1	Roof Hazard Index Class1 ***Normal roof ground***
FHIN 4 FHIN 6	Floor Hazard Index Class2 ***Moderately competent floor***	RHIN 2 RHIN 3	Roof Hazard Index Class2 ***Cautionary roof ground***
FHIN 7 FHIN 8 FHIN 9	Floor Hazard Index Class3 ***Incompetent floor***	RHIN 6 RHIN 7	Roof Hazard Index Class3 ***High Risk roof ground***

5.1.1 Floor Hazard Index Classification

The FHIN values were grouped by considering the lithological qualifier classes which inform on the "*hazardousness*" of the floor. The Floor Hazard Index Class one (FHIC 1) consists of floor conditions with all competent floor qualifiers (FHIN 1) and with up to two moderately competent floor qualifiers (FHIN 2 and FHIN 3). The Moderately Competent Floor Class two (FHIC 2) was created by combining FHIN 4 and FHIN 6. FHIN 5 was disregarded as it was not encountered in the research data base. All FHIN values higher than six were grouped together to form FHIC 3, the Incompetent Floor Class three. The bar chart showing the frequency in each FHIC class is presented in **Figure 12**. Most of the FHIN is contained within FHIC 2, with FHIC 3 occurring the least.

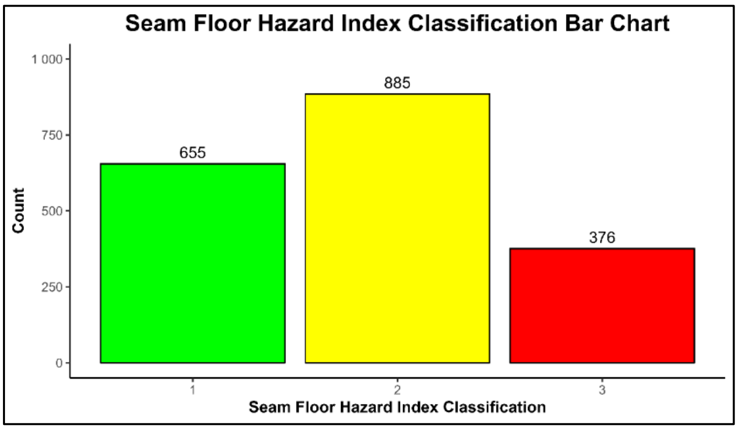

Figure 12: *Floor Hazard Index Classification Bar chart.*

The spatial locations of the FHIC appear in **Figure 13** and it clearly highlights that FHIC 2 and FHIC 3 commonly accompany each other spatially, whereas FHIC 1 is present throughout the study area.

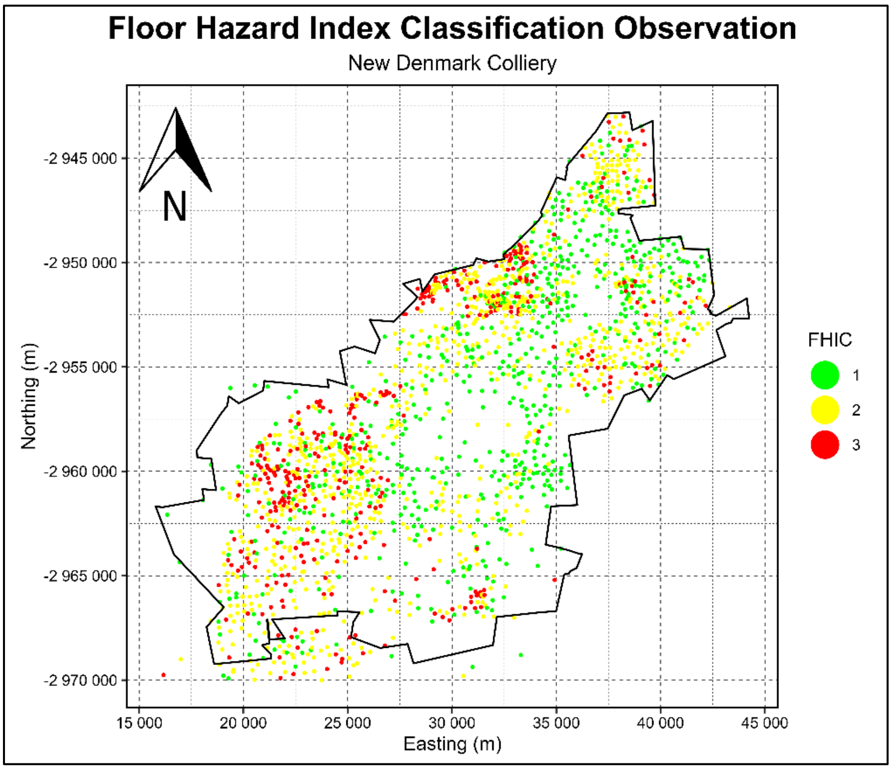

***Figure 13**: FHIC location plot within the study area.*

To further investigate the spread of the FHIC within the study area a Voronoi diagram was generated, see **Figure 14** below. This diagram informs on the density of the data (polygon sizes) and the spread of the FHIC (polygon colours). It is clear that on the outer edges of the NDC mining lease larger polygons exist. The polygon size is a function of the decrease in borehole density toward the outer edges of the mining lease. The polygons in the Voronoi Diagram smooths the point location information of **Figure 13** and the polygons accentuates that FHIC 3 polygons occur mostly close to or next to FHIC 2 polygons and FHIC 1 is present throughout the entire lease area. However, only small FHIC 1 polygons are close to FHIC 2 and FHIC 3 polygons. The small polygons represent areas where the data is spatially denser. Increased drilling in these areas can be attributed to infill drilling before mining, which has now mined out, or can be attributed to increased geological challenges requiring increased borehole density in FHIC 2 or FHIC 3 classes.

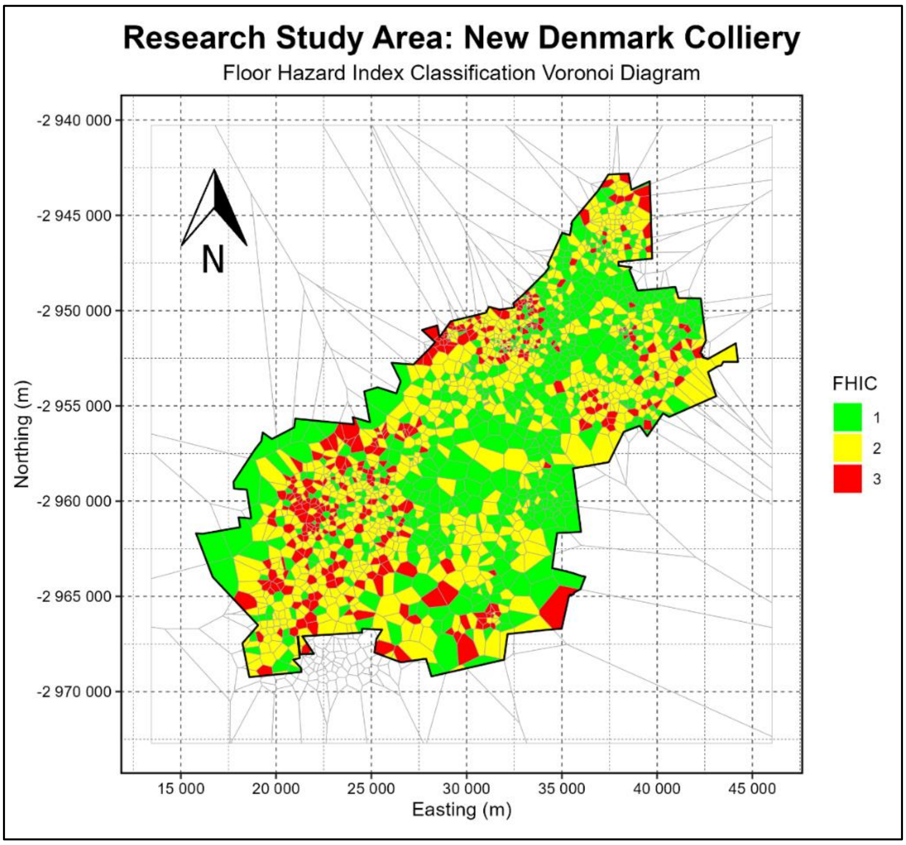

***Figure 14**: Floor HIC Voronoi Diagram.*

5.1.2 Roof Hazard Index Classification

The RHIN were grouped based on the spread of the data as well as considering that no data point with a qualifier in cautionary can be allowed to be classified as 'good ground'. As the safety of underground personnel is the main concern for the mine; the Rock Engineers will only allow data points with all qualifiers in 'Normal Ground' to be grouped into the Normal Ground Class (RHIC 1). Based on the bar chart frequencies of the of the data (**Figure 9**) the "Cautionary Class" RHIC 2, consist of RHIN 2 and RHIN 3, and the "High Risk Class", RHIC 3 consists of RHIN 6 and RHIN 7.

The RHIC frequency distribution is illustrated by the bar chart in **Figure 15** below. The RHIC classes are colour coded and most of the RHIC data points occur within the "Normal Ground Class". The spatial locations of the RHIC appear in **Figure 16**, and it appears that RHIC 2 and RHIC 3 are spatially random but seem to be spatially occurring together. RHIC 1, is however present throughout the entire study area.

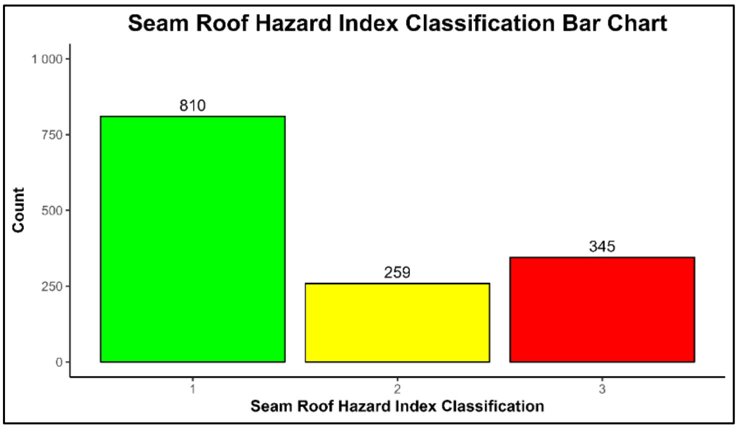

***Figure 15**: Roof Hazard Index Classification Bar Chart.*

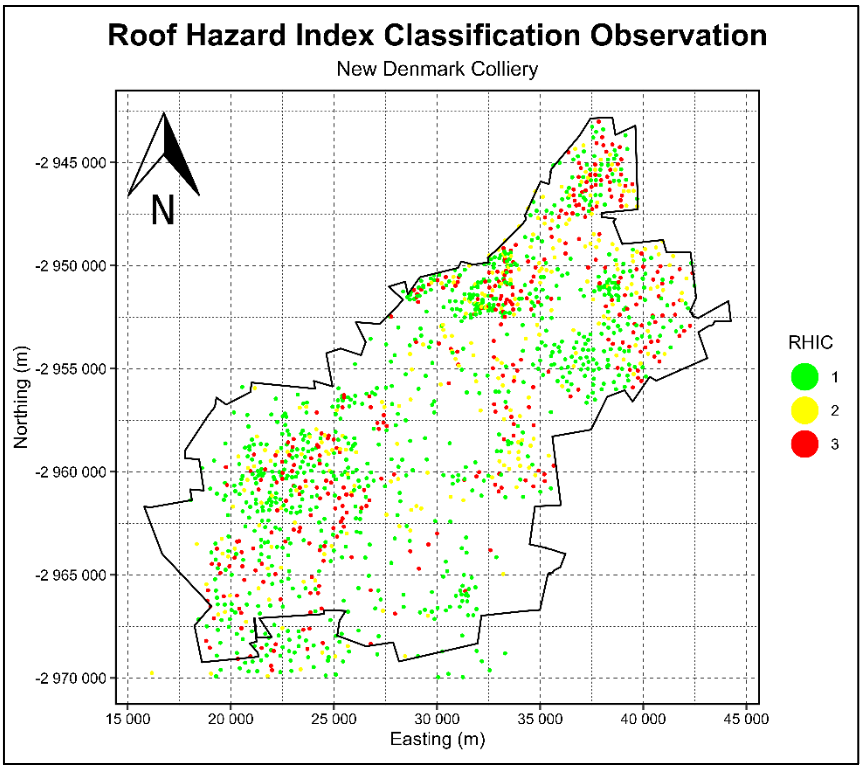

***Figure 16**: Roof HIC location plot within the study area.*

The RHIC Voronoi diagram is illustrated in **Figure 17**. As expected, the Voronoi polygons are similar to those in **Figure 14**, again highlighting the decreasing borehole density towards the edges of the mining lease. No clear patterns in the positions of the RHIC polygons were visually identified. Another difference would be that there are larger RIHC polygons present thought the mining lease than in **Figure 14** as there are less observations for the RHIC than FHIC (**Table 1**). It is also important to note that RHIC 1 dominates the study area. There does seem to be a slight spatial affinity between RHIC 2 and RHIC 3 polygons.

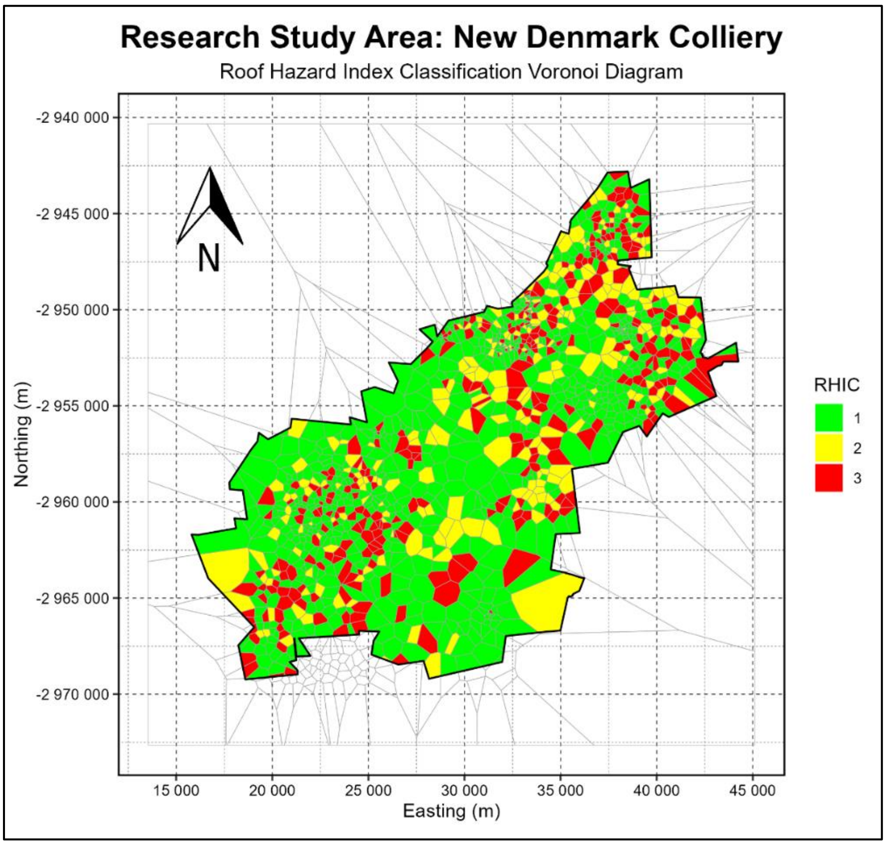

***Figure 17**: Roof HIC Voronoi Diagram.*

5.2 Structural Variable Correlations and Hazard Index Value Domaining

The measured structural data outnumbers the interpreted hazard data (**Table 1**) thus, ascertaining some form of spatial association between these two variables types would be beneficial to achieving the research objective. This subsection considers the investigation into establishing such association between hazard indexes and the three structural variables.

The same analytical process was followed for each structural variable and a description follows. The EDA performed on the variables include graphical summaries such as a histogram and cumulative frequency distribution (CFD) plots and basic statistics. A location plot for the variable is generated with meaningful colour classes selected based on the slope changes in the CFD. This location plot is then compared to the FHIC and RHIC location plots in an attempt to identify visual spatial association or correlation between the HIC and the structural variable. Then follows the geospatial analysis of the structural variable, where its spatial correlation is explored.

The spatial correlation is discovered with the aid of variogram maps (varmaps) which assist in identifying major and minor directions of spatial continuity (anisotropy). Thereafter spherical variogram models are fitted to the experimental variograms directions of maximum and minimum continuity as identified from the varmap. With variogram models in place the structural variable is estimated on a 25 m x 25 m grid applying Ordinary Kriging (OK) and IDW2. This is carried to enable comparison between the two methods of estimation of the structural variable to assess IDW2 against OK.

Subsequent to the generation of OK estimation maps for the structural variables the application of CSGS was explored to understand the spatial variability of the variables. In the simulation process the original variables undergo a NSCORE transformation. Followed by the geospatial investigation of the NSCORE values wherein experimental NSCORE variograms are calculated from which NSCORE varmaps are generated and anisotropy is identified. This process culminates in the NSCORE variogram model fitting for the anisotropic directions. These model parameters together with the kriging neighbourhood parameters are then used as input for the simulations. The simulated structural NSCORE data is then back transformed to original units of measurement. In the final step of the simulation process each node in the estimation grid now had 100 simulated values associated with it. These points were then used to calculate the E-type estimates (averages per node) for the variable. In the assessment of results the E-type estimation map is produced and spatially compared to the input data location plots and the IDW2 estimation maps.

5.2.1 No 4 Seam Thickness

Within the study area there are 3 290 seam thickness observations with an average of 1.89 m and standard deviation of 0.42 m. The maximum thickness is 3.60 m, and the minimum is 0.10 m. A graphical summary of the No 4 seam thickness is captured by the histogram shown in **Figure 18**. A normal probability density curve is drawn over the shape of the histogram and illustrates how the seam thickness frequency distribution compares to it. **Figure 19** presents the CFD of the seam thickness. It is concluded that the No 4 seam thickness in the study area closely resembles a Gaussian distribution.

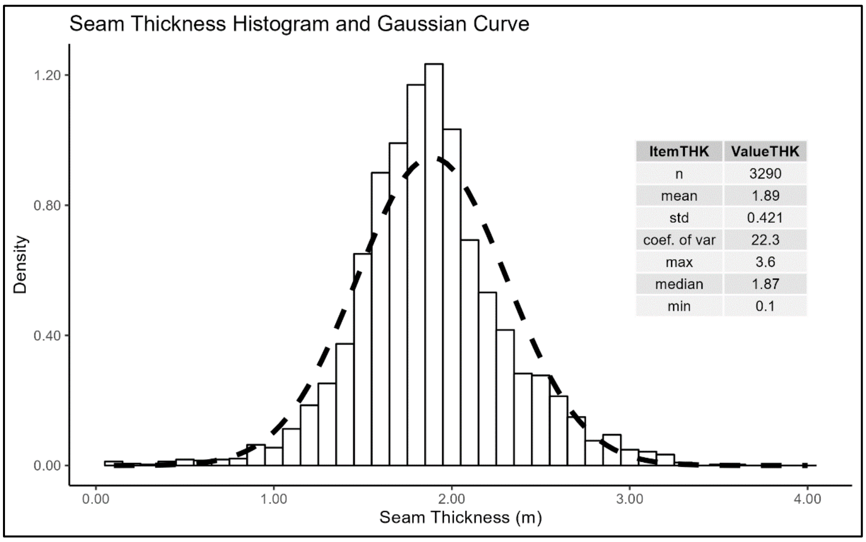

***Figure 18**: No 4 Seam Thickness Histogram and Normal Probability Curve.*

The seam thickness location plot within the study area appears in **Figure 20**. This colour coded spatial plot of seam thickness clearly emphasise anisotropy in the seam thickness. Clear ‘directional channels (‘streaks’) of similarly coloured observations are present in approximately an NNE direction. Within these directional “channels” the thickness variability is low, however across the “channels” in an approximately a WNW direction higher seam thickness variability is observed. This observation is expected to be confirmed in the variography analysis.

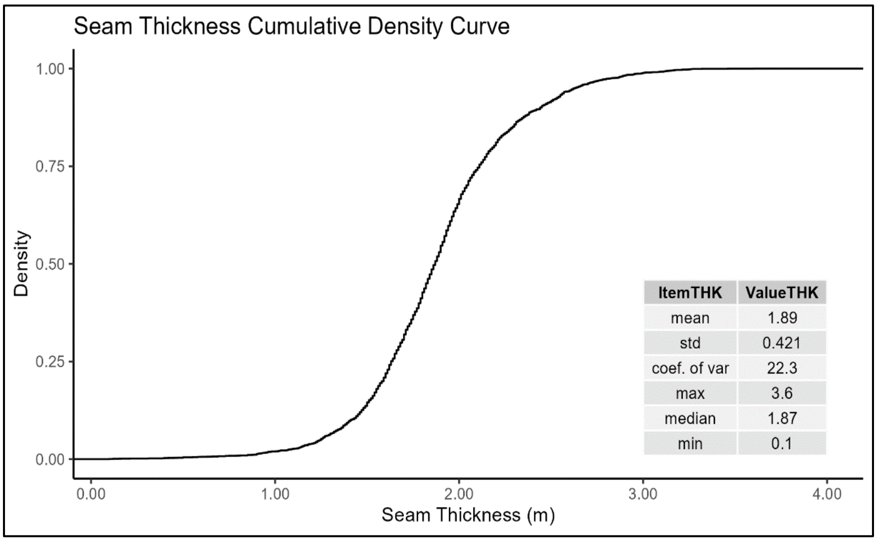

Figure 19: *Cumulative Density Curve of the Seam Thickness (m).*

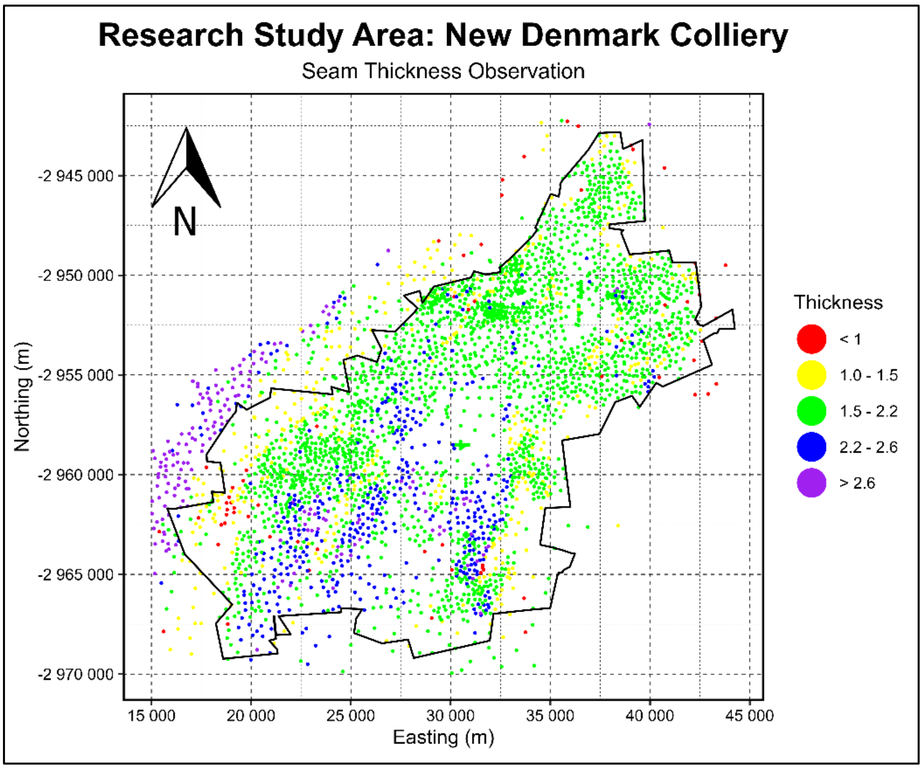

Figure 20: *Location plot for seam thickness in the study area.*

Hazard Index Spatial Correspondence to Seam Thickness

The HIC values are categorical, and it would have been difficult to identify statistical behaviour in the two variable types. Thus, it was decided to generate seam thickness box plots for each of the HIC categories (FHIC 1, FHIC 2 and FHIC 3 y-axis) corresponding to the continuous seam thickness variable (x-axis). The Box plots appearing in **Figure 21** and **Figure 22** respectively present a comparison between the FHIC and RHIC classes and seam thickness. The multiple box plots display the spread of the seam thickness in relation to the HIC and make it easier to identify similarities or peculiarities in the HICs.

The multiple FHIC Box Plots (**Figure 21**) shows that for FHIC 2 a wider spread in seam thickness is observed than for FHIC 1 and FHIC 3. The seam thickness spread is the least for FHIC 3. The median and inter quartile range (IQR) thickness are roughly similar in all FHIC categories, suggesting negligible difference in the seam thickness distributions within FHICs.

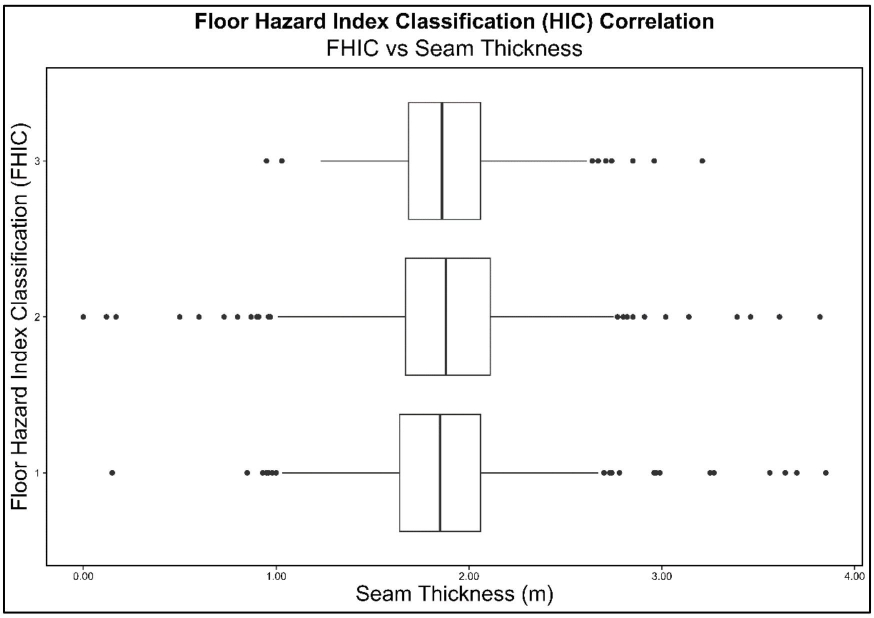

Figure 21: FHIC Box Plots vs No 4 Seam Thickness (m).

On the other hand, from the multiple seam thickness Box plots per RHIC (**Figure 22**), it is observed that the thickness spread for RHIC 2 is narrower compared to RHIC 1 and RHIC 3. The spread within RHIC 1 reveals more of outliers towards the thicker seam, whereas within RHIC 3 more outliers towards the thinner seams are observed. Despite this, the thickness median and IQR of the RHIC are similar over all three the RHIC.

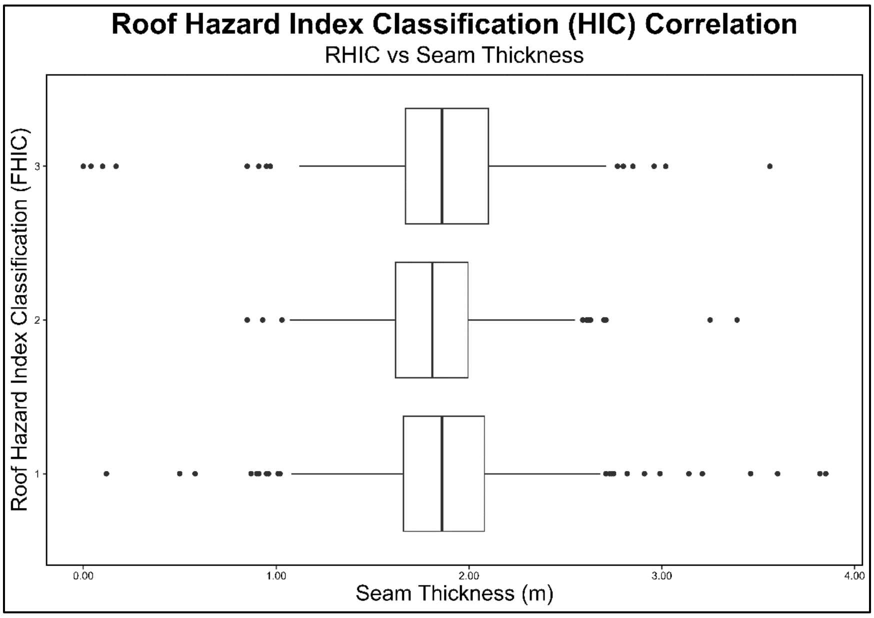

Figure 22: RHIC Box Plots vs No 4 Seam Thickness (m).

Although the graphically summarised FHIC and RHIC Box plot statistics do not show distinctive dissimilar behaviours in relation to the coal seam thickness, it was envisaged that there might be still remain visually observable spatial similarities or trends within location plots. If the seam thickness could be estimated there might be grounds for domaining of the hazard data accordingly.

Seam Thickness Variography

To determine the spatial correlation for coal seam thickness a 2D (two dimensional) a varmap was generated (**Figure 23**). As expected from the thickness location plot (**Figure 20**), the varmap highlights spatial anisotropy in the No 4 seam thickness. The highest spatial continuity and major direction of seam thickness continuity was identified to be at an angle of 33°, perpendicular to it at an angle of 123°, is the highest spatial variability or direction of minor seam thickness continuity.

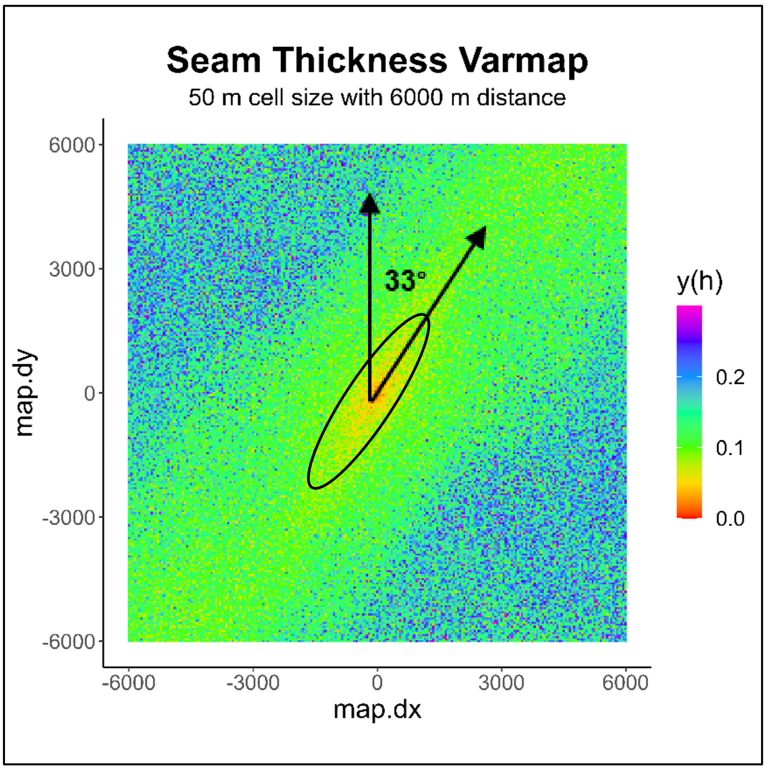

***Figure 23**: Varmap of seam thickness in the study area*

Once the anisotropy directions were identified the standardised experimental variograms in the major and minor directions were plotted and directional spherical variogram models fitted (**Figure 24**). The variogram model in the direction of high continuity is used along with a ratio which expresses the relative range of the direction of lowest continuity compared to the direction of highest continuity. This is illustrated by the model following the experimental variogram points in the 123° direction. The parameters of the final double structured spherical variogram modelled (in the direction of highest continuity) are:

Variogram Model Parameters:	Nugget effect (C_0 = 0.23),
	Sill 1 (C_1 = 0.31) and Range 1 (a_1 = 1500 m)
	Sill 2 (C_2 = 0.46) and Range 2 (a_2 = 5200 m)

The anisotropy ratio has been estimated at 0.5 for use in 'gstat'. This ratio represents the ellipsoid ratio between the direction of highest continuity and the direction of lowest continuity.

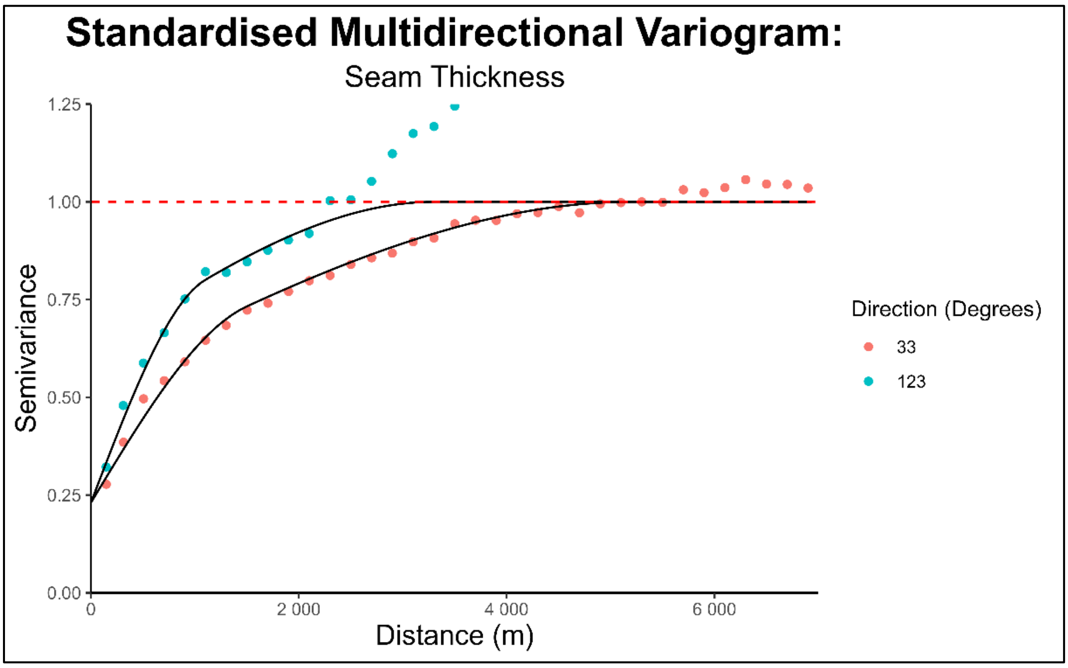

Figure 24: *No 4 seam thickness standardised experimental variograms and models for the major and minor directions of continuity.*

Estimation

For practical application purposes specifically in this research it was important to compare the OK estimates with the IDW2 estimates as only IDW type estimates can be generated at the mine. Comparing the results for these two estimation methodologies will inform similar comparisons when looking at the floor and roof HIC estimates later in the research.

The spatial maps of the seam thickness OK block estimates (25 m x 25 m) and associated KV, appear in **Figure 25**. Whilst the IDW2 seam thickness estimates together with the location plot of the colour coded observed seam thickness values are presented in **Figure 26**.

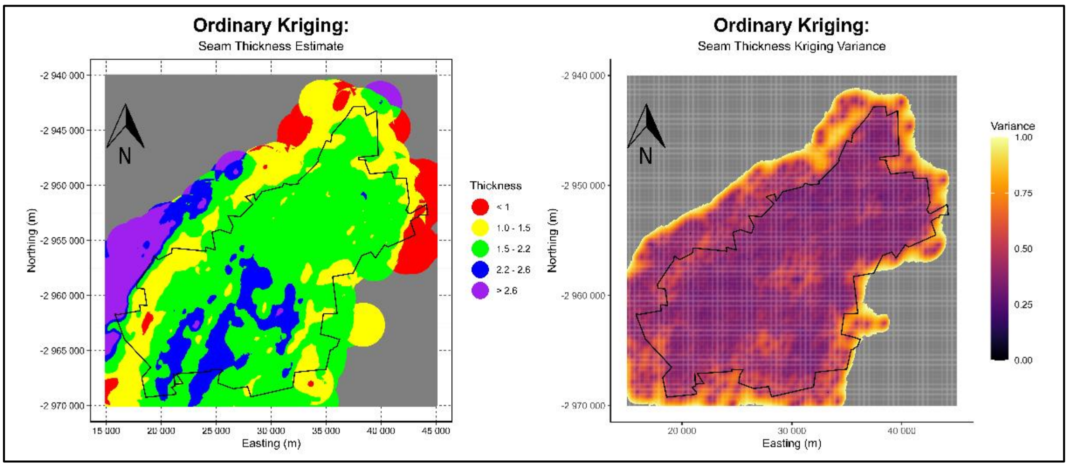

***Figure 25**: OK estimate and associated KV of the No 4 Seam thickness.*

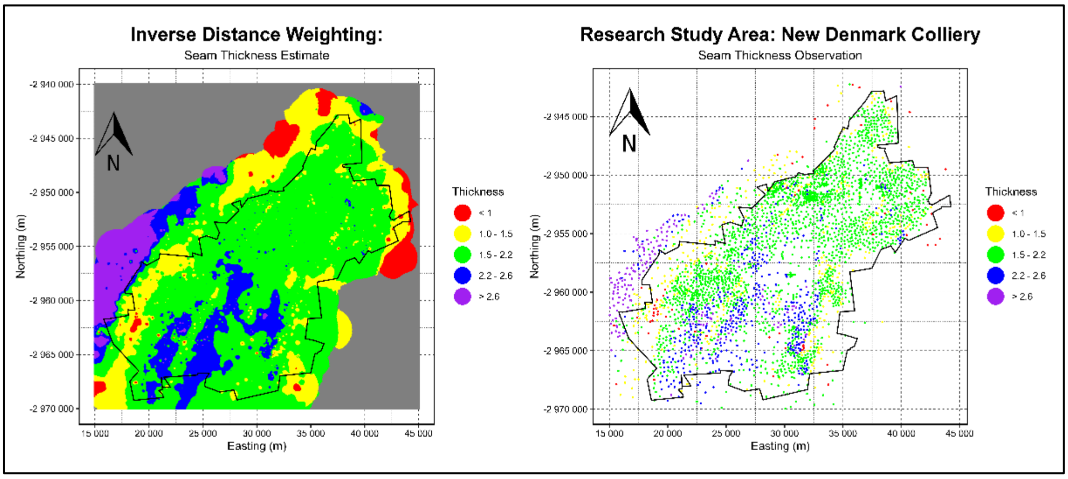

***Figure 26**: IDW2 estimate and location plot of the seam thickness observations.*

The same colour coding is applied to both the OK and IDW2 estimation maps. A clear visual difference observed between the two estimation maps, is in the smoothness of the results. OK produces an estimate that considers distances between the known points and the point to be estimated as well as the distances between all the known points used in the estimation. Whereas the IDW2 only considers the distance between the point being estimated and the known data points used in the estimation and ignores the spatial relationship between the known points, used in the estimate. IDW2 estimates appear more discrete (most weight goes to the closest point) than OK estimates where the point weights are optimised to produce the minimum estimation variance. Due to this technical difference between the two estimation methodologies the OK estimate map is spatially smoother than the IDW2 estimation. Whilst a difference in smoothness is observed similarities in the maps are also highlighted. It is seen that areas of thin and thick seam thickness are comparable and similar. Showing that for the purposes of this research IDW could be a proxy for OK.

An investigation of whether spatial domaining of the HIC data would be possible by using the seam thickness as a guide was carried out next. Seam thickness was simulated to capture its spatial variability and an e-type estimate generated from 100 simulations. The outcome thereof would then be compared to the spatial locations of the HIC data to establish if any spatial correspondence exists between the two variables. The results were also expected to inform on HIC estimations outside areas of dense data regions. The process of generating the simulations for the No 4 seam thicknesses is detailed below.

Seam Thickness NSCORE transformation

For simulation of the seam thickness the thickness values had to be transformed to Gaussian values through the NSCORE process. The CFD of the seam thickness data (quantiles) are allocated NSCORES based on the associated CFD values of a standard Gaussian CFD. In **Figure 27** the two CFDs for the seam thickness and normal distribution are displayed.

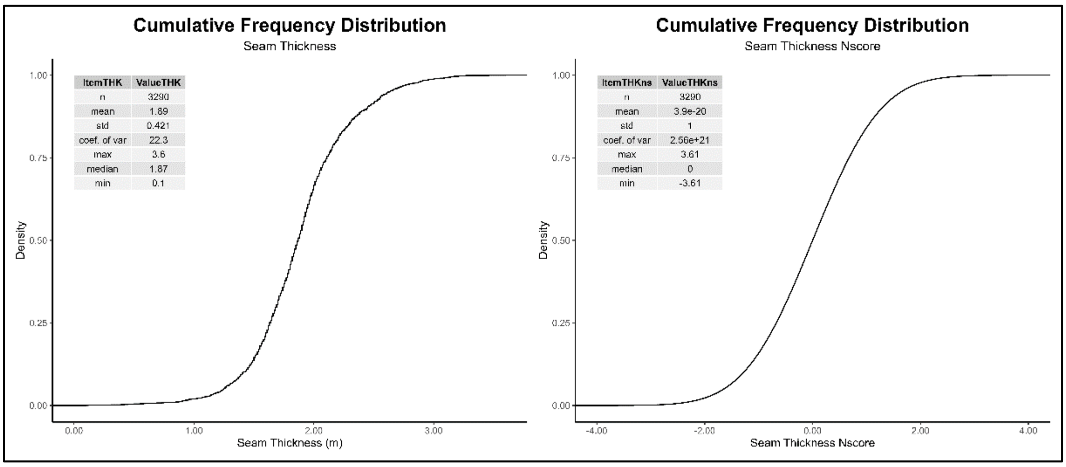

***Figure 27**: Seam thickness CFD vs the seam thickness NSCORE CFD.*

After the transformation a histogram was drawn to confirm that the seam thickness NSCORE is Gaussian (**Figure 28**).

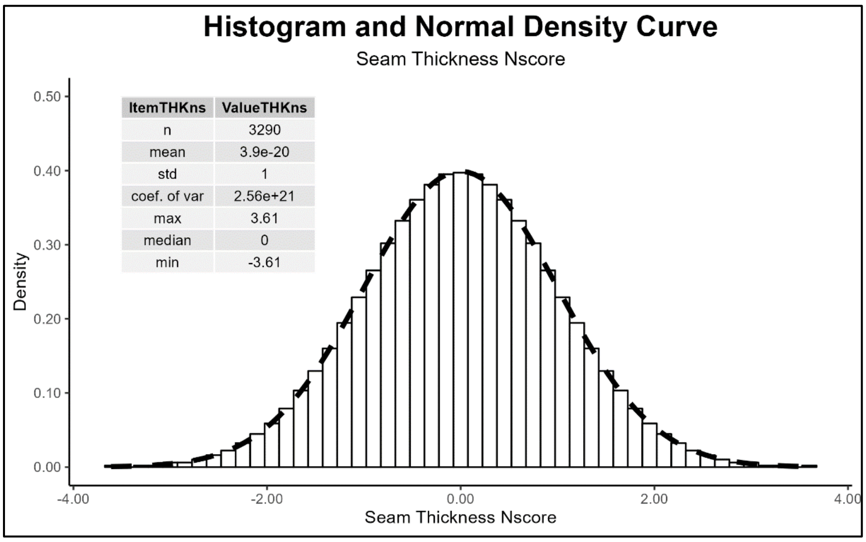

***Figure 28**: Seam thickness NSCORE histogram and normal density curve.*

The CSGS process requires an NSCORE variogram model. To achieve this a varmap of the NSCORE seam thickness data was generated. The resulting varmap presented in **Figure 29** and as expected (**Figure 18** seam thickness has a normal distribution) confirmed the anisotropy directions (major axis at 33°and minor axis at 123°) observed for the untransformed seam thickness (**Figure 23**).

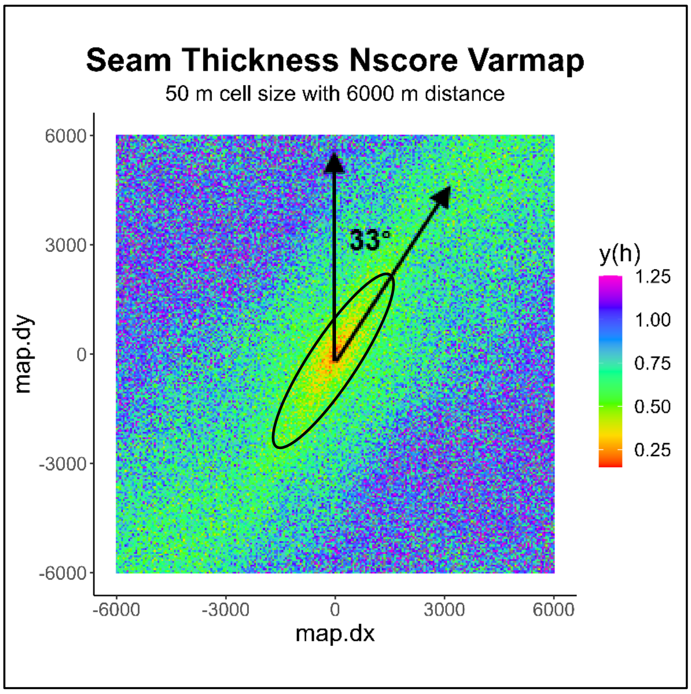

***Figure 29**: Seam thickness NSCORE varmap.*

Once the directions were identified the NSCORE variograms were plotted and double structured spherical models were fitted to both the major and minor directions (**Figure 30**). The double structured variogram models again match the shape of the untransformed seam thickness variograms. An anisotropy ratio of 0.5 was used and a spherical variogram model with parameters:

Nugget effect (C_0 = 0.29),
Sill 1 (C_1 = 0.33) and Range 1 (a_1 = 2000 m),
Sill 2 (C_2 = 0.38) and Range 2 (a_2 = 5200 m).

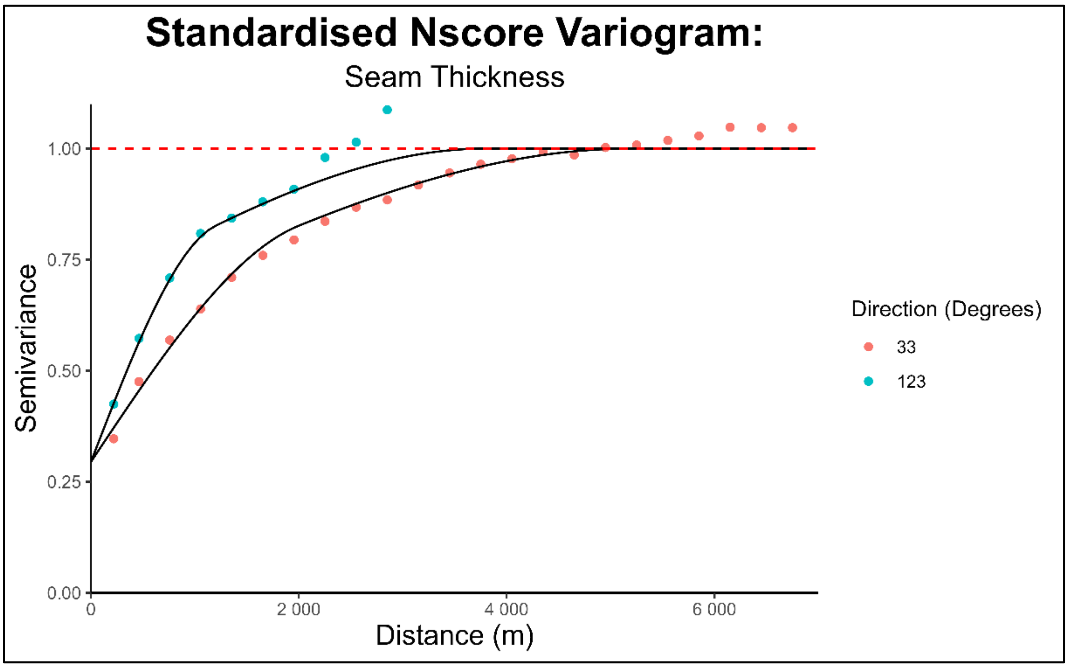

***Figure 30**: Standardised seam thickness NSCORE experimental and model multidirectional variogram.*

Simulation

This NSCORE spherical variogram model was used in CSGS to simulate the NSCORE coal seam thickness. A total of 100 realisations were simulated on a 25 m x 25 m grid. The simulated Gaussian data was back transformed to seam thickness format. This back transformation is the reverse of the process explained above (**Figure 27**). After the data transformation averages and probabilities were calculated, at each of the (1 440 000) nodes. For each node on the grid there is

100 seam thickness realisations from which a thickness distribution is generated. An E-type estimation is a plan which is generated from the simulation grid where the average of each node in the grid is calculated. In this case there are 100 realisations which means that an average of the 100 values is taken at each node.

The spatial results of the process described above is summarised in **Figure 31**. The E-type estimate, and the OK estimate closely resemble one another, and bears resemblance to the IDW2 estimation. It is also observed that the variability in the E-type estimate is low close to input data and increases in areas where the simulation is more model driven than data driven. Finally, the IDW2 and OK estimates were restricted with a range of 2000 m whereas the simulation was unrestricted. The reason the simulation estimate and variance plots on the other hand are unrestricted.

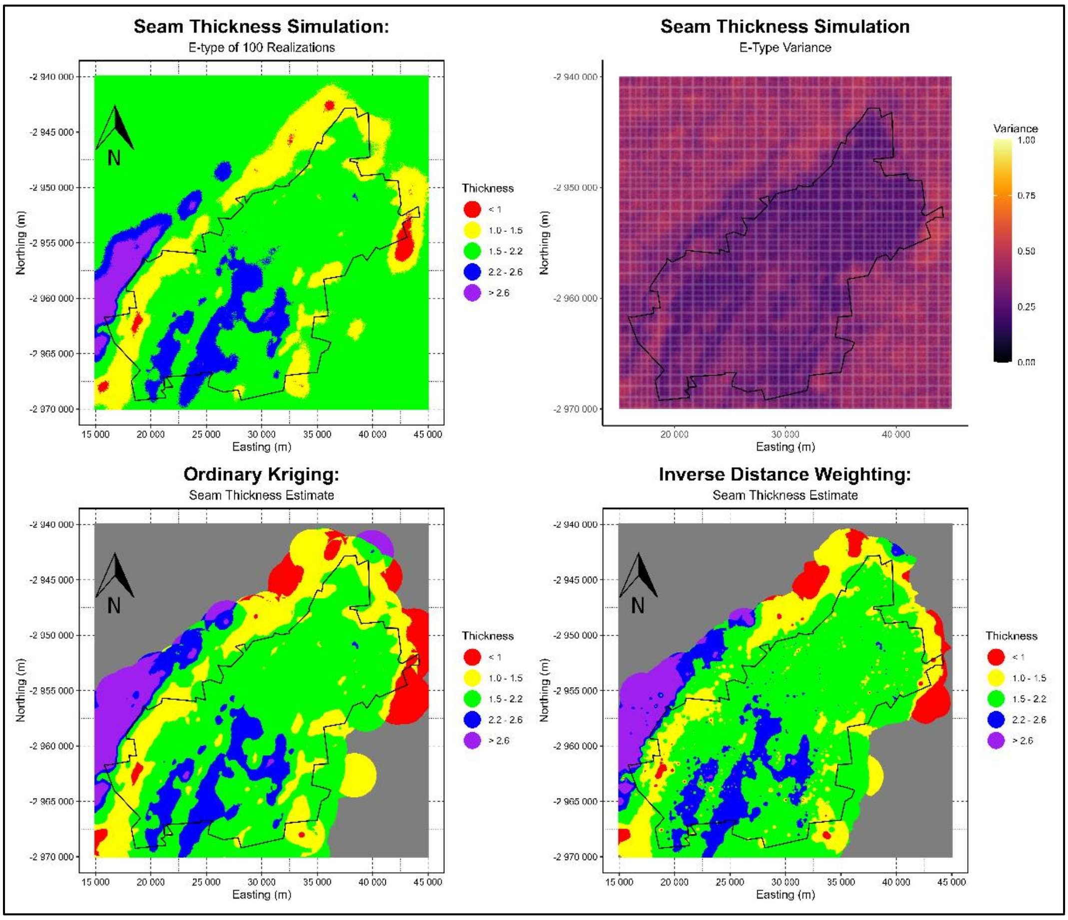

***Figure 31**: Seam thickness E-type estimate, E-type variance plot, OK estimate and IDW2 estimate.*

The seam thickness simulation (E-type), IDW2 estimate and HIC plans (floor and roof) are illustrated in **Figure 32**.

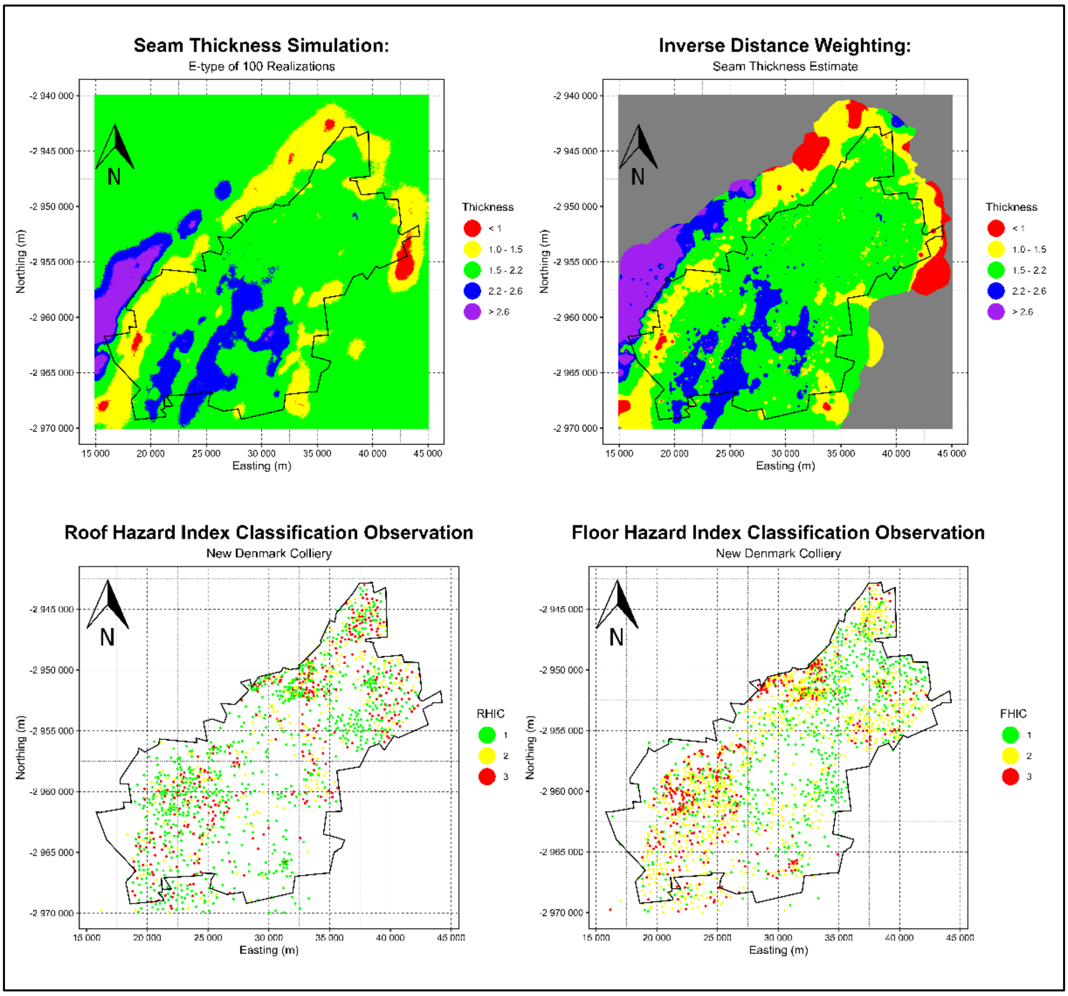

***Figure 32**: Seam thickness simulation and IDW2 estimated vs the RHIC and FHIC.*

The purpose of this section was to assess if domaining of the FHIC and RHIC can be done based on the seam thickness simulation e-type estimate. However, it is clear from **Figure 32** that there is no observable geospatial correspondence to suggest FHIC and RHIC domaining based on the seam thickness. Nonetheless, based on the results of this section it can be concluded that the OK and CSGS model are clearly aligned to the IDW2 estimates.

5.2.2 No 4 Seam Floor Elevation

The seam floor elevation is the elevation measured in metres from mean sea level (MSL) to the floor of the No 4 Seam. Within the study area there are 3 290 seam floor elevation points with an average of 1 418 m and standard deviation of 22 m. The maximum is 1 471 m, and the minimum is 1 348 m. **Figure 33** shows the histogram and spread of the observed seam floor elevation in the study area. The overlain normal density curve illustrates that compared, to the seam thickness the probability distribution of floor elevations conforms less well to a normal distribution. The cumulative density curve of the seam floor elevation data is illustrated in **Figure 34**.

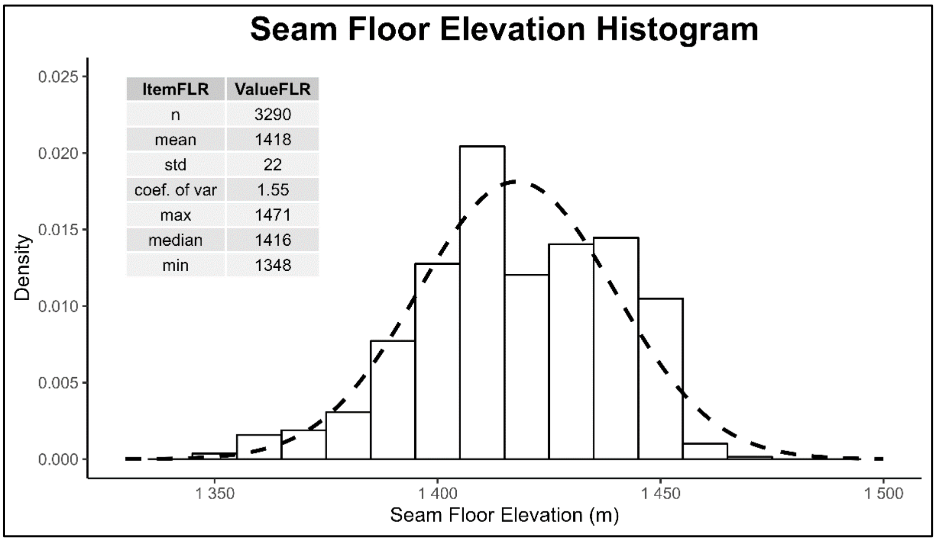

***Figure 33**: No 4 Seam Floor Elevation Histogram and Normal Probability Curve.*

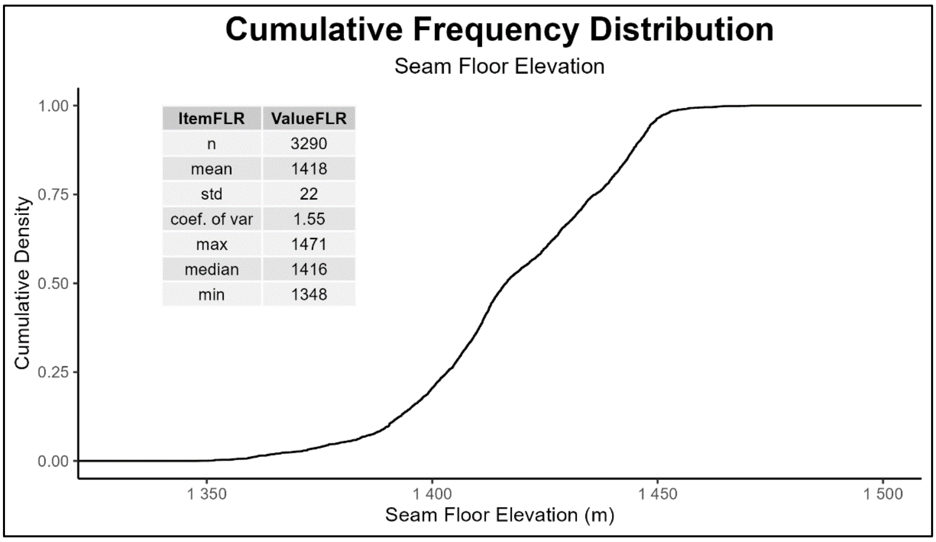

***Figure 34**: Cumulative Density Curve of the Seam Floor Elevation.*

A colour coded location plot for the seam floor elevation within the study area shown in **Figure 35**. The method for choosing the colour code for the seam floor elevation data is similar to that used for the seam thickness. The colours were chosen according to changes in the slope of the CFD of the variable, in this case the seam floor elevation CFD. This methodology allows for meaningful colour codes related to the statistical distribution of the data.

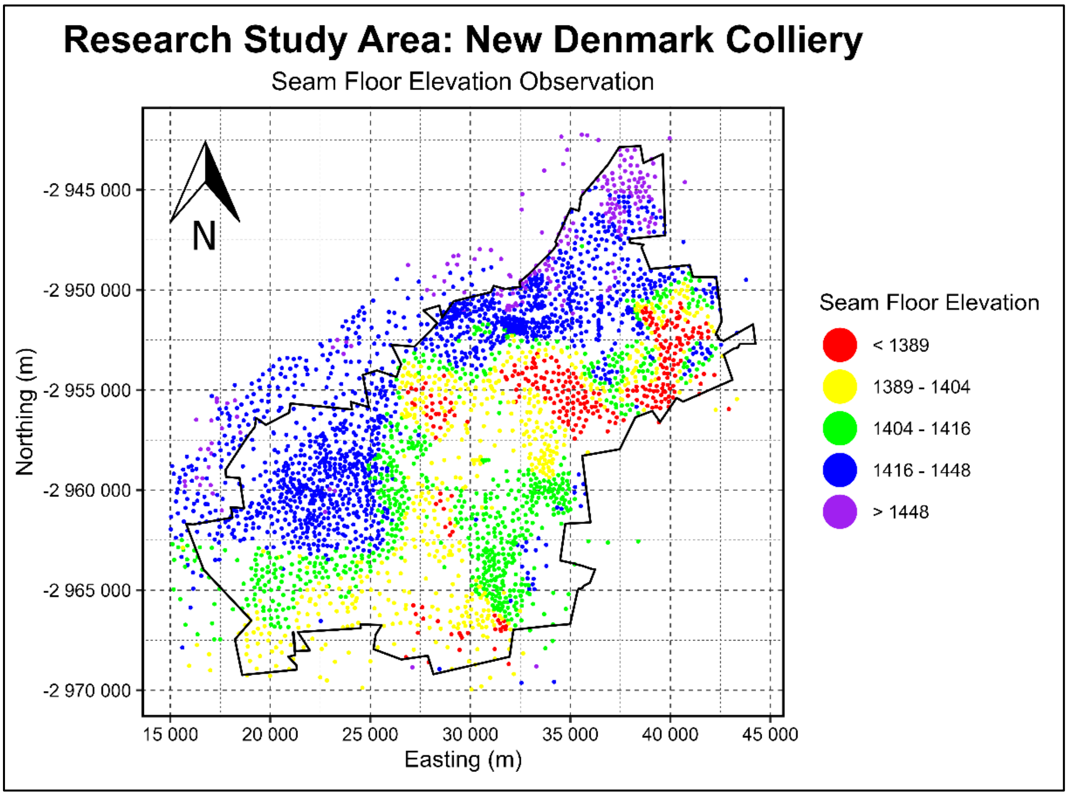

***Figure 35**: Location plot for seam floor elevation in the study area.*

From the colour coded seam floor elevation plot in **Figure 35** it was ascertained that a higher elevation is present in the north-west (NW) portion than in the south-east (SE) portion of the study area. A spatial trend in the seam floor elevation is evident, elevation changes across the study area is gradual in all directions. This observation suggests that the seam floor elevation is highly continuous and generally decreases from the NW to the SE.

Hazard Index Correspondence to Seam Floor Elevation

Box plots displaying the spread of the seam floor elevation in relation to the HICs were created to enable the identification of similarities or peculiarities in the seam floor elevation and the respective HICs. The seam floor elevation box plots for the different FHICs appear in **Figure 36**. From which a similar spread in seam floor elevation is observed across all three FHICs. What is different is the amount and position of floor elevation outliers for the FHICs. For FHIC 2 and FHIC 3 most of the floor elevation outliers are towards higher elevations. The outliers are however, closely spaced. It is also observed that the IQR of the floor elevation decreases with increasing FHIC. As with the seam thickness it is clear from this graph that there is no identifiable correspondence between the seam floor elevation and the three FHICs.

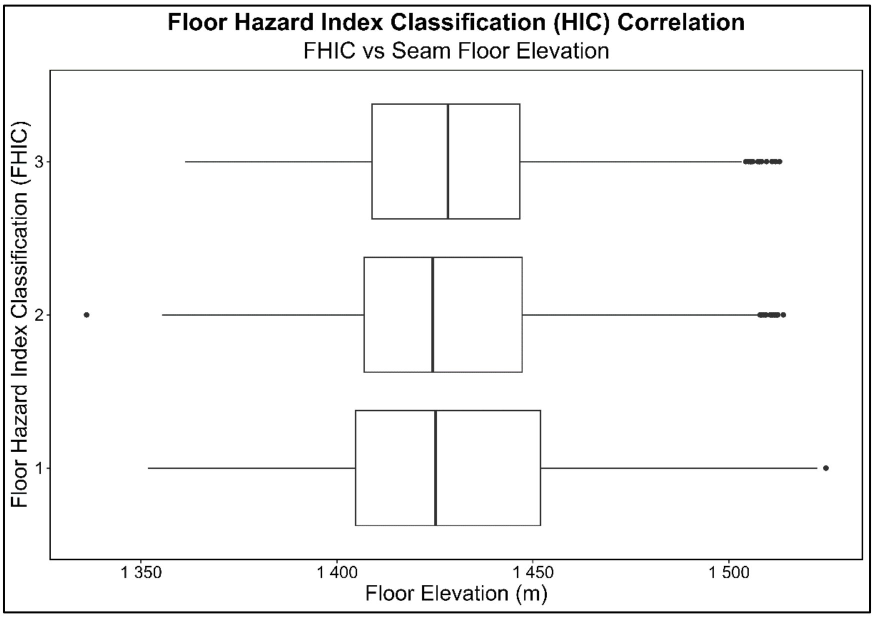

Figure 36*: Box plots of the FHIC vs Seam Floor Elevation.*

In **Figure 37** below the seam floor elevation box plots are compared to the RHIC. It is seen that the spread of the floor elevation across all three roof hazard classes is similar. However, in contrast to the floor hazard classes there are virtually no outliers in the roof hazard classes and only a few at the lower seam floor elevation of RHIC 1 and RHIC 3. Also, the floor elevation distributions are negatively skewed in the individual RHICs.

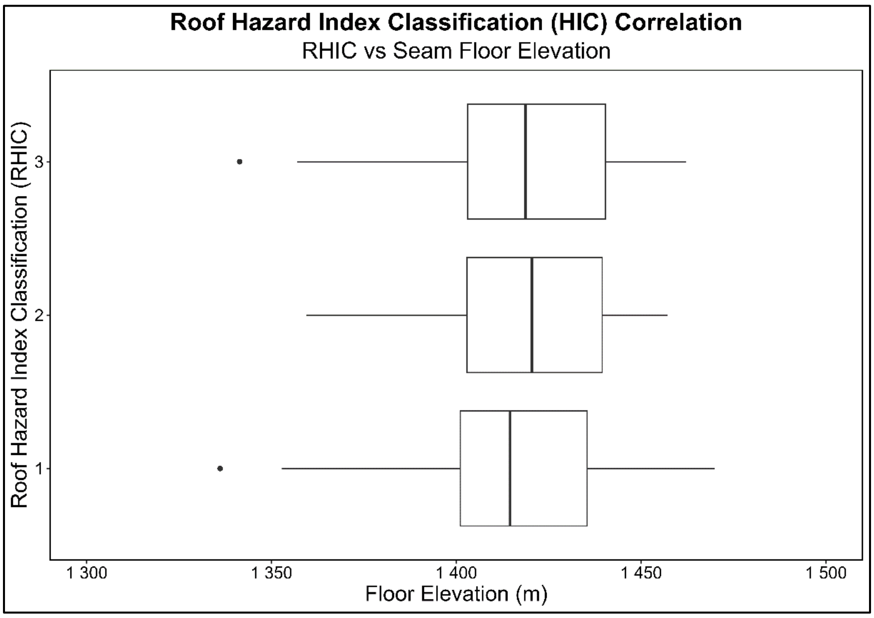

Figure 37: *Box plots of the RHIC vs Seam Floor Elevation.*

Based on the FHIC and RHIC box plots vs seam elevation comparisons there seems to be no correspondence between the seam floor elevation and the different FHICs and RHICs. The seam floor elevation means are within a close range in the and FHIC and RHIC. Despite small observed changes each floor and roof hazard category, individually have a similar distribution as the total seam floor elevation data set. This, strongly pointed to the conclusion that there is no correspondence between the seam floor elevations data and the floor and roof HIC data. Despite there not being any correspondence between the HIC data and seam floor elevation it does not mean that all options of spatially domaining the hazard data based on seam floor estimates or simulations have been explored.

Estimation

From the seam thickness assessment, it was established that the continuity of the structural variables results in OK estimates and simulations E-type estimates closely correspond to the IDW2 estimate. It was accepted that the NDC preferred IDW2 estimation can be used as a proxy for OK in this research. It was decided that, even though this analytic work was explored during the research, not to report on the variography, OK estimation and simulation results for the seam floor elevation as it did not add additional value to the research.

The spatial location plots of the seam floor elevation data points and the IDW2 estimate, the FHIC and RHIC data are displayed in **Figure 38**. Visually there again seems to be no geospatial correspondence to suggest domaining for FHIC and RHIC based on floor elevation.

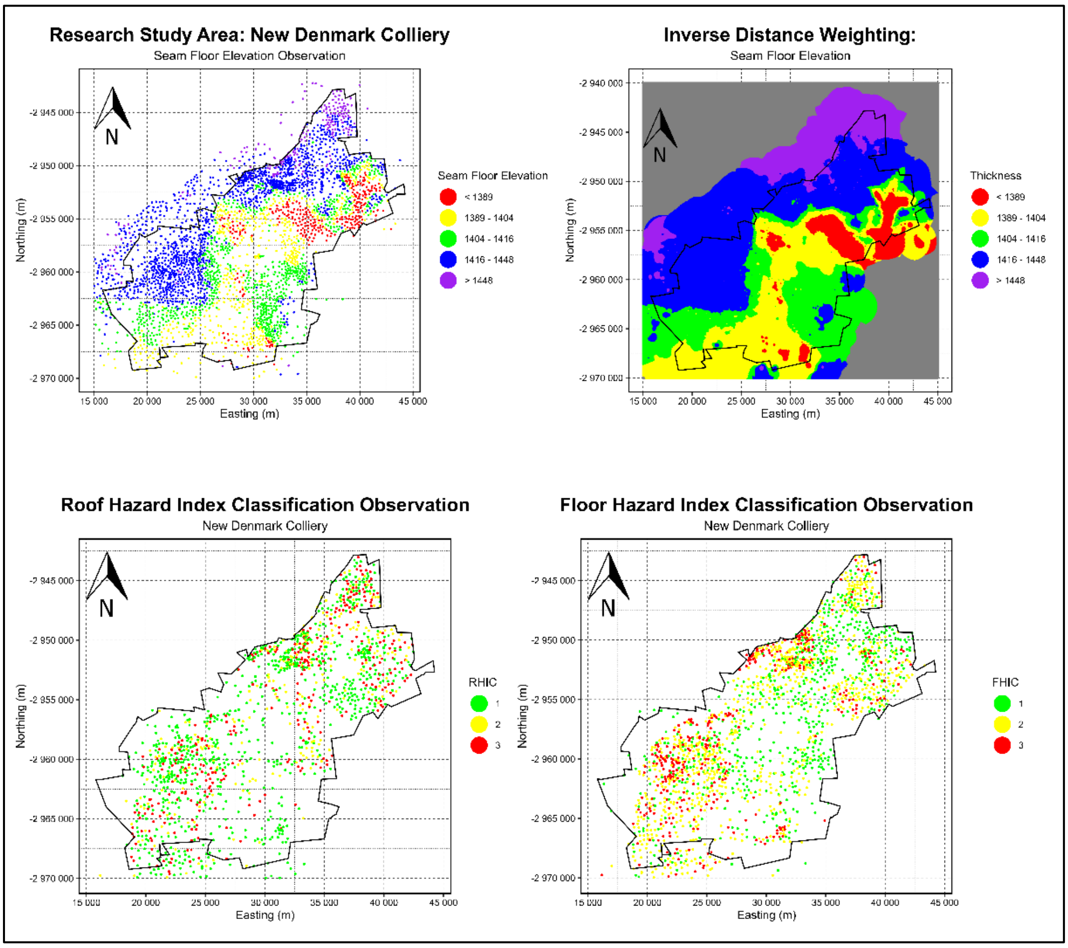

__Figure 38__: Location plots: Seam floor elevation, IDW2 estimates, RHIC and FHIC.

5.2.3 No 4 Seam Floor Depth

Within the study area there are 3290 seam thickness, floor elevation points and subsequently 3290 seam floor depth points. The seam floor depth has an average depth of 189 m and standard deviation of 26.40 m. The maximum depth is 282 m and the minimum depth is 104 m. The seam depth is the seam floor elevation subtracted from the digital terrain model (DTM), or topography.

The histogram in **Figure 39** shows the spread of the seam depth. The overlain normal density curve shows that the seam depth deviates from a normal distribution and appears to be slightly positively skewed.

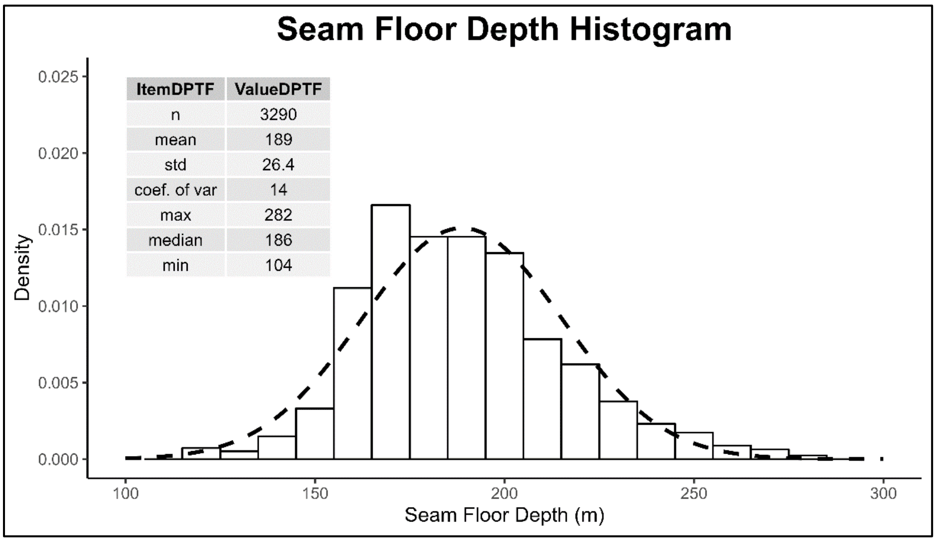

***Figure 39**: Seam Floor Depth Histogram and Normal Density Curve.*

In **Figure 40** the CFD curve of the seam floor depth data is shown. Visually it confirms that the seam floor elevation in the study deviates from a Gaussian distribution and does not resemble it as closely as the seam thickness.

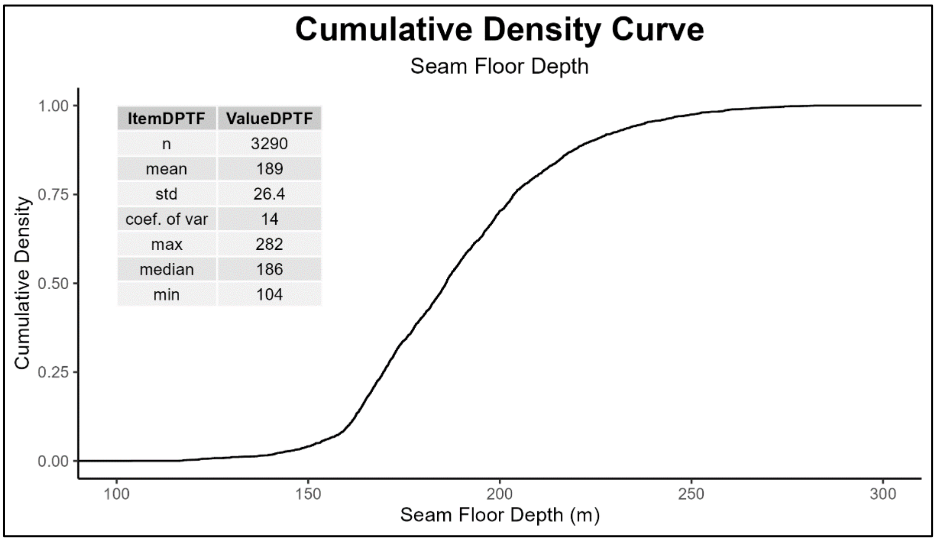

***Figure 40**: Cumulative density curve of the seam floor depth.*

The location plot in **Figure 41** presents the colour coded location plot for the seam floor depth within the study area. The colour code for the seam floor depth is based on the changes in slope on the seam floor depth CFD. From this colour plot it can be ascertained that on the western (W) side of the study area the seam floor is at a shallower depth than on the eastern (E) side. Despite this there appears to be no spatial trends to which the change in seam depth occurs. It is also clear that the changes in depth across the study area is gradual. This suggest that the seam floor elevation data is highly continuous. There is a deep area (purple/blue) towards East and the seam floor depth is shallower in the remainder of the area suggesting some trend in the floor depth

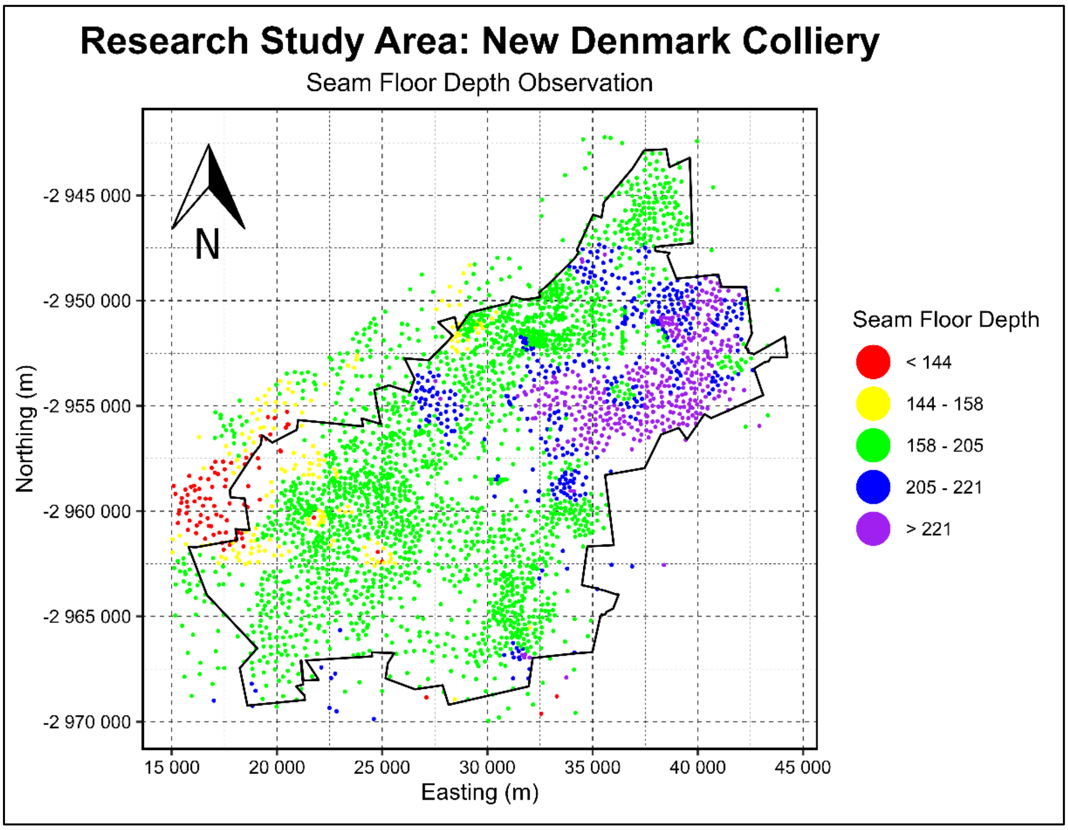

***Figure 41**: Location plot for seam floor depth in the study area.*

Hazard Index Correspondence to Seam Floor Depth

In **Figure 42** below the seam floor depth within the three FHICs are compared. On initial investigation there appears to be a trend in the mean and IQR positions of the floor depth in the FHICs. The floor depth means and IQR have an inverse relationship to hazard class, i.e., as the depth increases the more likely it is to encounter a lower FHIC. Although at first sight this seems to be a good agreement, it is not. The IQR has large areas which overlap, and despite there being a shift in the Q1, Q2 and Q3, position that only represents 50% of the data in each FHIC. The data outside the IQR do vary across the board, with all three FHICs having several outliers at the deeper floor depths. Holistically the box plots reveal the higher the FHIC the more positively skewed the population becomes.

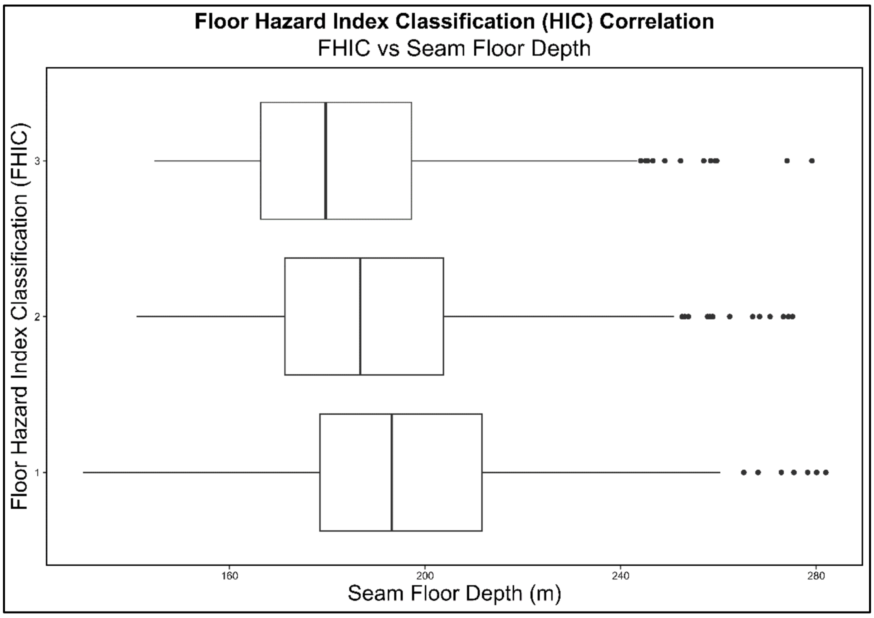

***Figure 42**: Box plots of the FHIC vs Seam Floor Depth.*

A comparison between the RHIC in relation to the seam floor depth appears in **Figure 43** and shows a similar behaviour to that observed in **Figure 36**.The other corresponding diagrams (with exception of **Figure 42**), have all the means of the floor depth within the hazard classes, close to the mean of the global population of seam floor depth. Also, the floor depth IQR of all the classes, essentially overlap with one another and the total data spread is very similar. **Figure 43** also compares to **Figure 36** in that all the outliers appear toward the upper and higher end of the x-axis that is floor depth and seam elevation respectively.

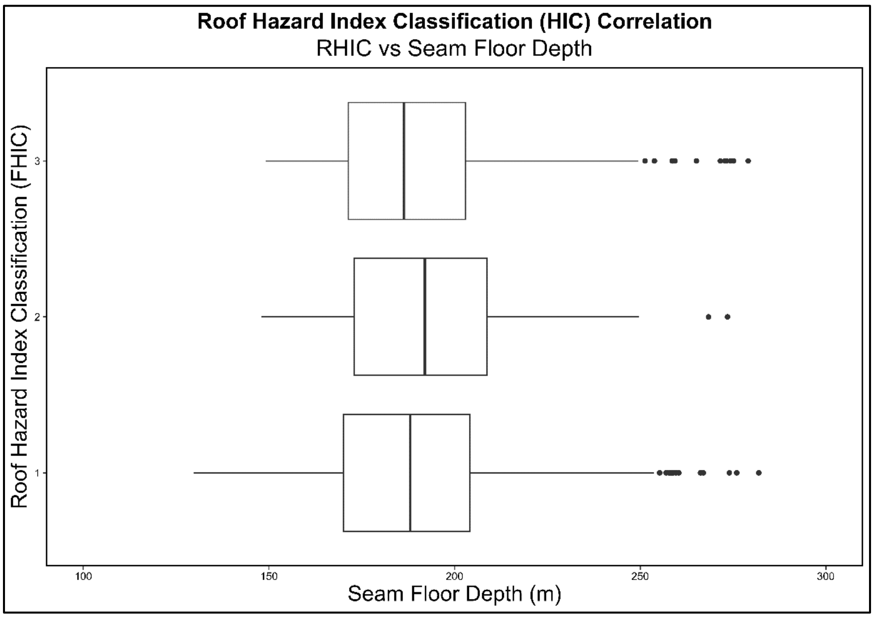

***Figure 43**: Box plots of the RHIC vs Seam Floor Depth.*

Similarly, to seam thickness and seam floor elevation, domaining might be an option to be used for domaining of the HIC. Thus, estimation and simulation on the seam floor depth data were also investigated.

Estimation

From the seam thickness assessment is clear that the continuity of the structural variables results in OK estimates and E-type estimates which closely correspond to the IDW2 estimate, which was a sufficient conclusion for the purposes of this research. Displayed in **Figure 44** are the location plots of the IDW2 seam floor depth estimate, the seam floor depth observations and the seam floor depth FHIC and RHIC. Visually, again there seems to be no geospatial correspondence to suggest domaining the FHICs and RHICs based on seam floor depth.

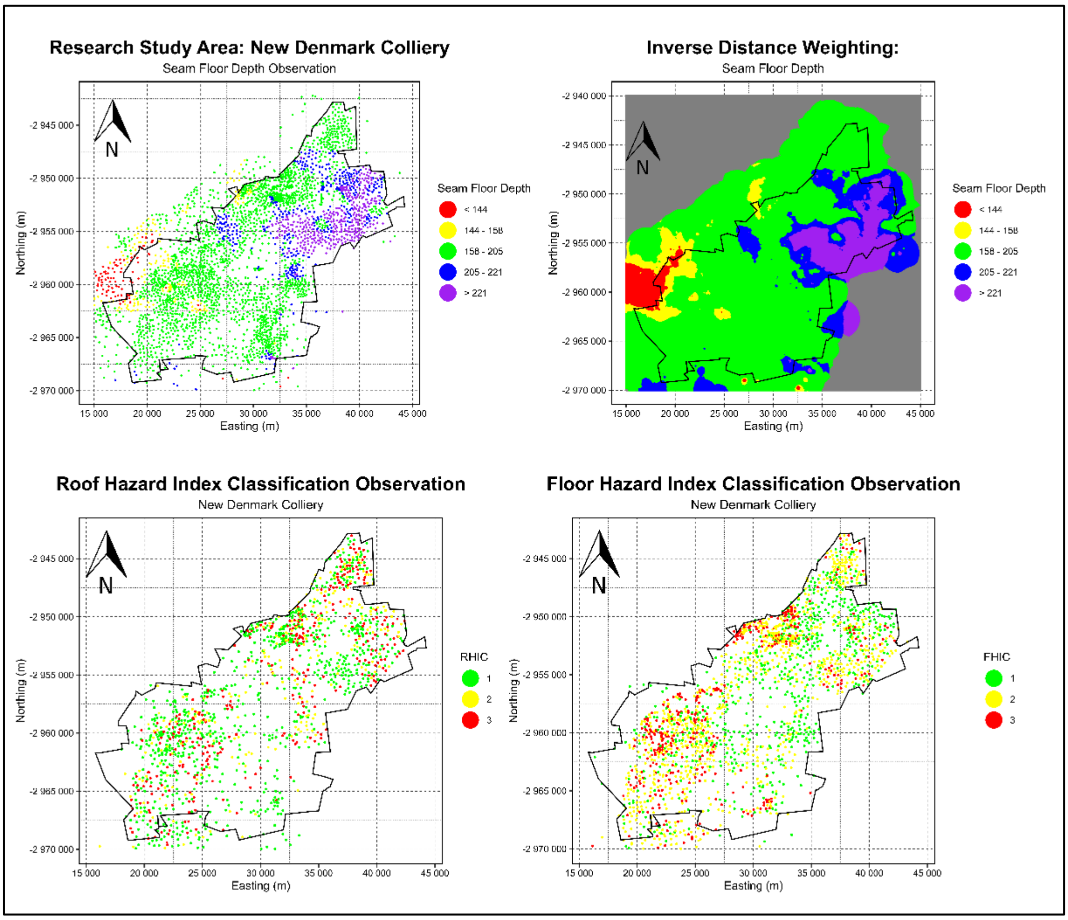

Figure 44*: NDC Seam floor depth, IDW2 estimates, RHIC & FHIC Location plots.*

5.3 Hazard Index Classification Estimation

Disappointingly the CSGS analysis of the structural variables did not reveal any option for domaining the roof and floor hazards and the structural variables also did not show any convincing spatial correspondence, to the HIC data sets. The hazard data sets were then individually analysed. To do this the FHICs and RHICs were each subdivided into 2 indicator data sets. The indicator data sets were constructed by combining two classes and then comparing it to the third, and the second set would be the where the last two classes are combined and compared to the first. **Figure 45** graphically illustrates the creation of these indicator data sets and **Figure 46** reflects the corresponding number of indicators per set.

	Floor Hazard Classes			Roof Hazard Classes		
	FHIC 1	FHIC 2	FHIC 3	RHIC 1	RHIC 2	RHIC 3
Set 1	0	1		0	1	
Set 2	0		1	0		1

Figure 45*: Illustration of the hazard indicator data set creation*

	FHIC Indicator Set Observations			RHIC Indicator Set Observations		
	FHIC 1	FHIC 2	FHIC 3	RHIC 1	RHIC 2	RHIC 3
Set 1	655	1261		810	601	
Set 2	1540		376	1069		345

Figure 46*: Number of observations per set of FHIC and RHIC indicators.*

All Indicator subsets are interpolated by applying IDW2 on a 25 m x 25 m grid. When spatially estimating values that are either zero or one, the resulting estimates will range between these two values which may be considered as “probabilities”; the higher the estimate the more likely it is to be close to indicator 1 is and the lower the estimate the more likely to be close to indicator 0. The final estimated indicator models will be used and compared to the final hazard plans.

5.3.1 Floor Hazard Classification

The FHIC data is divided into 2 data sets (**Figure 45**). In the first set FHIC1 is allocated an indicator value of 0 and the combined FHIC2 and FHIC3 are allocated an indicator value of 1. In the second set (**Figure 45**) the combination of FHIC1 and FHIC2 is allocated an indicator value of 0 and FHIC3 is allocated an indicator value of 1.

Set1 FHIC Indicator Analysis

Set1 FHIC indicators are: FHIC1 (0) $\sim 34\%$ and combined FHIC2 and FHIC3 (1) $\sim 66\%$. The Set1 FHIC indicator location plot is presented in **Figure 47** and that of the IDW2 indicator estimates appear in **Figure 48** below.

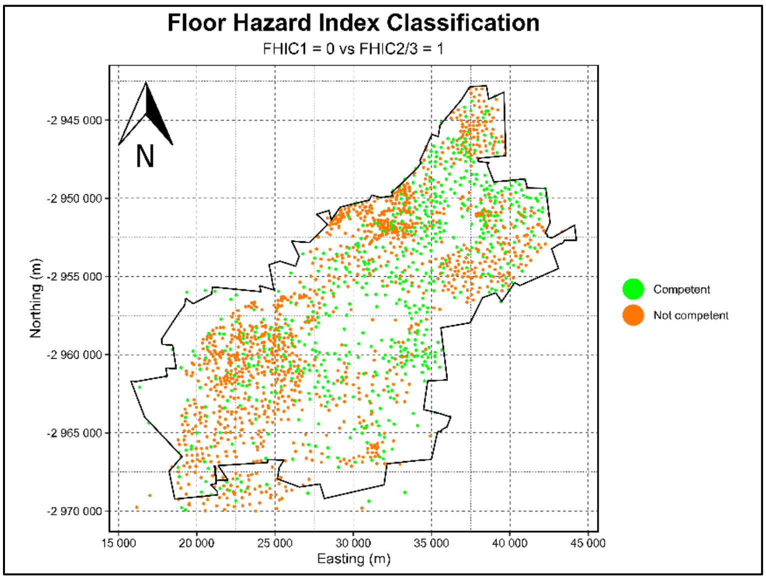

***Figure 47**: Location plot of Set1 FHIC indicators.*

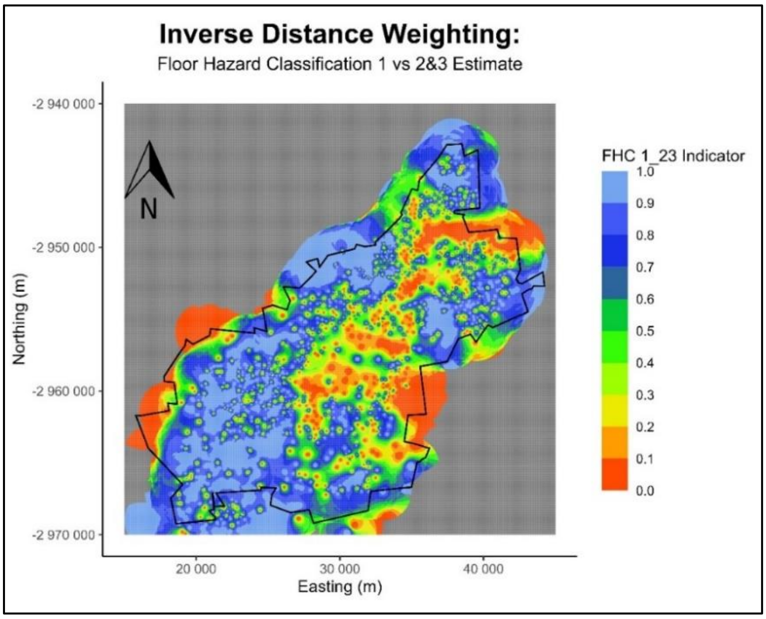

***Figure 48**: Location plot of the IDW2 estimate of Set1 FHIC indicators.*

Comparing **Figure 47** and **Figure 48** above it is seen that the warm colours (‘reds’) align with the zero indicator (**Competent floor** conditions) and the cold colours (‘blues’) align with the one (**Not competent floor** conditions). The default continuous scale applied to the location plot in **Figure 48** is impractical as it does not clearly reveal boundaries for the two floor conditions. To overcome this scale limitation, a cut-off on the Set1 FHIC indicator estimates was introduced. As before the change in slope of the CFD of the estimate shown in **Figure 49** was applied to define a more meaningful colour scale. A cut-off at 0.70 was selected to clearly distinguish the two floor conditions considered.

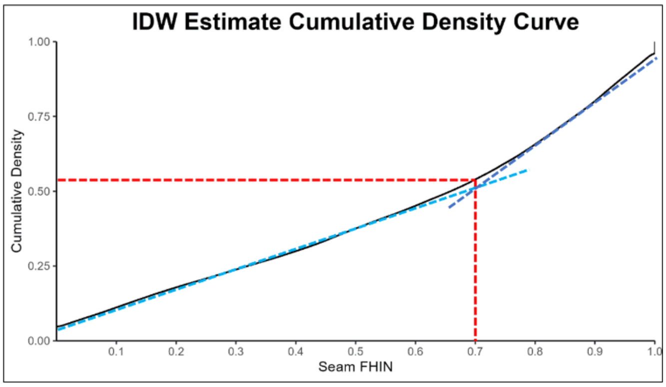

Figure 49*: CFD of the IDW2 estimate of Set1 FHIC indicators.*

The final IDW2 model for Set1 FHIC is reflected by the location plot in **Figure 50**. **Competent floor** conditions, green areas (indicator estimates up to and including 0.70) approximately cover 54% of the area and **not competent floor** (orange, indicator estimates greater than 0.70) approximately 46%.

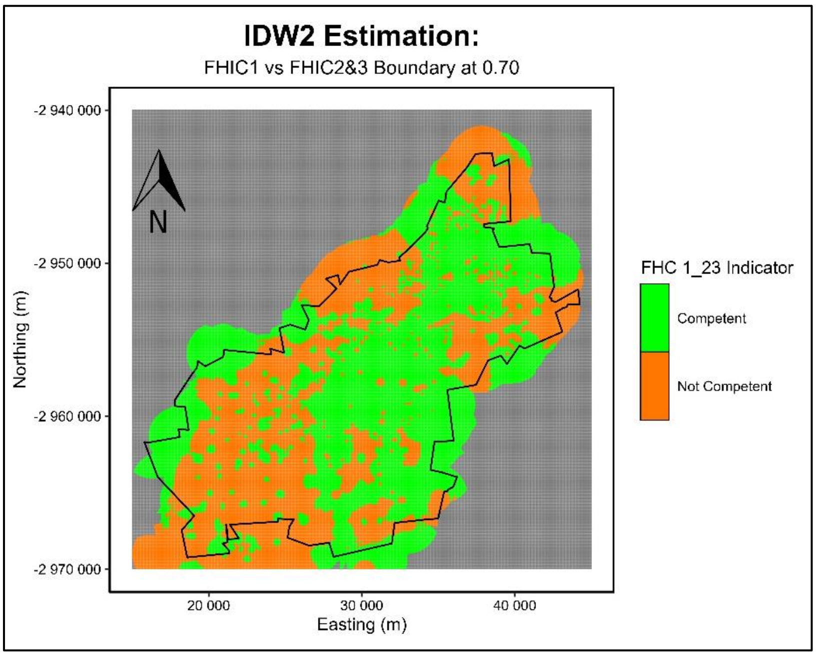

Figure 50*: Set1 FHIC IDW2 indicator model for competent and not competent floor conditions.*

Set2 FHIC Indicator Analysis

In this section Set2 FHIC indicator is considered, where FHIC1 and FHIC2 were combined and assigned (0) $\sim 80\%$ and FHIC3 was assigned (1) $\sim 20\%$. The location plot of these indicators appears in **Figure 51** and that of the associated IDW2 indicator estimates on a continuous scale in **Figure 52**.

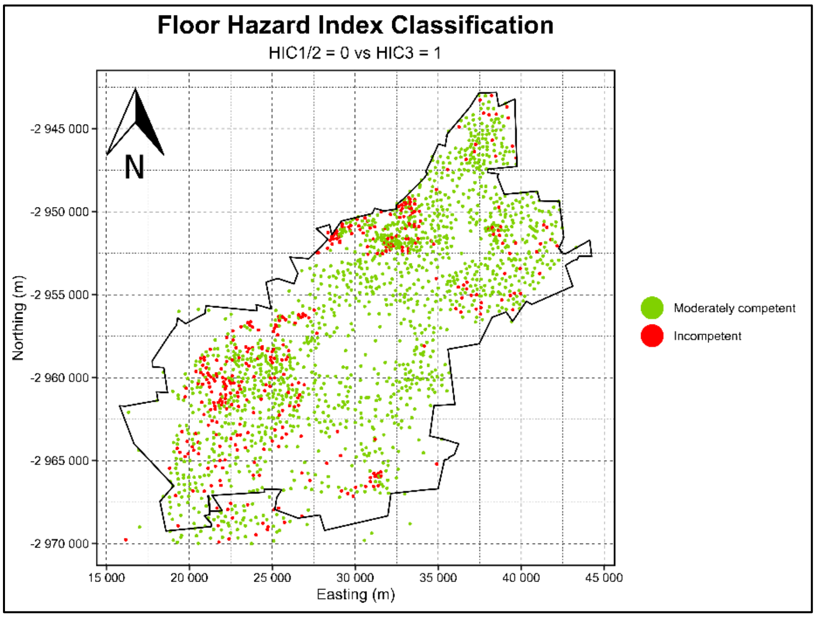

***Figure 51**: Location plot of Set2 FHIC indicators.*

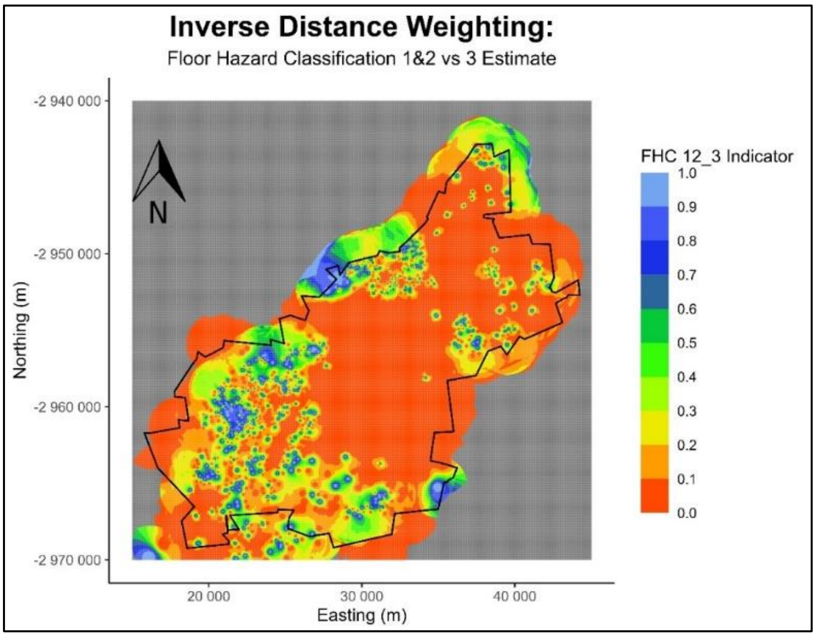

***Figure 52**: Location plot of the IDW2 estimate of Set2 FHIC indicators.*

To establish an indicator cut-off, point for colour coding the IDW2 indicator estimate CFD was used as before. **Figure 53** shows the CFD IDW2 indicator estimates with the slope change estimated at 0.35; this cut-off was then applied.

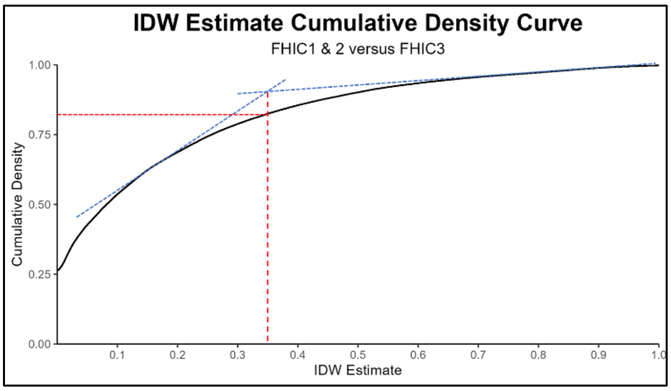

***Figure 53**: CFD of the IDW2 estimate of Set2 FHIC indicators.*

The final IDW2 model for Set2 FHIC is reflected by the location plot in **Figure 54**. **Moderately competent floor** conditions green areas, (indicator estimates up to and including 0.35) approximately 82% of the area and the **Incompetent floor** conditions, red areas (indicator estimates greater than 0.35) ~18% of the area.

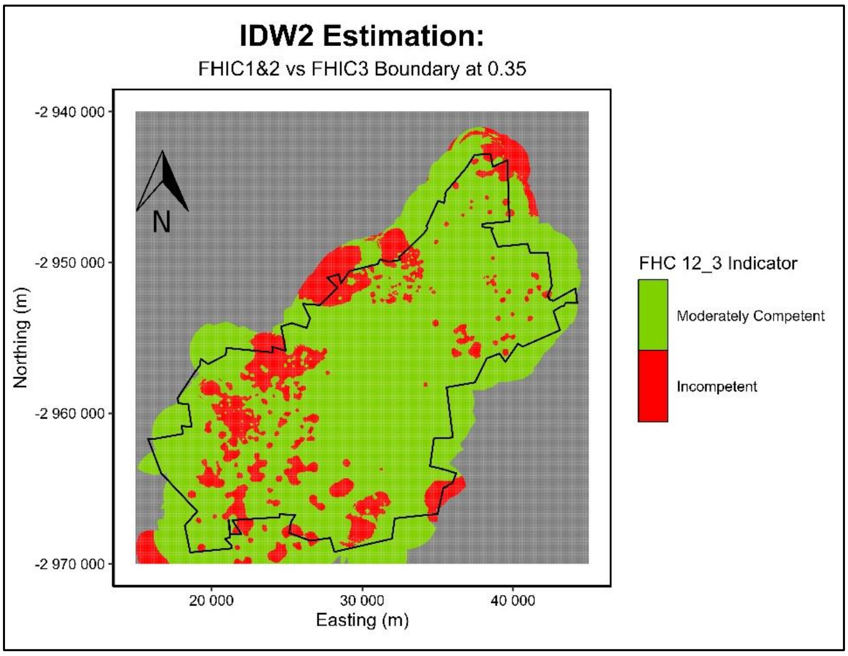

***Figure 54**: Set2 FHIC IDW2 indicator model for moderately competent and incompetent floor conditions.*

5.3.2 Roof Hazard Classification

The RHIC was also divided into 2 data sets (**Figure 45** and **Figure 46**). The indicator definition for Set1 RHIC, RHIC 1 is assigned (0) and the combined RHIC 2 and RHIC 3 assigned (1). For the Set2 RHIC, the combined RHIC 1 and RHIC 2 is assigned (0) and RHIC 3 (1). **Figure 55** illustrates the bar charts frequencies of the two new indicator data sets.

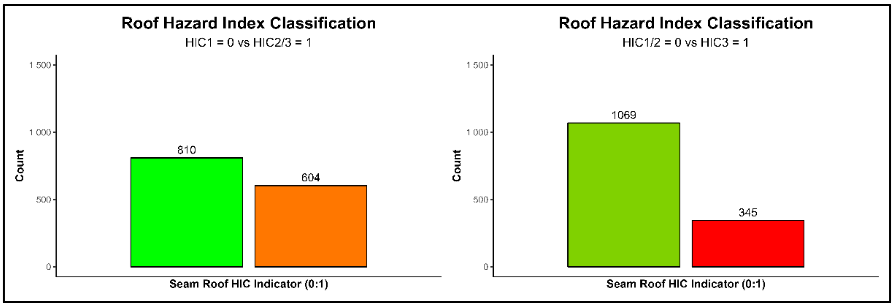

***Figure 55**: Indicator bar charts for the RHIC data.*

Set 1 RHIC Indicator Analysis

This analysis follows the same procedure as for the floor hazard indicators The location of Set 1 RHIC is presented n **Figure 56**.

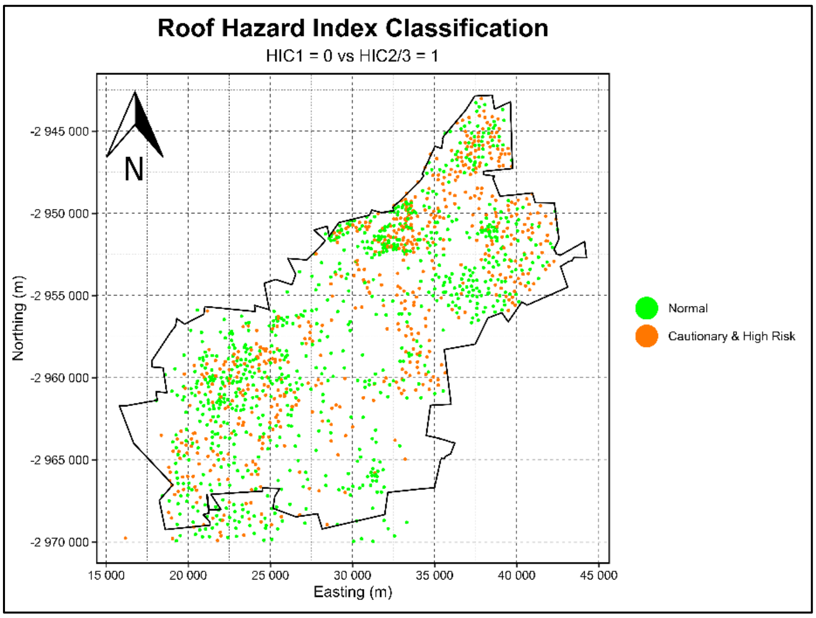

***Figure 56**: Location plot of the Set1 RHIC.*

The location plot of the IDW2 estimates of Set1 RHIC appears in **Figure 57**. In this figure it is noticed that the 'reds' align with the zero indicator and the 'blues' align with the one. In order to generate such a model a cut-off on the continuous variable is required. To establish a cut-off, point to distinguish between the roof conditions the CFD of the estimates was considered.

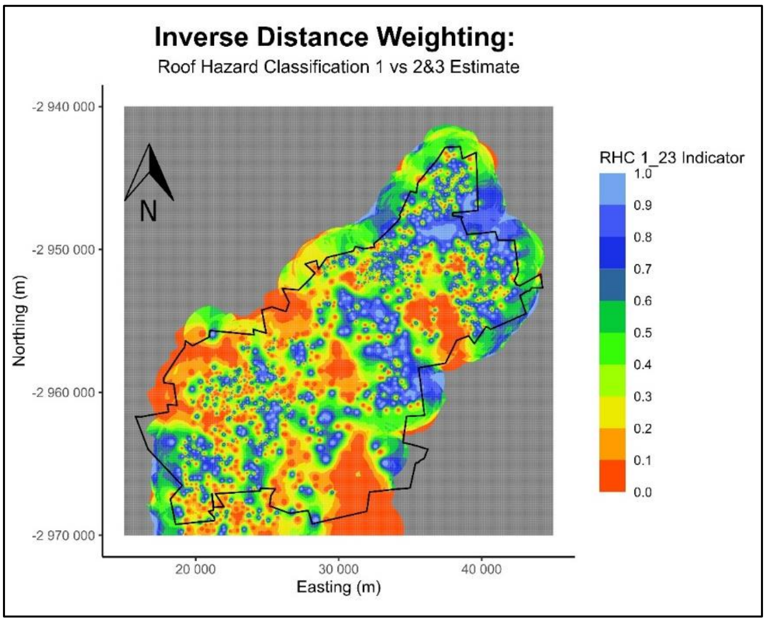

Figure 57*: IDW2 estimate for Set1 RHIC.*

In **Figure 58** the CFD of the RHIC 1 versus RHIC 2 and RHIC 3 is shown. Based on the change in the slope of the curve it seemed appropriate to estimate the indicator estimate cut-off for Set1 RHIC to be at 0.60.

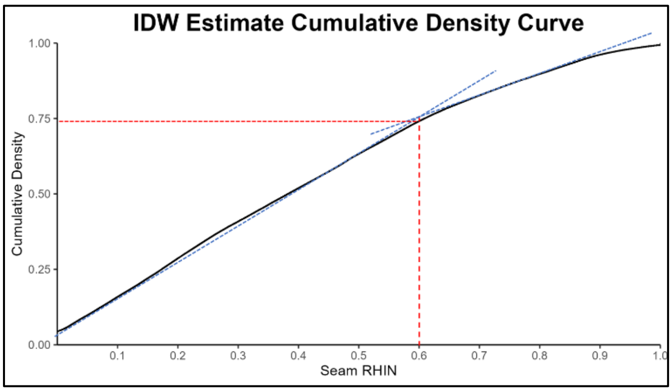

Figure 58*: CFD of the Set 1 RHIC IDW2 estimate.*

The location plot in **Figure 59** reflects Set1 RHIC areas (green, IDW2 estimates up to and including 0.60) to be **Normal roof condition** (74%) and the areas (orange, IDW2 estimates greater than 0.60) to be **Cautionary and High risk roof condition** (26%).

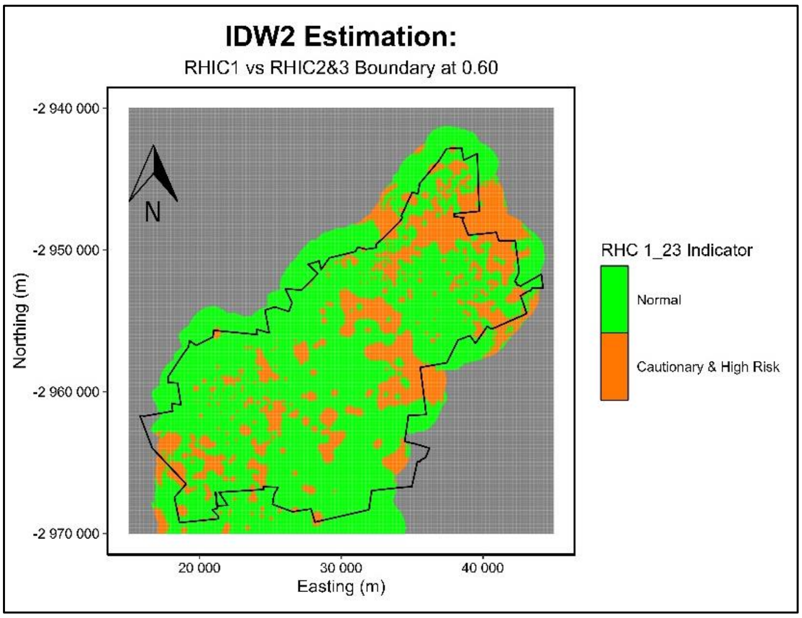

***Figure 59**: Set1 RHIC IDW2 indicator model for normal and cautionary/high risk conditions.*

Figure 60 represents the location of the second set of indicator data for the RHIC as described by **Figure 45**. This dataset is composed of RHIC data grouped into the following categories: RHIC 1 and RHIC 2 (0) versus RHIC 3 (1).

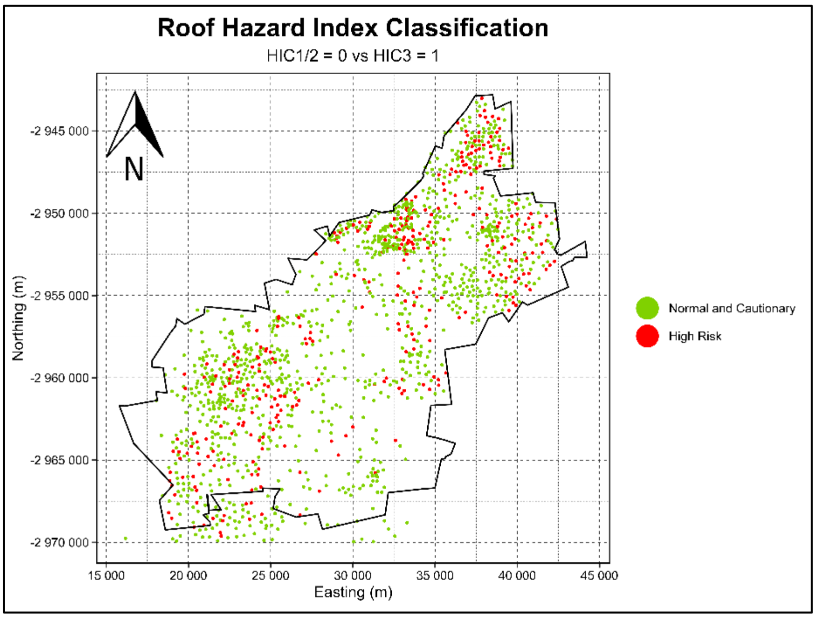

Figure 60*: Location plot of the Set2 RHIC.*

The Set2 RHIC IDW2 estimate is shown in **Figure 61**. From this figure it is evident that the 'reds' align with the zero indicator and the 'blues' align with the one. In order to generate such a model a cutoff on the continuous variable is required. To establish a cut-off, point a CFD of the IDW2 estimate was considered.

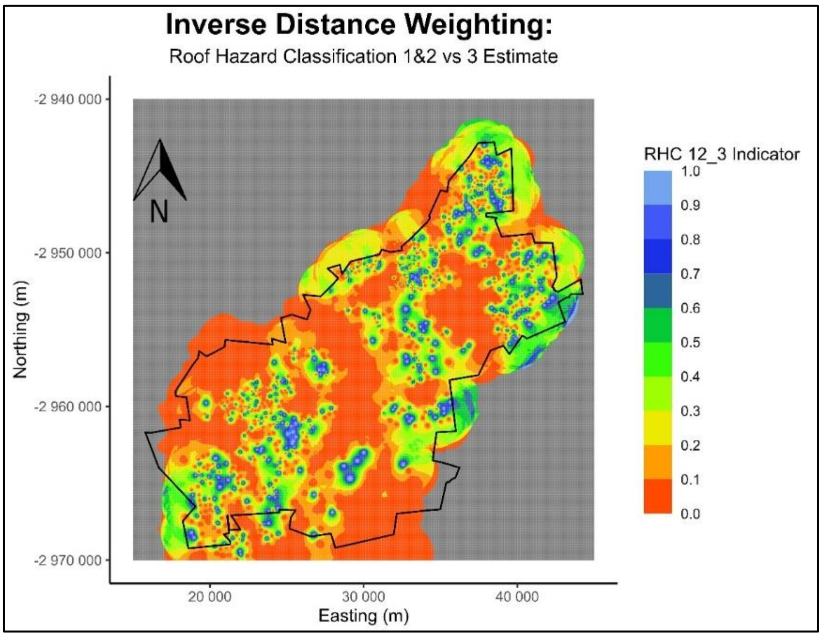

Figure 61*: IDW2 estimate for Set2 RHIC.*

Figure 62 shows the CFD of the RHIC 1 and RHIC 2 versus RHIC 3. Based on the change in the slope of the curve it seemed appropriate for the estimate the indicator estimate cut-off for Set2 RHIC at 0.47.

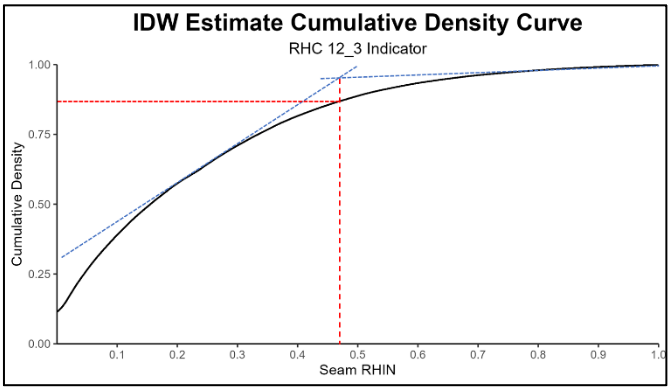

Figure 62*: CFD of the Set2 RHIC IDW2 estimate.*

The location plot in **Figure 63** reflects Set2 RHIC green areas (DW2 estimates up to and including 0.47) to be **Normal and Cautionary roof** and red areas (IDW2 estimates greater than 0.47) to be **High Risk roof** respectively at 87% and13% of the total estimates.

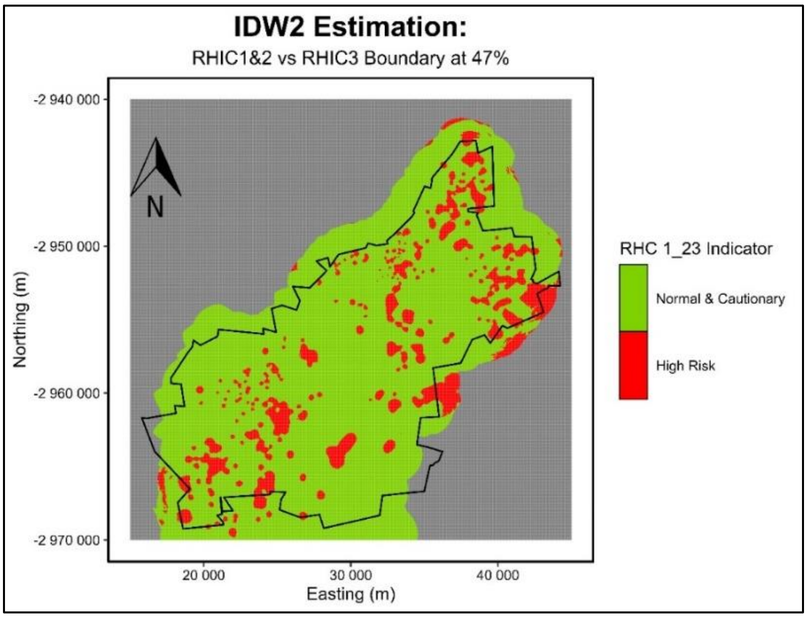

Figure 63*: Set2 RHIC IDW2 indicator model for normal/cautionary and high risk conditions.*

5.4 Hazard Plan Modelling

At this stage the two sets of indicator data have been modelled for the FHIC and RHIC. This process was necessary as the IDW2 indicator estimates in both instances together inform on a hazard plan. To construct the final Floor Hazard Plan (FHP) the combined sets Set1 FHIC and Set2 FHIC of the IDW2 indicator estimates are considered and the final Roof Hazard Plan (RHP) is similarly based on Set1 RHIC and Set2 RHIC IDW2 indicator estimates.

5.4.1 Floor Hazard Plan Modelling

To combine the two sets of FHIC indicator estimates the following algorithm was applied by considering Set1 FHIC and Set2 FHIC IDW2 estimates together with the cut-offs determined by changes in the slope of the CFDs, refer to (**Figure 49**, **Figure 53**).

Floor competency is identified by the following logic: If **Set1 FHIC** indicator estimate is less than or equal to 0.70 then "1", *(that is **the floor is Competent**)*, else if **Set2 FHIC** indicator estimate is less than or equal to 0.35 then Floor competency is "2", (*that is **the floor is Moderately Competent***) else "3" (*that is **the floor is Incompetent***)**.**

The FHP is spatially represented by assigning these three logically generated floor competency values, "1", "2" or "3", respectively to the colours green, yellow and red based on the floor competency logic above. The location plots of the FHP and the FHIC appear in **Figure 64**, a clear correspondence between estimated FHP is observed FHIC.

A noticeable advantage of this process and the methodology of using the floor hazard indicator classes and producing 25 m x 25 m grid IDW2 estimates for them is the fact that 'Incompetent' floor can border 'Competent' floor and more accurately represent the locations of the FHIC data. In other words, if IDW2 were applied to the FHIC without the indicator subsets, the 'Competent' floor would have to transition into 'Moderately competent' floor before reaching 'Incompetent' floor: which is not necessarily realistic: as the observed FHIC data do display instances where 'Incompetent' floor is surrounded by 'Competent' floor, and vica versa.

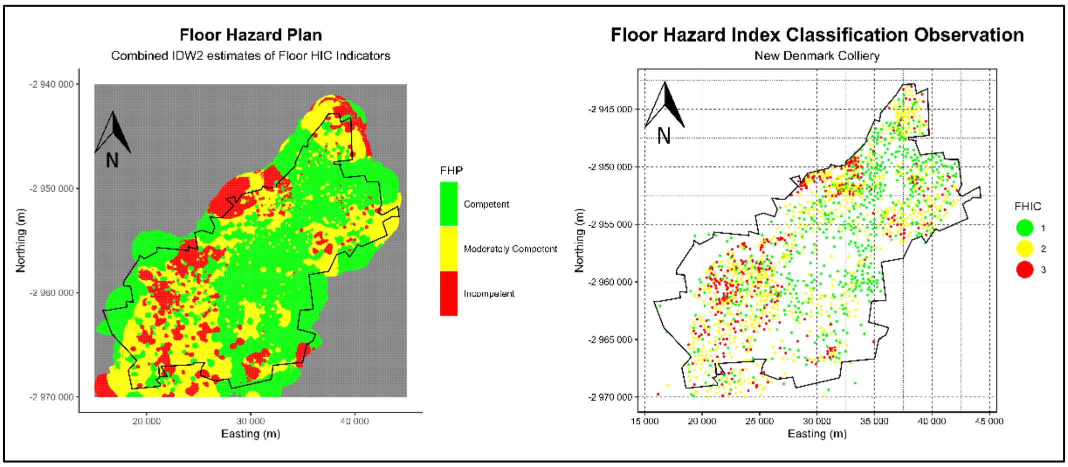

***Figure 64**: FHP and FHIC location plot.*

5.4.2 Roof Hazard Plan Modelling

Similarly, to the FHIC the RHIC indicator data sets were combined using the same procedure as for the FHIC indicator data sets. IDW2 estimates together with the cut-offs determined by changes in the slope of the CFDs, refer to (**Figure 58**, **Figure 62**) For the RHIC data the logic followed is detailed below.

Roof condition is identified by the following logic: If **Set1 RHIC** indicator estimate is less than or equal to 0.60 then “1”, (that is **the roof is Normal)**, else if **Set2 RHIC** indicator estimate is less than or equal to 0.47 then ”2”, (that is **the roof is Cautionary)** else ”3” (that is **the roof is High Risk).**

The RHP is spatially represented by assigning these three logically generated discrete roof conditions (“1”, “2” or “3”) respectively to the colours green, yellow and red based on the roof competency logic above. The location plots of the RHP and the RHIC are presented in **Figure 65**. This plan clearly illustrates the IDW2 hazard plan, which has as its foundation, the individual IDW2 indicator estimates of **Set1 RHIC** and **Set2 RHIC**. It is evident from these two plots that the RHP honours the conditioning input data (RHIC). Also, the method eliminates the transition zone as mentioned in the FHP section.

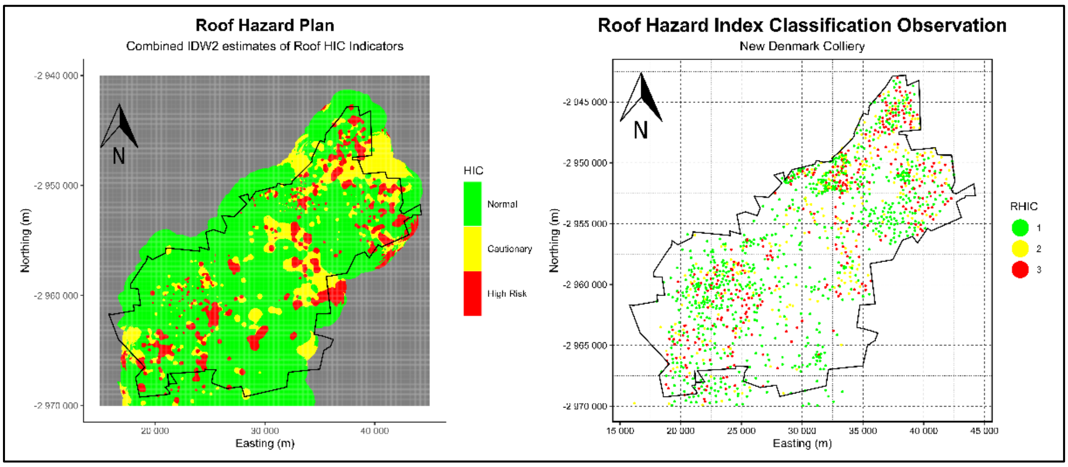

Figure 65: *RHP and RHIC location plot.*

In Chapter 5 the analysis and results of the research study was presented. The correspondence between HIC data and the estimation and simulation of structural variables was summarised. The potential for domaining of HIC in accordance with structural variables was also investigated. However, these analyses disappointingly did not yield any possibility for spatial domaining of the HIC based on the structural.

Nonetheless it was established that for the purposes of this research IDW2 is an acceptable spatial estimator to be used. The research took a turn when it was decided to consider the HIC values as indicators. The HIC indicators were estimated using IDW2. The correspondence between these estimates was compared. Finally, the IDW2 indicator datasets were combined and the FHP and RHP were generated and presented for implementation.

6 CONCLUSIONS AND RECOMMENDATIONS

Chapter 6 contains a reflection on the research. Concluding remarks are noted and detail shortcomings and the success of this research. In addition to these are the recommendations encompassing a clear outline for recommended future work to increase confidence in the FHP and RHP.

6.1 Conclusions

Borehole data types used in the research were both qualitative (interpretated-geological and rock properties) and quantitative (measured bed separation thicknesses and sill proximity). Hazard assessment scorecards were developed considering both data types and applied to the NDC vertical borehole logs. Resulting in the Floor Hazard Scorecard and the Roof Hazard Scorecard methodology to capture the hazardousness of the No 4 coal seam floor and roof conditions.

The two scorecards successfully produced numerical values which formed the foundation of the analytical research in the NDC study area. The developed hazard scorecard methodology is applicable to any borehole in the database and allow for updating of new borehole information as it becomes available. The method for the generation of the scorecard was developed at the onset of the research and is detailed in **APPENDIX A**.

The original nine HIN categories individually contained too few observations for sensible assessment. The HIN data was grouped to form more meaningful classes (HIC) for further analysis. Firstly, the HIC data was used to create Voronoi diagrams for FHIC and RHIC. With the Voronoi diagrams the spatial density of the data was evaluated. Small polygons in the centre of the NDC lease, where mining has taken place, and larger polygons towards the edge of the mining lease. Highlighted the spatial influence of borehole information.

The amount data for the structural variables are more than double the number of observations than that of the floor and roof hazard data. Because of this notable difference in sample size, it was envisaged that investigating the structural variables could shed light on the occurrence of the HIN and HIC variables through spatial correspondence with the structural variables.

Out of the three structural variables the ‘seam thicknesses were assessed with the use of estimates (IDW2 and OK) as well as simulation. Despite the high variability in the spatial continuity the OK estimate showed good correlation to the IDW2 estimates. This correlation is important as it gives geospatial significance to the IDW2 estimates because it is the preferred estimation methodology of NDC.

Regardless of this correspondence between the IDW2, OK and Simulation estimates for seam thickness, no spatial correspondence, envisaged at the onset of the research, between the FHIC or RHIC and the seam thickness could be identified. The ‘seam floor elevation’ and ‘seam floor depth’ were also assessed and again no correspondence or possibility for FHIC or RHIC domaining using these variables could be established. It was concluded that the structural variables did not contribute to identifying hazard domains. The research then focusses on the evaluation of the HIC information only and without perceived benefits of the larger structural dataset.

The FHIC location plot revealed that most of the FHIN 2 boreholes fall within the mined-out areas. On the other hand, most of the FHIN 6 fall within areas still to be mined. Thus, it is conclusionary that the mine is more likely to intersect incompetent floor conditions. It was not possible to draw similar conclusion for the RHIC due to the random spatial distribution of the RHIC indicator subsets.

To fully evaluate the HIC indicator subsets were defined Set1 FHIC and Set2 FHIC for the floor competency, and Set1 RHIC and Set2 RHIC for the roof conditions. IDW2 indicator estimates of the two sets of for the individual hazards were then used to identify the likelihood of distinct hazard conditions for each hazard resulting respectively in an FHP and an RHP. These hazard plans are the final outcomes of the research. They match their HIC location plots and represent the observed data more accurately. This accordance is an improvement as a standard IDW2 plot of the HIC data would create ‘moderately competent’ transition zones on the plans even in locations where there is no evidence of this. The plans created in this research study do not have this limitation. This procedure for updating the hazard plans is detailed in **APPENDIX B**.

The goals of this research were achieved, despite some setbacks. The gaps in the hazard modelling at NDC have been addressed by the research outcomes. Firstly, methodologies for the construction and validation of reliable and easily implementable hazard forecasting models were developed. Secondly, a formal procedure for updating the hazard models is presented.

6.2 Recommendations

This research is essentially a desktop study applied to information gathered from vertical boreholes which have been drilled in the NDC study area over a period of 50 years. Due to the fact that the hazard plans produced, will inform on areas of varying levels of hazardousness, validation of the proposed model correspondence to actual conditions will require continuous monitoring and reconciliation from the operation once the models are in use. The reconciliation will involve comparing the predictive model to actual conditions underground.

If reconciliations in the future cannot be linked to the hazard models with a certain degree of accuracy a re-evaluation of the scorecards can be initiated. The innovative usage of scorecards could further evolve and included in the prediction of lithological hazards in coal mining at NDC. The formal procedure for hazard model updating, presented in **APPENDIX A** needs to be refined to conform to an official standalone document to be adopted as a standard operating procedure (SOP) at NDC.

It has to be noted that there are some limitations to the scorecards. In the development of the hazard scorecard the hazard qualifies have implicitly been assumed to be independent. Future work to investigate links between the identified hazard qualifiers is recommended. If such an investigation is to be carried out, then the weighting of the qualifies might be different.

Because reconciliation is a paramount recommendation of this research it is further recommended that a formal procedure is written up on how the FHP and RHP are to be reconciled. This is important as it will inform on if and when the FHP and RHP process needs to be re-evaluated.

Finally, all boreholes drilled after the drill date of the most recent borehole in this research study needs to be added to the FHP and RHP.

REFERENCES

Abzalov, M (2016), *Applied mining geology*, vol. Volume 12, Modern Approaches in Solid Earth Sciences, Springer, Switzerland.

Aksoy, C (2008), 'Review of rock mass rating classification: Historical developments, applications, and restrictions', *Journal of mining science*, vol. 44, no. 1, pp. 51-63.

Anglo Coal Geological Services (Acgs) Resource Geology Department (2018), *'New NDC floor hazard plan.dgn'*, Anglo American Shared Services (A.C.G.S.), Standerton.

Aphalo, PJ (2023), *ggpmisc: Miscellaneous Extensions to 'ggplot2'*, R package version 0.5.3, <https://CRAN.R-project.org/package=ggpmisc>.

Atkinson, PM & Lloyd, CD (2009), 'Geostatistics and spatial interpolation', *The SAGE handbook of spatial analysis*, pp. 159-181.

Auguie, B (2017), *gridExtra: Miscellaneous Functions for "Grid" Graphics*, R package version 2.3, <<https://CRAN.R-project.org/package=gridExtra>>.

Bivand, RS, Pebesma, E & Gomez-Rubio, V (2013), *Applied spatial data analysis with {R}*, 2 edn, Springer, New York.

Cairncross, B & Cadle, A (1991), 'Fluvial depositional systems in the Vryheid Formation, northern Karoo basin', in *Conference on South AfricaLs Coal Resources: Geological Society of South Africa, Witbank*, vol. 11, pp. 6-9.

Chiles, J-P & Delfiner, P (1999), 'Modeling spatial uncertainty', *Geostatistics, Wiley series in probability and statistics*.

Clark, I & Harper, WV (2000), *Practical Geostatistics 2000*, vol. 1, Ecosse North America Llc., Columbus, Ohio, USA.

De Korte, G (2015), 'Processing low-grade coal to produce high-grade products', *Journal of the Southern African Institute of Mining and Metallurgy*, vol. 115, no. 7, pp. 569-572.

Dearlove, D & Crainer, S (2011), *Robert Kaplan & David Norton*, Thinkers50.com, viewed 13 June 2021, <https://thinkers50.com/biographies/robert-kaplan-david-norton/>.

Dunnington, D (2023), *ggspatial: Spatial Data Framework for ggplot2*, 1.1.9 edn, GitHub, <https://github.com/paleolimbot/ggspatial>.

Falcon, RMS (1986), 'The Coalfields of Southern Africa: An Introduction', in CR Anhaesser & S Maske (eds), *Mineral Deposits of Southern Africa*, Geological Society of South Africa, Johannesburg, vol. Vol. 2, pp. 1875–1878.

Garrett, RC, Nar, A & Fisher, TJ (2022), *ggvoronoi: Voronoi Diagrams and Heatmaps with 'ggplot2'*, R package version 0.8.5, <https://CRAN.R-project.org/package=ggvoronoi>.

Gräler, B, Pebesma, E & Heuvelink, G (2016), 'Spatio-Temporal Interpolation using gstat', *The R Journal*, vol. 8, no. 1, pp. 204-218.

Grills, A, Stiefenhofer, J & Thurston, M (2017), 'Development of a best-practice mineral resource classification system for the De Beers group of companies', *Journal of the Southern African Institute of Mining and Metallurgy*, vol. 117, no. 12, pp. 1127-1132.

Hagelskamp, H (1987), 'The Influence of Depositional Environment and Other Dolerite Intrusions on the Quality of Coal: A Study of the Twistdraai Mine Area Near Secunda, Southeastern Transvaal', Universiteit van Pretoria.

Hagelskamp, H, Eriksson, P & Snyman, C (1988), 'The effect of depositional environment on coal distribution and quality parameters in a portion of the Highveld Coalfield, South Africa', *International Journal of Coal Geology*, vol. 10, no. 1, pp. 51-77.

Hancox, PJ & Götz, AE (2014), 'South Africa's coalfields—A 2014 perspective', *International Journal of Coal Geology*, vol. 132, pp. 170-254.

Hvitfeldt, E (2021), *paletteer: Comprehensive Collection of Color Palettes*, R package version 1.3.0, <https://github.com/EmilHvitfeldt/paletteer>.

Jeffrey, L (2005), 'Characterization of the coal resources of South Africa', *Journal of the South African Institute of Mining and Metallurgy*, vol. 105, no. 2, pp. 95-102.

Jeffrey, L, Henry, G & Mcgill, J (2015), 'Introduction to South African coal mining and exploration', in Struik Nature.

Kaplan, RS & Norton, DP (1992), 'The Balanced Scorecard—Measures that Drive Performance', *Harvard business review*, no. January - February 1992.

Kassambara, A (2023), *ggpubr: 'ggplot2' Based Publication Ready Plots*, R package version 0.6.0, <https://CRAN.R-project.org/package=ggpubr>.

Krige, DG (1951), 'A statistical approach to some basic mine valuation problems on the Witwatersrand.', *Journal of the Chemical Metallurgical and Mining Society of South Africa*, no. December, pp. 119-139.

Lam, NS-N (1983), 'Spatial interpolation methods: a review', *The American Cartographer*, vol. 10, no. 2, pp. 129-150.

Laubscher, D (1990), 'A geomechanics classification system for the rating of rock mass in mine design', *Journal of the Southern African Institute of Mining and Metallurgy*, vol. 90, no. 10, pp. 257-273.

Ma, Y (2019), 'Geostatistical Estimation Methods: Kriging', in *Quantitative Geosciences: Data Analytics, Geostatistics, Reservoir Characterization and Modeling*, Springer, pp. 373-401.

Matérn, B (1987), *Spatial Variation*, vol. 36, Lecture Notes in Statistics, Springer, New York.

Matheron, G (1962), *Traité de géostatistique appliquée*, Editions Technip.

Matheron, G & Kleingeld, WJ (1987), 'The evolution of geostatistics', paper presented to APCOM 87. Proceedings of the Twentieth International Symposium on the Application of Computers and Mathematics in the Mineral Industries., Johannesburg.

Maxwell, K (2020), 'Review of the spatial interpolation techniques used for estimating economic coal properties', *Australian Institute of Geoscientists (AIG)*.

Mineral Council South Africa (2020), *Mineral Council South Africa*, <https://www.mineralscouncil.org.za/sa-mining/coal>.

New Denmark Colliery Geology Department (2016), *'Floor hazard plan_New Colours3.dgn'*, New Denmark Colliery, Standerton.

New Denmark Colliery Mine Survey Department (2019), *'New Roof Hazard Plan.dgn'*, New Denmark Colliery, Standerton.

Parker, H & Dohm, C (2014), 'Evolution of Mineral Resource Classification from 1980 to 2014 and Current Best Practice', in *FINEX 2014 Conference*.

Poonam, S, Lokhande, R & Jeena, S (2017), 'Impact of Geological Discontinuities on Underground Coal mining', paper presented to Indian Coal Mining Industry: Overcoming Challenges for a Better Tomorrow.

R Core Team (2022), *R: A language and environment for statistical computing.*, R Foundation for Statistical Computing, Vienna, Austria, <https://www.R-project.org/>.

Sichel, HS (1947), 'An experimental and theoretical investigation of bias error in mine sampling with special reference to narrow gold reefs', *Trans. Inst. Min. Metall*, vol. 56, no. 403-473, p. 3.1.

Snyman, C & Botha, W (1993), 'Coal in south Africa', *Journal of African Earth Sciences (and the Middle East)*, vol. 16, no. 1-2, pp. 171-180.

Snyman, CP (1991), 'The rank of coal as an indication of the structure of dolerite intrusions.', paper presented to Conference on South Africa's Coal Resources., Witbank, November.

Trueman, AM (2019), *truemoid/mstats: Some Miscellaneous Statistical Functions*, GitHub, <https://github.com/truemoid/mstats >.

Wickham, H (2016), *ggplot2: Elegant Graphics for Data Analysis*, Springer-Verlag, New York.

Wickham, H, Averick, M, Bryan, J, Chang, W, Mcgowan, LDA, François, R, Grolemund, G, Hayes, A, Henry, L, Hester, J, Kuhn, M, Pedersen, TL, Miller, E, Bache, SM, Müller, K, Ooms, J, Robinson, D, Seidel, DP, Spinu, V, Takahashi, K, Vaughan, D, Wilke, C, Woo, K & Yutani, H (2019), 'Welcome to the {tidyverse}', *Journal of Open Source Software*, vol. 4.

Wren, AE (1973), 'Trend surface analysis - A review.', *Canadian Society of Exploration Geophysics Journal*, no. 9, pp. 39-44.

Zhange, Y (2011), *Introduction to Geostatistics — Course Notes*, University of Wyoming, Wyoming.

APPENDIX A

FLOOR AND ROOF HAZARD SCORECARD PROCEDURE

The logic of scoring the floor competency for is borehole is as follows, each of the floor hazard qualifiers are considered in turn and a competency identifier (“X”) is placed in the appropriate informed floor competency column for that qualifier. Then the number of ‘X’ occurrences in each competency column are totalled.

The scorecard is designed to assign the worst-case competency scenario to a borehole. In other words, if 1 qualifier is regarded as incompetent the borehole has to be incompetent in terms of the seam floor. Allocating a floor hazard score or floor hazard index number (FHIN) for any borehole in the database is based on the following logic:

- ✓ If all floor hazard qualifies are ***competent*** the borehole is allocated FHIN of one
- ✓ If one of the floor hazard qualifiers are in the ***moderately competent*** column the FHIN will increase to two. The FHIN will increase by one for every additional qualifier that is classified as moderately competent. Thus. if all four qualifiers are classified as moderately competent the FHIN would be five.
- ✓ If one floor hazard qualifier is ***incompetent*** the borehole floor is deemed to be incompetent floor and is allocated a FHIN of six, irrespective of where the other qualifiers rank (competent or moderately competent). The count for incompetent will increase by one for every qualifier that is classified as incompetent. If all qualifiers are classified as incompetent the borehole will have a FHIN of nine.

The algorithm for applying this logic to produce a FHIN for any qualifying borehole in the database is:

```
if (count(Number of "X's" in the Incompetent column)>0) {
        count(Number of "X's" in the Incompetent column) + 5
        } else if (count(Number of "X's" in the Moderately competent column)>0) {
                count(Number of "X's" in the Moderately competent column) + 1
                } else {
                1
```

This method of scoring the competency of the floor always considers the worst-case scenario for the competency of the floor. This is important as encountering for example a carbonaceous floor will be hazardous for a section even if all other qualifiers are competent. This method of assessing the hazard qualifiers will result in 9 potential categories for a FHIN to fall within.

Allocating a roof hazard score or roof hazard index number (FHIN) for any borehole in the database is based on the following logic:

- ✓ If all roof hazard qualifies are ***normal*** the borehole is allocated RHIN of one
- ✓ If one of the roof hazard qualifiers are in the ***cautionary*** column the RHIN will increase to two. The RHIN will increase by one for every additional qualifier that is classified as cautionary. Thus. if all four qualifiers are classified as cautionary the RHIN would be five.
- ✓ If one floor hazard qualifier is ***high risk*** the borehole roof is deemed to be high risk and is allocated a RHIN of six, irrespective of where the other qualifiers rank (normal or cautionary). The count for high risk will increase by one for every qualifier that is classified as high risk. If all qualifiers are classified as high risk the borehole will have a RHIN of nine.

In this case the code for applying this logic in an algorithm and produce a RHIN for any qualifying borehole in the database is detailed below:

```
if (count(Number of "X's" in the High Risk column)>0) {
        count(Number of "X's" in the High Risk column) + 5
        } else if (count(Number of "X's" in the Cautionary column)>0) {
                count(Number of "X's" in the Cautionary column) + 1
                } else {
                1
                }
```

The graphical scorecard for the FHIN is represented by **Figure 6** and for the roof represented by **Figure 10**.

APPENDIX B

HAZARD MODEL UPDATE PROCEDURE

The process for the updating of the FHP and RHP is as follows:

1. Score the floor and roof of the new boreholes using the floor and roof hazard scorecards methodologies (**Figure 6** and **Figure 10**). This will result in FHIN and RHIN values for each borehole.

2. Update the geological database with the FHIN and RHIN.

3. Create hazard indicator classes (HIC) by combining the respective HINs (**Section 5.1, Table 2**).

   For FHIC:
   a. For FHIC 1 combine FHIN 1, FHIN 2 and FHIN 3
   b. For FHIC 2 combine FHIN 4, FHIN 5 and FHIN 6
   c. For FHIC 3 combine FHIN 7, FHIN 8 and FHIN 9

   For RHIC:
   a. For RHIC 1 the RHIN 1 values are taken as is.
   b. For RHIC 2 combine RHIN 2, RHIN 3, RHIN 4 and RHIN 5
   c. For RHIC 3 combine RHIN 6, RHIN 7, RHIN 8 and RHIN 9

4. Generate two FHIC and two RHIC indicator subsets according to the logic provided in **Section 5.3**; which **must be adhered** to, as it affects the interpretation of the final hazard plans; see refer to **Figure 45** and **Figure 46**.

   a. **Set1 FHIC** indicators are:

      FHIC 1 (**0**) and combined FHIC 2 & FHIC 3 (**1**), spatially reflecting **Competent** and **Not competent floor conditions** (**Figure 47**).

   b. **Set2 FHIC** indicators are:

      Combined FHIC 1 & FHIC 2 (**0**) and FHIC 3 (1), spatially reflecting **Moderately Competent** and **Incompetent floor conditions** (**Figure 51**).

c. **Set1 RHIC indicators are:**

RHIC 1 (**0**) combined RHIC 2 & RHIC 3 (**1**), spatially reflecting **Normal** and **Cautionary/High Risk roof conditions** (**Figure 56**).

d. **Set2 RHIC** indicators are:

Combined RHIC 1 & RHIC 2 (**0**) and RHIC 3 (**1**), spatially reflecting **Normal/Cautionary** and **High Risk roof conditions** (**Figure *63***).

5. Generate IDW2 indicator estimates for each of the four indicator sub-sets defined in the previous step.

6. In this step distinct spatial areas reflecting the likelihood of the floor and roof hazard conditions are identified from the results of the previous step. Create the cumulative relative frequency distribution plots for the individual IDW2 indicator estimates for **Set1 FHIC, Set2 FHIC, Set1 RHIC and Set2 RHIC** (**Figure 49**, **Figure 53**, **Figure 58** and **Figure 62**).

7. Apply the technique of identifying sensible colours for spatial representation of the estimates by considering changes in the slope of the CFD plots. On the x-axis of the CFD identify the point of inflection (all estimates less than or equal to it will be plotted in green and all above it plotted in red. The green proportion can be read off on the y-axis of the CFD plot and the red proportion on is one minus that proportion **Figure 49**, **Figure 53**, **Figure 58** and **Figure 62**).

8. The hazard plans for the NDC floor and roof conditions are generated in the final step by respectively considering the estimates of **Set1 FHIC and Set2 FHIC** together for the floor hazard plan and **Set1 RHIC** and **Set2 RHIC** together for the roof hazard plan. With the geological software evaluate all the nodes of the IDW2 grids estimates.

   a. **<u>For the FHP</u>**: Floor competency is distinguished by using the cuff-offs identified for Set1 FHIC and Set2 FHIC in step 7 using following logic: *If* Set1 FHIC indicator estimate is less than or equal to the cut-off identified *then* “1”, (that is the floor is Competent), *else if* Set2 FHIC indicator estimate is less than or equal to the cut-off identified *then* Floor competency is ”2”, (that is the floor is Moderately Competent) *else* ”3” (that is the floor is Incompetent).

b. **<u>For the RHP</u>**: Roof competency is distinguished by using the cuff-offs identified for Set1 RHIC and Set2 RHIC in step 7 using following logic: *If* Set1 RHIC indicator estimate is less than or equal to the cut-off identified *then* “1”, (that is the roof is Normal), *else if* Set2 RHIC indicator estimate is less than or equal to the cut-off identified *then* ”2”, (that is the roof is Cautionary) *else* ”3” (that is the roof is High Risk).

9. Use the discrete values for the floor hazard and the roof hazard generated in step 8 to plot a colour coded FHP and RHP (**Figure 64** and **Figure 65**)